UNIVERSIDADE FEDERAL DE MINAS GERAIS
Programa de Pós-Graduação em Engenharia de Produção

Samantha Rodrigues de Araújo

A tactical optimization framework for equitable allocation and distribution of routine and emergency vaccines

Belo Horizonte
2026

Samantha Rodrigues de Araújo

A tactical optimization framework for equitable allocation and distribution of routine and emergency vaccines

Thesis presented to the postgraduate course degree in Industrial Engineering from Federal University of Minas Gerais as partial requirement for obtaining the degree PhD in Industrial Engineering.

Advisor: Profa. Dra. Lásara Fabrícia Rodrigues

Co-advisor: Prof. Dr. João Flávio de Freitas Almeida

Belo Horizonte
2026

Araújo, Samantha Rodrigues de.
A663t A tactical optimization framework for equitable allocation and distribution of routine and emergency vaccines [recurso eletrônico] / Samantha Rodrigues de Araújo. – 2026.
1 recurso online (112 f. : il., color.) : pdf.

Orientador: Lásara Fabrícia Rodrigues.
Coorientador: João Flávio de Freitas Almeida.

Tese (doutorado) – Universidade Federal de Minas Gerais, Escola de Engenharia.

Inclui bibliografia.

1. Engenharia de produção – Teses. 2. Framework (Programa de computador) – Teses. 3. Vacinas – Controle de produção – Teses. 4. Modelos epidemiológicos – Teses. 5. Otimização – Teses. I. Rodrigues, Lásara Fabrícia. II. Almeida, João Flávio de Freitas. III. Universidade Federal de Minas Gerais. Escola de Engenharia. IV. Título.

CDU: 658.5(043)

Ficha catalográfica elaborada pelo bibliotecário Marcio A. A. Gomes CRB/6 2812
Biblioteca Prof. Mário Werneck, Escola de Engenharia da UFMG

UNIVERSIDADE FEDERAL DE MINAS GERAIS

Escola de Engenharia

Programa de Pós-Graduação em Engenharia de Produção

FOLHA DE APROVAÇÃO

A TACTICAL OPTIMIZATION FRAMEWORK FOR EQUITABLE ALLOCATION AND DISTRIBUTION OF ROUTINE AND EMERGENCY VACCINES.

SAMANTHA RODRIGUES DE ARAÚJO

Tese submetida à Banca Examinadora designada pelo Colegiado do Programa de Pós-Graduação em ENGENHARIA DE PRODUÇÃO, como requisito para obtenção do grau de Doutor em ENGENHARIA DE PRODUÇÃO, área de concentração PESQUISA OPERACIONAL E INTERVENÇÃO EM SISTEMAS SOCIOTÉCNICOS, linha de pesquisa Otimização e Simulação de Sistemas Logíst. e de Grande Porte.

Aprovada em 05 de março de 2026, pela banca constituída pelos membros:

Prof(a). Lásara Fabrícia Rodrigues - Orientador

UFMG

Prof. João Flávio de Freitas Almeida - Coorientador

UFMG

Prof. Reinaldo Morabito Neto

UFSCAR

Prof(a). Patrícia Nascimento Pena

UFMG

Prof. Edilson Fernandes de Arruda

University of Southampton

Prof. Luiz Ricardo Pinto

Belo Horizonte, 05 de março de 2026.

Documento assinado eletronicamente por **Lásara Fabrícia Rodrigues**, **Professora do Magistério Superior**, em 05/03/2026, às 13:00, conforme horário oficial de Brasília, com fundamento no art. 5º do Decreto nº 10.543, de 13 de novembro de 2020.

Documento assinado eletronicamente por **João Flavio de Freitas Almeida**, **Professor do Magistério Superior**, em 05/03/2026, às 13:33, conforme horário oficial de Brasília, com fundamento no art. 5º do Decreto nº 10.543, de 13 de novembro de 2020.

Documento assinado eletronicamente por **Patricia Nascimento Pena**, **Professora do Magistério Superior**, em 06/03/2026, às 05:20, conforme horário oficial de Brasília, com fundamento no art. 5º do Decreto nº 10.543, de 13 de novembro de 2020.

Documento assinado eletronicamente por **Luiz Ricardo Pinto**, **Professor do Magistério Superior**, em 06/03/2026, às 12:36, conforme horário oficial de Brasília, com fundamento no art. 5º do Decreto nº 10.543, de 13 de novembro de 2020.

Documento assinado eletronicamente por **Edilson Fernandes de Arruda**, **Usuário Externo**, em 09/03/2026, às 12:57, conforme horário oficial de Brasília, com fundamento no art. 5º do Decreto nº 10.543, de 13 de novembro de 2020.

Documento assinado eletronicamente por **Reinaldoi Morabito Neto**, **Usuário Externo**, em 09/03/2026, às 18:35, conforme horário oficial de Brasília, com fundamento no art. 5º do Decreto nº 10.543, de 13 de novembro de 2020.

A autenticidade deste documento pode ser conferida no site https://sei.ufmg.br/sei/controlador_externo.php?acao=documento_conferir&id_orgao_acesso_externo=0, informando o código verificador **5000914** e o código CRC **CF28333A**.

Referência: Processo nº 23072.212564/2026-92 SEI nº 5000914

ABSTRACT

Ensuring equitable access to vaccines is as important as vaccine development. Without widespread access, the full benefits of immunization cannot be achieved. To ensure universal vaccine access, vaccine supply chain (VSC) planning must enable coordinated decision-making for both routine and emergency immunization while considering equity constraints. VSC management addresses strategic, tactical, and operational decisions at the production, storage and distribution, and vaccination echelons, as well as the links between hierarchical levels and the VSC echelons. In VSC tactical planning, the Vaccine Allocation Problem (VAP) and the Vaccine Distribution Problem (VDP) must be jointly addressed due to the interdependent decisions that determine the effectiveness of the VSC, particularly in an epidemic context where timeliness is critical and can be life-saving. The VAP aims to allocate vaccines to each site, reducing deaths in epidemic scenarios while maintaining routine immunization coverage. The VDP addresses the logistical challenges of vaccine distribution by selecting the most cost-effective modes of transportation to supply each warehouse, addressing the constraints of each mode. However, current VSC tactical planning does not jointly consider vaccine allocation and distribution for both routine and emergency vaccines while addressing equity constraints. This work presents a systematic approach to address the Vaccine Allocation and Distribution Problem at the tactical level of VSCs. This method integrates a susceptible-exposed-infected-recovered-susceptible (SEIRS) epidemiological model with an optimization model to support equitable vaccine allocation strategies in epidemic scenarios, reducing deaths and infections. This approach also addresses the allocation of routine vaccines based on immunization coverage. Maintaining routine immunization, even during epidemic situations, is essential to prevent setbacks in diseases that are already under control. Following allocation, vaccines are distributed to warehouses using a multimodal distribution optimization model that determines cost-effective transportation decisions across the supply chain, subject to vehicle-capacity and trip-time constraints. We use Brazilian National Immunization Program data to test the proposed method. We then developed alternative scenario configurations that combine different epidemiological settings and vaccine types (routine and emergency) to demonstrate the application of the method in different epidemic and non-epidemic situations. Allocation plans are generated over a one-year planning horizon. The Covid-19 results highlight the efficiency equity trade-off. Equity policies allocate vaccines to less populated and more vulnerable regions, resulting in higher cumulative deaths compared to an efficiency-based allocation solution. For influenza, the allocation also changes across strategies, but predicted deaths remain low, and differences in mortality are minimal. In turn, the number of routine vaccine quantities is maintained constant across months over the planning horizon. In the distribution stage, we select the peak month of each scenario, i.e., the month with the highest transport quantity, to evaluate feasibility under vehicle-capacity and trip-time constraints. The developed approach is flexible enough to be applied to other countries or regions and sets of vaccine-preventable diseases to support tactical allocation and distribution in VSCs.

Keywords: vaccine; vaccine allocation; vaccine distribution; vaccine supply chain; epidemiological model; equity; epidemics; optimization.

RESUMO

Garantir o acesso equitativo às vacinas é tão importante quanto o seu próprio desenvolvimento. Sem acesso generalizado, os benefícios da imunização não podem ser alcançados. Para assegurar o acesso universal às vacinas, o planejamento da cadeia de suprimentos de vacinas (CSV) deve permitir a tomada de decisões coordenadas tanto para a imunização de rotina quanto para a de emergência, considerando restrições de equidade. A gestão da CSV aborda decisões estratégicas, táticas e operacionais nos níveis de produção, armazenamento e distribuição, e vacinação, bem como as conexões entre os níveis hierárquicos e os escalões da CSV. No planejamento tático da CSV, o Problema de Alocação de Vacinas (PAV) e o Problema de Distribuição de Vacinas (PDV) devem ser abordados conjuntamente devido às decisões interdependentes que determinam a eficácia da CSV, particularmente em um contexto epidêmico, em que a vacinação antecipada é crucial e pode salvar vidas. O PAV visa alocar vacinas a cada região, reduzindo mortes em cenários epidêmicos e mantendo a cobertura da imunização de rotina. O PDV aborda os desafios logísticos da distribuição de vacinas, selecionando os meios de transporte mais econômicos para abastecer cada armazém, considerando as limitações de cada meio. No entanto, o atual planejamento tático das CSVs não considera conjuntamente a alocação e distribuição de vacinas de rotina e de emergência, levando em conta as restrições de equidade. Este trabalho apresenta uma abordagem sistemática para abordar o Problema de Alocação e Distribuição de Vacinas no nível tático dos CSVs. Este método integra um modelo epidemiológico suscetíveis-expostos-infectados-recuperados-suscetíveis (SEIRS) com um modelo de otimização para apoiar estratégias equitativas de alocação de vacinas em cenários epidêmicos, reduzindo mortes e infecções. Esta abordagem também considera a alocação de vacinas de rotina com base na cobertura vacinal. Manter a imunização de rotina, mesmo durante cenários epidêmicos, é essencial para evitar retrocessos em doenças que já estão sob controle. Após a alocação, as vacinas são distribuídas para armazéns utilizando um modelo de otimização de distribuição multimodal que determina decisões de transporte custo-efetivas ao longo da cadeia de suprimentos, sujeitas a restrições de capacidade de veículos e tempo de viagem. Utilizamos dados do Programa Nacional de Imunização do Brasil para testar o método proposto. Em seguida, desenvolvemos configurações de cenários alternativos que combinam diferentes contextos epidemiológicos e diferentes tipos de vacinas (de rotina e de emergência) para demonstrar a aplicação do método em diferentes situações epidêmicas e não epidêmicas. Os planos de alocação são gerados para um horizonte de planejamento de um ano. Os resultados da Covid-19 destacam a relação entre eficiência e equidade. Políticas equitativas alocam vacinas para regiões menos populosas e mais vulneráveis, resultando em um número cumulativo de mortes maior em comparação com uma solução de alocação baseada na eficiência. Para a influenza, a alocação também varia entre as estratégias, mas as mortes previstas permanecem baixas e as diferenças na mortalidade são mínimas. Por sua vez, a quantidade de vacinas de rotina é mantida constante ao longo dos meses durante o horizonte de planejamento. Na etapa de distribuição, selecionamos o mês de pico de cada cenário, ou seja, o mês com a maior quantidade de transporte, para avaliar a viabilidade sob restrições de capacidade de veículos e tempo de viagem. A abordagem desenvolvida é suficientemente flexível para ser aplicada a outros países ou regiões e conjuntos de doenças preveníveis por vacinação, a fim de apoiar a alocação e distribuição táticas nas CSVs.

Palavras-chave: vacina; alocação de vacinas; distribuição de vacinas; cadeia de suprimentos de vacinas; modelo epidemiológico; equidade; epidemias otimização.

LIST OF FIGURES

LIST OF TABLES

LIST OF ABREVIATIONS

BRL	Brazilian Real
C	Constraint
Covid-19	Coronavirus Disease 2019
CS	Case Study
CW	Central Warehouse
DM	Deterministic Model
DY	Dynamic
GA	Genetic Algorithms
IVS	Social Vulnerability Index
LP	Linear Programming
LW	Local Warehouse
OF	Objective Function
M	Multiple
MAPE	Mean Absolute Percentage Error
MILP	Mixed Integer Linear Programming
MINLP	Mixed- Integer Nonlinear Programming
MIP	Mixed-Integer Programming
MOGWO	Multi-Objective Grey Wolf Optimizer
ML	Machine Learning
MOPSO	Multi-Objective Particle Swarm Optimization
MTVRP	Multi Trip Vehicle Routine Problem
NLP	Non-Linear Programming
NPIs	Non-Pharmaceutical Interventions
NSGA-II	Non-Dominated Sorting Genetic Algorithm II
PE	Production Echelon
PNI	National Immunization Program
PSO	Particle Swarm Optimization
RO	Robust Optimization
RSP	Robust Stochastic Programming

RW	Regional Warehouse
SCs	Supply Chains
S	Single
SA	Scenario Analysis
SD	System Dynamics
SDE	Storage and Distribution Echelon
SEIRS	Susceptible-Exposed-Infected-Recovered-Susceptible
SIM	Simulation
SO	Stochastic Optimization
SP	Stochastic Programming
SUS	Unified Health System
ST	Static
UBS	Basic Health Units
USD	United States Dollar
VAP	Vaccine Allocation Problem
VDP	Vaccine Distribution Problem
VE	Vaccination Echelon
VSC	Vaccine Supply Chain
VRP	Vehicle Routine Problem
WHO	World Health Organization

CONTENTS

1 INTRODUCTION

Immunization, through vaccination, improves health and international development, saving millions of lives yearly (Chen et al., 2014; Araújo et al., 2023; Mihigo et al., 2016; WHO, 2024a). However, about one-third of the global population remains unvaccinated, increasing the death toll (Nature, 2022). Access to vaccines is also inequitable and often not aligned with the vulnerabilities of populations and the epidemiological risks faced.

Due to innovation in vaccine development, since 2010, 116 countries have introduced vaccines in their national immunization programs, including those for pneumococcal pneumonia, diarrhea, cervical cancer, typhoid, cholera, and meningitis (WHO, 2024b). New vaccines have been developed against malaria, dengue, and ebola, while vaccines against respiratory syncytial virus, tuberculosis, and all strains of influenza are currently being researched.

Ensuring equitable vaccine allocation is just as important as vaccine development; without widespread access, the full benefits of immunization cannot be achieved (Duijzer; Van Jaarsveld; Dekker, 2018; Kargar et al., 2024). According to WHO (2023), many people, including about 20 million children each year, do not have adequate access to vaccines. Since 2022, the WHO has been negotiating the Pandemic Agreement to improve pandemic prevention and response, focusing on vaccine equity. The reluctance of wealthier nations to share vaccines and maintain measures to reduce the transmissibility of the severe acute respiratory syndrome coronavirus 2 (SARS-CoV-2) led to a significant loss of life, estimated at between 200,000 and 1.3 million by the end of 2021, primarily affecting low- and middle-income countries (Moore et al., 2022).

Successful immunization programs also depend on supply chain and logistics systems to prevent compromising the effectiveness and composition of vaccines, which are temperature-sensitive medicines (Almaraj et al., 2026; Dey et al., 2024; Lopes et al., 2022; Wang et al., 2023; WHO, 2023). Unlike typical pharmaceutical products, vaccines require strict temperature control (often between 2°C and 8°C) and have a limited shelf life once opened, requiring precise logistics planning (Dey et al., 2024; Duijzer; Van Jaarsveld; Dekker, 2018).

Immunization plans include both routine and emergency vaccines. Routine vaccines protect against common and predictable diseases and have a more stable and predictable supply. In contrast, emergency vaccines control highly contagious outbreaks that require rapid and widespread distribution; their availability is initially limited due to the need for vaccine development (Matrajt; Halloran; Longini, 2013).

The vaccine supply chain (VSC) consists of complex and hierarchically organized networks responsible for ensuring and maintaining the quality of vaccines during storage, transport, and handling under appropriate temperature conditions. It includes facilities, vehicles, and people who follow numerous procedures to transport vaccines from production centers to vaccination centers (Almaraj et al., 2026; Ribeiro et al., 2016).

The VSC begins with the production of vaccines in production centers and includes activities such as raw material reception, antigen manufacturing, formulation, filling, and packaging. After production, the vaccines are sent to the Storage and Distribution echelon, which is responsible for ensuring vaccine quality during storage, transport, and handling. Finally, at the vaccination centers, the vaccines are received, stored, prepared, and administered to patients.

The Storage and Distribution echelon requires an integrated approach that jointly addresses the Vaccine Allocation Problem (VAP) and the Vaccine Distribution Problem (VDP). The VAP focuses on determining the number of vaccines to be allocated to each site, aiming to reduce deaths in epidemic scenarios while maintaining routine immunization coverage. The VDP addresses the logistical challenges of vaccine distribution by selecting the most cost-effective modes of transportation to supply each warehouse, addressing the constraints of each mode.

Challenges in immunological demand forecasting have also been pointed out in previous works (Duijzer; Van Jaarsveld; Dekker, 2018; Lemmens et al., 2016). Vaccine demand is influenced by both government tenders and individual choice. Government demand, regulated by tenders, requires an early start of production due to long lead times. In addition, individual demand, which is influenced by the perceived risk of infection and vaccine safety, should also be considered by public health organizations and governments when ordering vaccines.

Before the Covid-19 epidemic, research on VSCs was scarce (Chowdhury et al., 2022) and concentrated on influenza. Since then, a growing number of studies have focused on vaccine allocation and distribution, particularly in the context of the Covid-19 epidemic. However, most studies still focus on a single emergency vaccine (influenza or coronavirus) and few on routine vaccines. Among them, Chen et al. (2014) and Hirsh Bar Gai et al. (2018) deal with several routine vaccines, and Lopes (2022) addresses BCG. However, even in epidemic scenarios, routine immunization is essential to prevent setbacks in diseases already under control (UNICEF, 2022; WHO, 2021a).

Most research addresses only the Vaccine Allocation Problem (VAP) or the Vaccine Distribution Problem (VDP). However, few studies integrated vaccine allocation and distribution to improve the efficiency of VSCs (see Jahed, Molana and Tavakkoli-Moghaddam

(2025), Kargar et al. (2024), Valizadeh et al. (2023)). Vaccine allocation decisions affect vaccine distribution, and inefficient distribution impacts vaccine allocation.

Regarding the strategic and tactical planning of VSCs, Bertsimas et al. (2022) and Roy, Dutta and Ghosh (2021) demonstrate the importance of integrating the epidemiological behavior of epidemics with optimization methods to address VSC management. Optimization approaches may not adequately capture the spread of disease, while epidemiological models only estimate future deaths and cases based on specific conditions. In this context, the susceptible-exposed-infected-recovered-susceptible (SEIRS) epidemiological model is used to assess the impact of vaccination of high-risk groups, early vaccination strategies, and non-pharmaceutical interventions (NPIs) on epidemic scenarios. The Centers for Disease Control and Prevention in the United States employs the Differential Equations Lead to Predictions of Hospitalizations and Infections (DELPHI) epidemiological model to predict epidemic progression (Bertsimas et al., 2022). On the other hand, Lopes (2022) notes that Brazil does not use tools to analyze and predict the spread of disease, and vaccine distribution strategies rely on manual analyses of demographic data, including population growth and age, without the systematic use of predictive modeling. However, to the best of our knowledge, no previous work has combined allocation and distribution decisions for both epidemic and routine immunizations while considering epidemiological dynamics and equity at the tactical planning level of VSCs.

In this sense, this work presents a systematic approach to address the Vaccine Allocation and Distribution Problem at the tactical level of Storage and Distribution echelon of VSCs. It combines allocation and distribution decisions from the central warehouse to regional warehouses and, subsequently, from regional warehouses to local warehouses within this echelon. This method integrates an SEIRS model and an optimization model to support equitable vaccine allocation strategies in epidemic scenarios, reducing the number of deaths and infections. This approach also addresses the allocation of routine vaccines based on immunization coverage. Then, emergency and routine vaccines are jointly distributed, minimizing transportation costs and ensuring the pre-determined allocation.

To demonstrate the applicability of the developed approach, the method is applied to the Brazilian National Immunization Program (PNI, from the Portuguese acronym for Programa Nacional de Imunização), which is part of the Unified Health System (SUS). The Brazilian Public VSC is responsible for distributing approximately 300 million doses of 49 immunobiologicals per year (Brazil, 2021), with an acquisition cost of approximately US$ 848 million (Domingues et al., 2020). However, the Ministry of Health faces imbalances in the

allocation of vaccines (shortages in some regions and surpluses in others), leading to losses due to the shelf-life (Lopes, 2022). Since 2016, vaccination coverage has declined (Butantan Institute, 2022; Domingues et al., 2020) due to factors such as a lack of knowledge about the importance of vaccination and misinformation about vaccine risks (Brazil, 2023; Frugoli et al., 2021) and by operational challenges of vaccine distribution throughout the national territory and limited access to health facilities (Domingues et al., 2020). In this context, tactical allocation and distribution planning, based on an optimization model and under equity policies, are important for improving vaccination coverage.

1.1. Research Objectives

This thesis addresses the routine and emergency immunization allocation and distribution problems in tactical planning within the Storage and Distribution echelon of Vaccine Supply Chains, considering equity policies.

1.2. Specific objectives

- Address the epidemiological behavior of diseases in the allocation of emergency vaccines.
- Incorporate equity policies based on population size and vulnerability indices in emergency vaccine allocation.
- Develop tactical plans considering routine and emergency vaccine allocation.
- Develop distribution plans that minimize the transportation costs of vaccines from the central warehouse to regional warehouses, and from regional warehouse to local warehouses.
- Integrate vaccine allocation and distribution decisions in a framework, minimizing the number of deaths and transportation costs.
- Evaluate allocation and distribution decisions under different epidemic conditions and equity policies using multiple outbreak scenarios.

1.3. Document structure

This thesis is divided into five chapters. The first is an introduction to the subject, where we present the objectives of the study and the structure of the thesis. The second chapter summarizes the VSC, describing its echelons and decisions at each planning horizon, and the

most important studies conducted in the optimization of vaccine allocation and distribution are presented. It also addresses equity in the VSC, presenting definitions, modeling approaches, and equity metrics. The third chapter describes the problem and proposes an approach to jointly address the Vaccine Allocation and Distribution Problem under equity policies. The fourth chapter presents the data sources used, the calibration of the SEIRS epidemiological model for Covid-19 and Influenza, a comparison between predictions and historical data for Covid-19, and the allocation and distribution results for four scenarios. Finally, the fifth chapter presents the conclusions of the thesis, discussing the findings, their practical implications, and directions for future research.

2 VACCINE SUPPLY CHAIN

This chapter summarizes the Vaccine Supply Chain, describing its echelons and decisions at each planning horizon. In addition, the studies conducted in the optimization of vaccine allocation and distribution are reviewed.

2.1. Vaccine Supply Chain

VSCs differ from other supply chains (SCs) in cold chain management and vaccine-specific characteristics, such as specific storage requirements (shelf-life, doses per vial, and cold storage) and dosing protocols (single or multiple doses), which affect transportation, allocation, and distribution logistics (Dey et al., 2024).

Vaccines are also sensitive to temperature changes and vibration during transport (Brazil, 2017; CDC, 2024). Unlike most drugs, vaccines have a strict temperature range (typically between 2°C and 8°C), and exposure to conditions outside this range reduces their effectiveness (Chen et al., 2014; Lin; Zhao; Lev, 2020; Moalla; Bouras; Neubert, 2007; Souza et al., 2019; WHO, 2023). Vibrations can cause microcracks in the vial, resulting in leakage and microbiological contamination of the vaccines (Brazil, 2017). Furthermore, VSCs face uncertainties in both supply and demand (Almaraj et al., 2026; Lopes et al., 2022) and involve multiple stakeholders, resulting in a misalignment of objectives due to the decentralization of decision-making at different levels of the chain (Dey et al., 2024; Lemmens et al., 2016; Oliveira, 2009).

From an economic standpoint, the challenges of high production costs and complex pricing structures highlight the particularities of VSC, given that determining the price of vaccines goes beyond financial viability and should consider ethical and public health issues. Several factors determine the price of a vaccine, including accessibility, health outcomes (Yu et al., 2024) development and production costs (Light; Andrus; Warburton, 2009; Martonosi; Behzad; Cummings, 2021), supply, investments, subsidies, government regulations, intellectual property, patents, and future development costs (Geng; Shi, 2024). In China, for example, the decline in vaccine innovation and research has been attributed to price control policies (Geng; Shi, 2024). In Brazil, the Chamber of Regulation of the Medicines Market regulates vaccine and other drug prices and monitors marketing to ensure that pharmacies and related entities comply with the established price limits (Anvisa, 2026).

VSCs entail political and equity complexities and are typically led by public health organizations, with the patient generally not bearing the cost (Duijzer; Van Jaarsveld; Dekker,

2018). In addition, most immunization programs face challenges with the introduction of new vaccines, population growth, increased demand on the cold chain, and limited financial resources (Brown et al., 2014).

Recognizing the complexity of VSC, previous works have addressed the design of VSC. Oliveira (2009), for instance, states that the VSC is composed of suppliers, national producers, international producers, national distribution centers, state distribution centers, regional distribution centers, municipal distribution centers, health posts, and patients. Hovav and Tsadikovich (2015) propose a multi-echelon structure VSC: manufacturers, distribution centers, healthcare organizations, and clinics. Ribeiro (2016) describes the VSC as comprising of the suppliers, manufacturers, warehouses, customers, and consumers. Fantini (2021) presents the VSC as composed of laboratories, the national warehouse, municipality warehouses, and vaccination centers. Georgiadis and Georgiadis (2021) present a generic design of the VSC, consisting of three echelons: manufacturing plants, hubs, and vaccination centers. Gilani and Sahebi (2022) designed a VSC consisting of domestic and foreign suppliers, international packaging centers, storage and distribution centers, and health centers. Kargar et al. (2024) proposed a multi-echelon VSC including four layers, namely manufacturers, regional warehouses, state repositories, and healthcare facilities. The World Health Organization (WHO) also presented the Immunization Agenda (IA) 2030 (WHO, 2021b), which shows the structure of the VSC and provides resources and guidance on immunization SC (WHO, 2023). In the IA 2030, the VSC consists of the national storage, subnational storage, district storage, service delivery point, and vaccination centers. These works address different VSC representations, ranging from complex multi-level configurations to simplified models.

Based on previous works on VSCs and SCs, we design a VSC composed of three echelons: Production, Storage and Distribution, and Vaccination, as presented in Figure 1. This configuration summarizes the hierarchical structure of the VSCs discussed below.

The VSC begins by acquiring raw materials, including pharmaceutical inputs, primary packaging, and various types of packaging (suppliers) (Oliveira, 2009; Souza et al., 2019). Thus, the first echelon of the chain involves the production of vaccines, which includes the reception of raw materials, antigen manufacturing, formulation, filling, packaging, and lot release (Ribeiro et al., 2016). Production centers can be located either domestically or internationally and can serve various storage and distribution facilities at different levels, including central, regional, or local levels. At this stage, decisions are made on lot sizing and production times. The production stage can take up to 24 months, which represents a significant

lead time in the delivery of vaccines from laboratories to warehouses (Duijzer; Van Jaarsveld; Dekker, 2018; Lopes et al., 2022; Ribeiro et al., 2016). Afterward, vaccines are sent to the storage and distribution supply chain echelon.

Figure 1- Decisions levels in the Vaccine Supply Chain

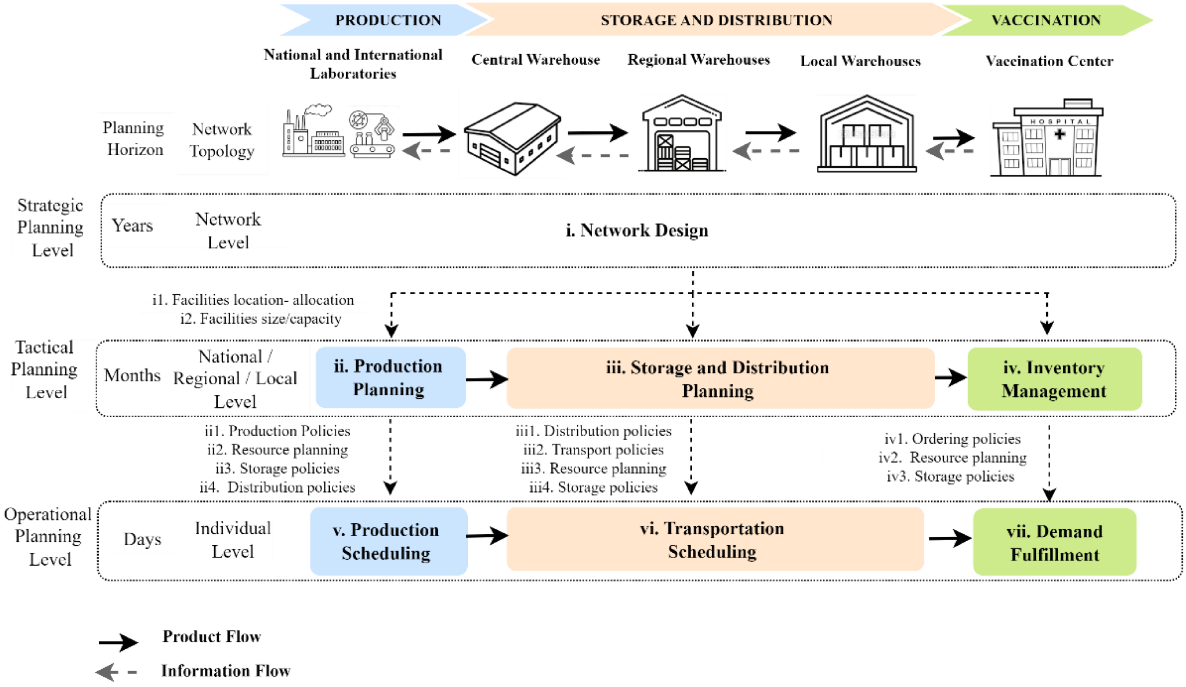

Storage and Distribution is the second echelon of the chain and aims to ensure the availability of vaccines at vaccination centers and to maintain the quality of vaccines during storage, transport, and handling under appropriate temperature and humidity conditions. Storage areas require refrigerated zones, and equipment like stabilizers and generators. The central, regional, and local warehouses manage vaccine distribution with designated rooms for receiving, preparing, and distributing vaccines in thermal boxes (Brazil, 2022). Air, road, and water transport, or a combination of them, can be used to distribute vaccines.

In the last echelon, at the local level, vaccines are received, stored, prepared, and administered to patients in the vaccination centers located in Basic Health Units (UBS) (Brazil, 2022). It also includes the coordination and implementation of immunization activities such as routine immunization, vaccination campaigns, and emergency actions, as well as the reporting and investigation of adverse events and deaths related to vaccination, as established by the PNI. Vaccination centers, along with other facilities in the supply chain, are responsible for vaccine

inventory management and information system management, including data collection, processing, and transmission.

Regarding the planning horizon, VSC management should address strategic, tactical, and operational decisions, as well as the links between hierarchical levels and the echelons (Figure 1). At the strategic planning level, VSC decisions focus on its design, including the layers configuration (central, regional, and/or local), the facilities locations (laboratories, storage and distribution centers, and vaccination centers), and the vaccines assignment. The network design problem involves long-term planning and affects several aspects at the tactical planning level. For example, the decision on the optimal location of a vaccination center is inherently linked to the decision on vaccine distribution (Goentzel et al., 2023).

In the production planning at the tactical level, VSC decisions include the setting of targets for the weekly or monthly amount of vaccine to be processed at production sites. The planned production is then used as input for daily scheduling. At the operational level, the production scheduling involves the setting of the timescale and the vaccine to be produced.

Storage and distribution planning, at the tactical level, addresses decisions on how to allocate vaccines among vaccination centers, considering vaccine characteristics, production capacity, available transport, and storage capacity. The arrival of vaccines from international transport of vaccines and central/district/regional storage occurs at this stage. At the operational level, transportation scheduling specifies the plan for storage and distribution of the quantities of specific vaccines and, defines when and where each vehicle goes and what it carries.

Inventory management at the tactical level requires considering available regional storage space, capacity, and power supply. In addition, the order quantities of each vaccine for each vaccination center are defined, and the request is sent to the warehouses. At the operational level, the capacity and size of the vaccination centers should be used to determine the number of vaccines to be stored and administered at these sites.

For comprehensive works addressing the main characteristics and challenges of VSC, we refer the reader to the review studies of Dey et al. (2023), Lopes et al. (2022), Jordan et al. (2021), Boeck et al. (2019), and Lemmens et al. (2016).

2.2. Optimization of Vaccine Allocation and Distribution

The pioneering research on vaccine allocation optimization was conducted by Longini, Ackerman and Elveback (1978) and aimed to minimize the number of influenza infections under limited supply. Despite this early work, few studies in the recent supply chain

optimization literature focus specifically on VSC (Chowdhury et al., 2022; Jahed; Hadji Molana; Tavakkoli-Moghaddam, 2025). However, since the Covid-19 pandemic, the Operations Research/Management community has published a significant set of research involving modeling and optimization studies to solve problems in the VSC (Dey et al., 2024). Despite the growing interest, most papers in the VSC literature focus on specific stages (production or distribution), resulting in isolated clusters of papers and ignoring the other stages and the linkages between them (Almaraj et al., 2026). Table 1 shows the main characteristics of these studies and their gaps compared to this work.

VSC literature addresses the vaccine allocation problem (VAP) and/or vaccine distribution problem (VDP). Works on vaccine allocation seek to identify which locations should receive vaccines and in what quantities, considering political and equity factors (Sun; Andoh; Yu, 2021). Conversely, works on vaccine distribution aim to determine the method of vaccine distribution (Duijzer; Van Jaarsveld; Dekker, 2018). This includes decisions about inventory management, facility location, routing, and temperature control. In addition, decisions about vaccine allocation and distribution are tactical and must be continually revised to incorporate the latest information throughout the immunization campaign (Bertsimas et al., 2022).

VAP has been more explored in literature. However, the terminology is not yet standardized. While some studies use VAP to refer to vaccine allocation (Enayati; Özaltın, 2020; Hu; Zhang; Zhou, 2023; Jadidi et al., 2021; Jarumaneeroj et al., 2022; Rao; Brandeau, 2021; Rey; Hammad; Saberi, 2023; Yarmand et al., 2014), others use the term to refer to broader aspects, such as distribution (Roy; Dutta; Ghosh, 2021).

To summarize, the models used in the works presented in Table 1 (*Model* column) can be classified into: (i) mathematical modeling and (ii) combinations of simulation and optimization. The studies on mathematical modeling aid in optimizing resources for vaccination programs, enabling the formulation of effective strategies to minimize the impact of disease outbreaks. The methods used in these studies are NLP, LP, DM, MIP, MILP, MILNP, RO, SO, SP, ML, PSO, and AG, and help reduce VSC costs and estimate vaccine demand. These methods are summarized and described in Annex A.

Table 1- Main research in VSC literature

Reference	VAP	VDP	Model	SEIR	Objective		Function Objective	Disease	Epidemics	CS	Echelon			Equity
					S	M					PE	SDE	VE	
Longini, Ackerman and Elveback (1978)	✓		*NLP*	✓	✓		*Min. years of life lost*	*Influenza*	✓	*Hong Kong*				
Patel, Longini and Halloran (2005)	✓		*SIM, GA*		✓		*Min. deaths*	*Influenza*	✓	-				
Chick, Mamani and Simchi-Levi (2008)			*NLSD, NLP*	✓	✓		*Min. total cost*	*Influenza*	✓	-				
Medlock, Meyers and Galvani (2009)	✓		*NLSD*	✓		✓	*Min. deaths, Min. hospitalizations*	*Influenza*	✓	*USA*				
Savachkin and Uribe (2012)	✓		*SIM, NLP*	✓	✓		*Min. total costs*	*Influenza*	✓	*USA*		✓		
Matrajt, Halloran and Longini (2013)	✓		*DM, AG*	✓	✓		*Min. people infected*	*Influenza*	✓	*Southeast Asia*				✓
Yarmand et al. (2014)	✓		*SIM, LP*	✓	✓		*Min. total cost*	*Influenza*	✓	*USA*		✓		✓
Ndeffo Mbah et al. (2014)	✓		*DM*		✓		*Min. dengue hemorrhagic fever cases*	*Dengue*	✓	*Thailand and Brazil*				
Chen et al. (2014)		✓	*LP*		✓		*Max. vaccine availability at the lower levels of the hierarchy*	*Tuberculosis, Tetanus, Measles, Polio, Yellow Fever, DTC-HepB-HiB, Rotavirus and PCV*		*Nigeria, Thailand, and Vietnam*		✓	✓	
Hovav and Tsadikovich (2015)	✓	✓	*MIP*		✓		*Min. total cost*	*Influenza*	✓	*Israel*	✓	✓	✓	
Hovav and Herbon (2017)	✓	✓	*MIP*		✓		*Min. total cost*	*Influenza*	✓	*Israel*	✓	✓	✓	
Hirsh Bar Gai et al. (2018)		✓	*SO*		✓		*Min. distance traveled between states and regional hubs*	*Tuberculosis, Polio, Yellow Fever, Tetanus Toxoid, Hepatitis B*		*Nigeria*		✓		
Sadjadi, Ziaei and Pishvaee (2019)		✓	*MILP*			✓	*Min. total cost, Min. unsatisfied demands*	*Influenza*	✓	*Iran*		✓		
Enayati and Özaltın (2020)	✓		*NLSD, MINLP*	✓	✓		*Min. number of vaccine doses distributed*	*Influenza*	✓	-		✓		✓
Bertsimas et al. (2020)	✓		*NLP*	✓	✓		*Min. number of deaths*	*Covid-19*	✓	*USA*		✓		✓
Abbasi et al. (2020)	✓	✓	*MILP*		✓		*Min. vaccine oversupply, transshipment time*	*Covid-19*	✓	*AUS*		✓		✓
Buhat et al. (2021)	✓		*LP*		✓		*Min. deaths*	*Covid-19*	✓	*Philippines*		✓		✓

Reference	VAP	VDP	Model	SEIR	Objective		Function Objective	Disease	Epidemics	CS	Echelon			Equity
					S	M					PE	SDE	VE	
Sun, Andoh and Yu (2021)		✓	*SIM, MIP*		✓		*Max. total coverage*	*Covid-19*	✓	*Norway*		✓		✓
Roy, Dutta and Ghosh (2021)	✓	✓	*NLSD, NLP*	✓	✓		*Min. transportation cost*	*Covid-19*	✓	*USA*		✓		✓
Rao and Brandeau (2021)	✓		*LP*	✓		✓	*Min. new infections, Min. deaths, Min. life years lost, Min. quality adjusted life years*	*Covid-19*	✓	*USA*				
Rastegar et al. (2021)	✓	✓	*MILP*		✓		*Max. minimum vaccine distributed-to demand ratio*	*Covid-19*	✓	*Iran*		✓		✓
Munguía-López and Ponce-Ortega (2021)	✓		*LP, NLP*			✓	*Max. total vaccines allocated, Max. smallest allocated vaccines, Max. social welfare*	*Covid-19*	✓	*Mexico*		✓		✓
Minoza, Bongolan and Rayo (2021)	✓		*SIM, LP*	✓		✓	*Max. vaccine to be allocated foreach location, Max. priority factor*	*Covid-19*	✓	*Philippines*		✓		✓
Jadidi et al. (2021)	✓		*NLP*	✓	✓		*Max. total immunity among populations*	*Covid-19*	✓	-				
Fantini (2021)	✓	✓	*MILP*			✓	*Min. risk of virus exposure to the vulnerable population, Max. set of accessibility indicators*	*Covid-19*	✓	*Mexico*		✓	✓	✓
Tavana et al. (2021)	✓	✓	*MILP*		✓		*Max. the minimum delivery-to-demand ratio*	*Covid-19*	✓	*India*	✓	✓		✓
Georgiadis and Georgiadis (2021)		✓	*MILP*		✓		*Min total cost*	*Covid-19*	✓	*Greece*	✓	✓	✓	
Yang et al. (2022)	✓		*PSO*	✓	✓		*Min. total number of confirmed cases*	*Covid-19*	✓	-		✓		✓
Mak, Dai and Tang (2022)		✓	*NLSD*	✓	✓		*Max. the number of people witch partial immunity*	*Covid-19*	✓	-				

Reference	VAP	VDP	Model	SEIR	Objective		Function Objective	Disease	Epidemics	CS	Echelon			Equity
					S	M					PE	SDE	VE	
Mohammadi et al. (2022)	✓	✓	*MINLP, RO*			✓	*Min. deaths, Min. total cost*	*Covid-19*	✓	*France*			✓	✓
Lopes (2022)	✓	✓	*ML, SO*		✓		*Min. operating cost of the entire chain*	*BCG*		*Brazil*			✓	
Jarumaneeroj et al. (2022)	✓		*NLSD, NLP*	✓	✓		*Min. stress on healthcare system*	*Covid-19*	✓	*Thailand*		✓		✓
Chowdhury et al. (2022)		✓	*MIP*			✓	*Min. operational cost, Min. environmental cost, Max. job opportunities*	*Covid-19*	✓	*Bangladesh*	✓	✓	✓	
Gilani and Sahebi (2022)	✓	✓	*MILP, RO*			✓	*Min. economical cost, Min. environmental cost, Min. social cost*	*Covid-19*	✓	*Iran*	✓	✓		✓
Bertsimas et al. (2022)	✓	✓	*NLSD, NLP*	✓		✓	*Min. deaths, Min. exposed, Min. distance*	*Covid-19*	✓	*USA*		✓		✓
Thul and Powell (2023)	✓		*SP*		✓		*Max. expected sum of cumulative rewards*	*Covid-19*	✓	*USA*		✓		✓
Rey, Hammad and Saberi (2023)	✓		*ML*	✓	✓		*Min. size of their susceptible population*	*Covid-19*	✓	*World*		✓		✓
Valizadeh et al. (2023)	✓	✓	*MIP, RO*			✓	*Min. risk of distribution inequality of the vaccine, Min. risk of mortality, Min. costs*	*Covid-19*	✓	*Iran*		✓	✓	✓
Hu, Zhang and Zhou (2023)	✓		*NLSD*	✓	✓		*Min. infected people*	*Covid-19*	✓	*World*			✓	
Holleran, Martonosi and Veatch (2023)	✓		*NLSD, LP*	✓	✓		*Min. deaths*	*Covid-19*	✓	*USA*		✓		✓
Kargar et al. (2024)	✓	✓	*SIM, MIP*			✓	*Min. total costs, Min. environmental impacts*	*Covid-19*	✓	*USA*	✓	✓	✓	✓
Jahed, Molana and Tavakkoli-Moghaddam (2025)	✓	✓	*RSP, NSGA-II, MOPSO, MOGWO*			✓	*Min. purchasing or producing vaccines, inventory holding, and transportation costs. Max. effectiveness of the vaccination process*	*Covid-19*	✓	*Iran*	✓	✓	✓	

Reference	VAP	VDP	Model	SEIR	Objective		Function Objective	Disease	Epidemics	CS	Echelon			Equity
					S	M					PE	SDE	VE	
Kheybari et al. (2025)		✓	*MILP, AG*			✓	*Min. total costs, and Min. maximum service user density of the service centers*	*Covid-19*	✓	*Iran*		✓	✓	✓
Almaraj et al. (2026)		✓	*MILP, RO*			✓	*Min. distance between echelons, Min. total costs, and Min. environmental impact*	*Covid-19*	✓	*Saudi Arabia*	✓	✓	✓	
This work	✓	✓	*NLP, SD, MIP*	✓	✓		*Min. deaths, Min. logistics costs*	*24 vaccines*	✓	*Brazil*		✓		✓

Note: VAP: Vaccine Allocation Problem, VDP: Vaccine Distribution Problem, CS: Case Study, SD: System Dynamics, NLP: Non Linear Programming, LP: Linear Programming, S: Single; M: Multiple; SIM: Simulation, DM: Deterministic Model, MIP: Mixed-Integer Programming, GA: Genetic Algorithms; PSO: Particle Swarm Optimization; NSGA-II: Non-Dominated Sorting Genetic Algorithm II; MOPSO: Multi-Objective Particle Swarm Optimization; MOGWO: Multi-Objective Grey Wolf Optimizer; RO: Robust Optimization, RSP: Robust Stochastic Programming; SO: Stochastic Optimization; MILP: Mixed Integer Linear Programming; MINLP: Mixed-Integer Nonlinear Programming, ML: Machine Learning; SP: Stochastic Programming; PE: Production Echelon; SDE: Storage and Distribution Echelon; VE: Vaccination Echelon.

Recently, the modeling efforts in vaccine allocation have focused on combining the simulation-based approaches with optimization structures to improve model accuracy and usefulness in practical contexts. Significant contributions in this area include the studies of Patel, Longini and Halloran (2005), Savachkin and Uribe (2012), Yarmand et al. (2014), Minoza, Bongolan and Rayo (2021), Sun (2021), and Kargar et al. (2024). These works combine simulation techniques with LP, MILP, NLP, and AG.

Some papers use the SEIR model to estimate the virus spreading and policy evaluation (*SEIR* column). Most of these works aim to minimize the negative health impacts of pandemic parameters, such as years of lost life, deaths, cases of infection, and susceptible populations.

The sixth and seventh columns (*Objective* columns) of Table 1 deal with the objectives of the works, classifying models into single- or multi-objective and clarifying the objective(s) adopted in each work. Most single-objective works aim to minimize chain costs (such as operational, environmental, logistical, etc.). Other objectives, such as minimizing the number of infected individuals and minimizing the number of deaths, were also widely adopted. Multi-objective work addresses these objectives simultaneously and aims to find solutions that go beyond minimizing deaths or costs. Only four of the twelve multi-objective works use the SEIR model (Bertsimas et al., 2022; Medlock; Meyers; Galvani, 2009; Minoza; Bongolan; Rayo, 2021; Rao; Brandeau, 2021). Based on Table 1, we observed a reduction in the proportion of works with a single objective. Before the pandemic, the majority (87.5%) of works had a single objective, while after the beginning of the pandemic, this proportion dropped to 58.3%. This suggests that researchers are incorporating more complex characteristics from real world situations into their investigations by using multiple objectives.

Most studies (95.5%) address only one disease, primarily epidemic diseases such as Covid-19 or influenza (see *Disease* column in Table 1). The work of Ndeffo Mbah et al. (2014) stands out as the only study to address the dengue pandemic. On the other hand, Chen et al. (2014) and Dor Hirsh Bar Gai (2018) are the only ones that do not consider pandemics in their analyses. Chen et al. (2014) and Dor Hirsh Bar Gai (2018) address multiple types of vaccines in their works.

Some studies calibrated or validated the models using specific data (population, epidemiological, demographic) from a country (see Case Study column in Table1). The papers used data from countries in Asia (Hong Kong, Southeast Asia, Thailand, Vietnam, Israel, Iran, Philippines, Saudi Arabia, and Bangladesh) and the Americas (Brazil, USA, and Mexico), accounting for about 46% and 43% of the studies listed in Table1, respectively. The remaining

studies are from European, African, and Oceanian countries. The studies by Patel, Longini and Halloran (2005), Chick, Mamani and Simchi-Levi (2008), Enayati and Ozaltın (2020), Jadidi et al. (2021), Yang et al. (2022), and Mak, Dai and Tang (2022) used artificially generated data to simulate a hypothetical situation, i.e., the data are not derived from actual observations or epidemiological situations in a specific region. Hu et al. (2023) and Rey et al. (2023) developed global studies to evaluate the allocation of vaccines for the Covid-19 pandemic to minimize the number of infected and susceptible individuals in each country.

The *Echelon* column of Table 1 shows echelons of the VSC addressed in each study. Most works address only the Storage and Distribution Echelon (SDE) of the VSC. Only Hovav and Tsadikovich (2015), Hovav and Herbon (2017), Georgiadis et al. (2021), Chowdhury et al. (2022), Kargar et al. (2024), and Almaraj et al. (2026) address all echelons of the vaccine network chain (PE, SDE, VE). The scarcity of works that integrate VSC echelons reflects the complexity and challenges associated with this integration, which involves several variables and uncertainties, in addition to the difficulty of integrating data from different sources and the need for collaboration between multiple agents.

Additionally, twenty-four of the forty-four papers reviewed address equity in VSC (*Equity* column), and most works from 2013 onward deal with this issue. The equity in VSCs is discussed in Section 2.2.1.

Finally, Table 1 summarizes the main characteristics of the present study. Specifically, this work addresses both the VAP and the VDP at the Storage and Distribution Echelon (SDE) of VSCs. The SDE is comprised of central, regional, and local warehouses. In this study, vaccines are allocated and distributed from the central warehouse to the regional warehouses and from the regional warehouse to the local warehouses. Since vaccines are typically transported together at the SDE, this approach also ensures that each vaccine is transported appropriately while maximizing the use of shared logistics resources.

To the best of our knowledge, this study is the first attempt to develop a tactical tool that addresses all emergency and routine vaccines of national immunization plans and is adaptable to deal with different national or regional configuration scenarios. The epidemiological behavior of diseases was embedded in an optimization method using the SEIRS model, deriving a SEIRS-based optimization approach. This approach enables the dynamic adjustment of vaccine allocation in response to reinfection and equity policies, whereas most previous work has only addressed the SEIRS framework. Addressing equity in vaccine allocation and

distribution aims to ensure a fair distribution of health resources and reinforces the social relevance of the proposed method.

Figure 2 provides an overview of the gaps addressed and key contributions of the present study. This study simultaneously addresses the VAP and VDP for both emergency and routine vaccines, as well as equity in vaccine allocation and the epidemiological behavior in epidemic scenarios using the SEIRS model.

Figure 2 - Integrated contributions of this work

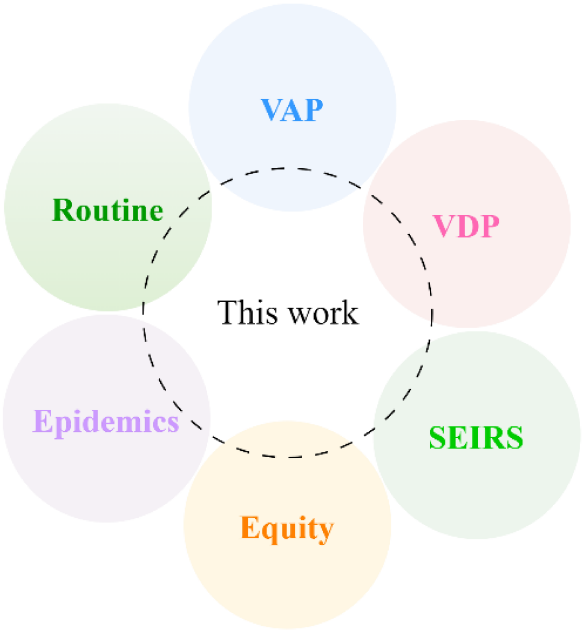

2.2.1. Equity Policy in VSCs

The principle of equity in public health means that everyone has the right to access health services and resources, and the government is responsible for ensuring this access is universal (Béland et al., 2021; Hogan et al., 2025; Marmot; Allen, 2014). Similarly, the Centers for Disease Control and Prevention defines health equity as the condition in which all individuals have a fair opportunity to achieve the highest level of health (Calanan et al., 2023). The responsibility for securing this right is distributed among federal and state agencies, regional and local health administrations, hospitals, and services. These government entities, in turn, interact with businesses, doctors and pharmacists, hospitals, insurers, international vaccine manufacturers, and civil society organizations.

The concept of equity replaced the idea of equality by recognizing heterogeneity and distinct needs among individuals (Fiocruz, 2009). Equality seeks a homogeneous distribution of goods or services, whereas equity establishes a criterion for a heterogeneous distribution adjusted to each individual's needs (Brazil, 2025a; Calanan et al., 2023; Johns Hopkins Medicine, 2022).

Health inequities are defined as unfair differences in health conditions of some socio-demographic groups compared to others (Hogan et al., 2025). These disparities are derived from the inequitable social, political, and economic structures that determine the conditions in which people live. In this sense, the increase in inequality and the challenges of reducing poverty, despite economic growth, have attracted considerable attention and concern from researchers (Béland et al., 2021).

To address these disparities, equity is implemented through fairness criteria that must consider the heterogeneous health conditions across populations (Marmot; Allen, 2014). Although biological factors (i.e., sex and age) influence morbidity and mortality, health outcomes and health inequities are strongly impacted by social determinants, including income, education, housing, and access to healthcare (Fiocruz, 2009). Consequently, some high-risk groups for disease have limited access to treatment and are more likely to become severely ill or die from treatable and even preventable conditions.

Fairness is not a single and universal concept due to subjective interpretations and the different characteristics of the problems addressed (Alem; Caunhye; Moreno, 2022; Béland et al., 2021; Fiocruz, 2009). Bertsimas, Farias and Trichakis (2011) present several approaches to address this challenge in resource allocation problems. These approaches include utilitarian, Rawls, Nash, Kalai–Smorodinsky, *max-min* fairness, and proportional fairness. The authors demonstrate that imposing fairness schemes can reduce utilitarian efficiency relative to an efficiency benchmark, defined as the allocation that maximizes the sum of individual utilities. However, such a solution may be regarded as inequitable by some parties because it is achieved at the expense of some individuals. Thus, relative to this benchmark, they defined the “price of fairness” as the loss in performance that occurs when allocations are made under fairness schemes (*max–min* fairness and proportional fairness).

Most studies address equity using *max-min* fairness and proportional fairness schemes. In this regard, the *max-min* fairness scheme consists of maximizing the lowest benefit among all parties, prioritizing the worst-served (Bertsimas; Farias; Trichakis, 2011; Rastegar et al., 2021). Proportional fairness, on the other hand, seeks fair allocation and assumes that the aggregate proportional change is less than or equal to zero for any other feasible allocation of resources

(Bertsimas; Farias; Trichakis, 2011). The authors showed that for a small number of self-interested parties, the price of fairness remains relatively low. This suggests that in problems with a small number of self-interested parties, the central decision-maker can achieve fair allocations without incurring a large reduction in the sum of utilities. The price of fairness increases significantly with the number of self-interested parties in both schemes. However, the proportional fairness scheme has a considerably lower price compared to the *max-min* fairness scheme.

Table 2 shows the twenty-four studies identified in the literature (see Table 1) that address equity in VSC optimization. Among these works, equity is addressed more often in the VAP than in the VDP. Of the 24 studies, 22 use fairness mechanisms in the allocation stage. Only Sun, Andoh and Yu (2021) and Kheybari et al. (2025) focus on fairness exclusively in the distribution stage. Most papers address equity in the SDE, and all of them focus on epidemic scenarios and disregard routine vaccinations. Additionally, single-objective formulations and mixed-integer linear programming (MILP) are the most commonly used, while the SEIR model is used to capture disease progression in nearly half of the studies.

Regarding fairness schemes, most of the studies are based on a proportional fairness scheme, only Rastegar et al. (2021), Munguía-López and Ponce-Ortega (2021), and Tavana et al. (2021) explicitly use the *max-min* fairness scheme.

The second column shows the terminology employed to describe equity and related concepts. The terms equity, fairness, and equitable allocation are the most common; however, their meanings vary depending on the author's approach. Bertsimas et al. (2020), Buhat et al. (2021), Jarumaneeroj et al. (2022), Kargar et al. (2024), Matrajt, Halloran and Longini (2013), Sun, Andoh and Yu, (2021), Thul and Powell (2023) and Yarmand et al. (2014) use the term "pro rata strategy" to describe the proportional allocation of vaccines between regions. Abbasi et al. (2020), Enayati and Özaltın (2020), Gilani and Sahebi (2022), Minoza, Bongolan and Rayo (2021) and Tavana et al. (2021) prioritize high-risk groups in vaccine allocation. In Roy, Dutta and Ghosh (2021), Rastegar et al. (2021), Fantini (2021), Bertsimas et al. (2022), Rey, Hammad and Saberi (2023), Valizadeh et al. (2023) and Holleran, Martonosi and Veatch (2023), models address equity by combining a guaranteed minimum quantity of vaccines for each region with a residual distribution based on risk groups. Yang et al. (2022) and Mohammadi et al. (2022) refer to equity as the allocation of vaccines to prioritize regions with the greatest potential for preventing future cases.

The third column specifies how equity is included in each model. Most studies incorporate equity via constraints (C), using fairness criteria to define the feasible solution space. Matrajt, Halloran, and Longini Jr. (2013) and Thul and Powell (2023) adopt the "pro rata strategy", which involves multiplying the population size of each region by the vaccination coverage rate. Yarmand et al. (2014) and Tavana et al. (2021) impose a minimum coverage proportional to the regional population. Enayati and Özaltın (2020) consider inequality through the Gini coefficient. Bertsimas et al. (2020) define the minimum share of each region in the daily vaccine quantities based on its population. Buhat et al. (2021) ensure vaccination coverage proportional to the size of the priority group (healthcare workers and older adults) in each region. Roy, Dutta and Ghosh (2021) introduce epidemiological restrictions based on the number of susceptible and infected individuals. Jarumaneeroj et al. (2022) and Rey et al. (2023) explore the potential of regional vaccination capacity as a strategy to address equity questions.

Some studies incorporate equity into the objective function (OF) by treating it as a variable to be minimized or maximized. In this sense, Abbasi et al. (2020) minimize the risk of disease transmission by prioritizing groups and adjusting the exposure coefficient. The authors aim to balance care for at-risk groups by giving greater weight to large populations or those that have a high concentration of individuals in a given area or service point, i.e., regions with high population density. Rastegar et al. (2021) aim to maximize vaccination coverage for the worst-served, ensuring that the most disadvantaged group receives the largest possible fraction of their demand. Fantini (2021) aims to balance accessibility criteria with maximizing the total volume of vaccines distributed. Tavana et al. (2021) aim to minimize the largest deviation between the population-proportional coverage targets, so that no region falls below the minimum required number of vaccines. Mohammadi et al. (2022) aim to minimize the number of deaths and logistical costs, considering uncertainties and analyzing epidemiological priority scenarios. Gilani & Sahebi (2022) aim to minimize inequality in vaccine access through a model based on real regional access data (average travel time, local infrastructure, and distance to vaccination centers). Bertsimas et al. (2022) developed a multi-objective framework in which one of the objectives is to minimize the number of deaths by considering demographic and geographic inequalities (age, comorbidities, and pandemic progression). Munguía-López and Ponce-Ortega (2021) developed different objective functions that represent Rawls's, Nash's, and social welfare justice criteria to maximize equity. According to the authors, the social welfare criterion favors regions with larger populations, resulting in a distribution proportional to the population. Rey et al. (2023) aim to minimize the number of susceptible individuals, infections, and deaths over

time based on the population proportion, vaccine effectiveness, and individual mobility between regions.

Conversely, Matrajt, Halloran and Longini (2013), Sun, Andoh and Yu (2021), Minoza, Bongolan and Rayo (2021), and Yang et al. (2022) incorporate equity through scenario analysis (SA) by evaluating multiple allocation strategies without directly embedding fairness into constraints or objective functions. Matrajt, Halloran and Longini (2013) evaluate a pro-rata strategy that distributes vaccines based on population size and employ a Genetic Algorithm (GA) as a search heuristic to identify population-proportional allocations that balance fairness and minimize the predicted cases and deaths by the model. Sun, Andoh and Yu (2021) use the expected lead time as an equity metric to determine the fleet compositions that yield the most uniform service levels across regions using a simulation model. Minoza, Bongolan and Rayo (2021) integrate a multi-objective linear model with an agent-based SEIR model to test five vaccination-priority scenarios, ranging from no vaccination to targeted schemes for essential workers, the mobile workforce, and the elderly. The authors use two equity indicators (percentage of reduction in infections and percentage of increase in protected individuals) to identify the scenario that promotes more balanced coverage between regions and age groups. Finally, Yang et al. (2022) compare twelve health-oriented allocation scenarios, ranging from an equal pro-rata distribution to various risk-adjusted heuristics, to identify the strategies that would minimize disparities in infection and mortality across regions.

The fourth column presents the metrics used to quantify equity in the models, considering minimum coverage and performance metrics. Minimum coverage metrics ensure that each region or population group receives a minimum number of doses. Specifically, these metrics are implemented in the constraints (C). In turn, performance metrics evaluate the effectiveness of vaccine allocation outcomes and are incorporated either as objective functions (OF) or as part of multi-objective formulations to maximize vaccination coverage and social welfare indices or minimize deaths, lead time, or inequality indices.

Table 2 - Equity policy in VSC

Reference	Terminology	Fairness mechanism	Equity metric	ST/DY
Matrajt, Halloran and Longini (2013)	Fair strategy, equality	*SA*	Attack rate	*ST*
Yarmand et al. (2014)	Equitable allocation, fairness constraint	*C*	Minimum vaccination coverage in all regions	*ST*
Enayati and Özaltın (2020)	Distribution with equity, equity measure	*C*	Inequity tolerance	*ST*
Bertsimas et al. (2020)	Fairness parameter, equitable distribution	*C*	Minimum regional allocation fraction	*ST*
Abbasi et al. (2020)	Equity, equitable allocation of vaccines	*OF*	Weight of vaccination of a person in priority group	*ST*
Buhat et al. (2021)	Equitable allocation of vaccines,	*C*	Minimum coverage for priority groups	*ST*
Sun, Andoh and Yu (2021)	Equitable vaccination, fairness of vaccine distribution	*SA*	Expected Lead Time	*ST*
Roy, Dutta and Ghosh (2021)	Allocate vaccines equitably, fairness condition	*C*	Minimum number of vaccines a region must receive	*ST*
Rastegar et al. (2021)	Equitable vaccine distribution, fair distribution	*OF*	Minimum percentage of group i to be covered	*ST*
Munguía-López and Ponce-Ortega (2021)	Fair Allocation, equitable allocation	*OF*	Social welfare, Nash, Rawlsian justice, social welfare	*ST*
Minoza, Bongolan and Rayo (2021)	Equitable vaccine distribution	*SA*	Priority Factors	*ST*
Fantini (2021)	Accessibility for vaccine allocation, equitable allocation	*OF*	Vulnerability index	*ST*
Tavana et al. (2021)	Equitable vaccine distribution	*OF, C*	Minimum percentage coverage rate for group	*DY*
Yang et al. (2022)	Health-oriented fairness, equal allocation	*SA*	Confirmed infection cases	*ST*
Mohammadi et al. (2022)	Equity of vaccine distribution	*OF*	Total number of deaths	*ST*
Jarumaneeroj et al. (2022)	Unfair allocation strategy, vaccine-access equity	*C*	Proportional to the population size, vaccination capacity	*ST*
Gilani and Sahebi (2022)	Equitable access, fair delivery vaccination	*OF*	Social index	*ST*
Bertsimas et al. (2022)	Fair interstate equity, Fair intercenter equity	*OF, C*	Hyperparameter that controls the trade-off between efficiency and fairness	*DY*
Thul and Powell (2023)	Fairness in allocation, fairness policies	*C*	Percentage of each region's population with access to vaccines	*DY*

Reference	Terminology	Fairness mechanism	Equity metric	ST/DY
Rey, Hammad and Saberi (2023)	Fair and ethical allocation, equitable access to vaccines	*OF, C*	Weight of infections and vaccination capacity	*DY*
Valizadeh et al. (2023)	Risk of inequality in the distribution of the vaccine, fair distribution	*OF, C*	Risk of inequality, risk of mortality	*ST*
Holleran, Martonosi and Veatch (2023)	Vaccine willingness, equitable distribution of Vaccines	*C*	Trade-off between self-interest and altruism, proportion of the population willing to be vaccinated	*DY*
Kargar et al. (2024)	Equitable distribution of vaccines, fairness considerations	*C*	Each region has at least one distribution center, vaccine acceptance rate	*ST*
Kheybari et al. (2025)	Fairness, equitable access	*OF, C*	Full coverage by distance	*ST*
This work	Equitable allocation of vaccines	*C*	Proportional to the population size, proportional to the population weighted by the Social Vulnerability Index (IVS)	*DY*

Note: SA: Scenario Analysis, C: Constraint, OF: Objective Function, DY: Dynamic, ST: Static.

Of the twenty-three studies, while Enayati and Özaltın (2020) use the Gini coefficient to directly measure socioeconomic inequalities, both Fantini (2021), with a vulnerability index, and Gilani & Sahebi (2022), with a social index, also include social vulnerability metrics. Kargar et al. (2024) and Holleran, Martonosi and Veatch (2023) incorporate vaccine hesitancy and willingness into their models, respectively. In turn, Jarumaneeroj et al. (2022) and Rey, Hammad and Saberi (2023) considered the vaccination capacity of regions to be the most important factor in fair vaccine allocation. These authors assume that, besides sending enough vaccines, it is necessary to ensure that the vaccines can be administered.

Most studies that incorporate SEIRS into their formulations recognize that minimizing cases or deaths only objective may produce inequitable solutions i.e., allocations in which some regions receive no vaccines. Accordingly, equity criteria are incorporated to guarantee access for vulnerable regions and high-risk groups. However, Bertsimas et al. (2020), Enayati and Özaltın (2020), Holleran, Martonosi and Veatch (2023), Minoza, Bongolan and Rayo (2021) recognize the trade-off between reducing cases or deaths and limiting inequalities. A common approach to addressing this challenge is to ensure minimum allocation by establishing a minimum number of doses that all regions must receive based on their population size, such as Bertsimas et al. (2020), Jarumaneeroj et al. (2022), Roy, Dutta and Ghosh (2021) and Yarmand et al. (2014), and then allocate additional doses using the equity metric employed in each work.

Equity can be addressed considering time-varying interactions (dynamic models) or without considering it (static models) (fifth column). In static models, the equity criteria remain with the values unchanged throughout the decision horizon. While this facilitates communication with decision-makers, it fails to incorporate evolving epidemiological conditions. In contrast, dynamic models recalculate and update equity criteria based on novel information, such as changes in risk levels, vaccination rates, or individuals' willingness to be vaccinated. Of the twenty-three studies, eighteen adopt a static formulation (ST). Conversely, five employ a dynamic (DY) approach, recalculating and updating their equity criteria as the epidemic progresses. Tavana et al. (2021) periodically re-evaluate minimum coverage. Bertsimas et al. (2020) apply the DELPHI-V model to successive optimization horizons. Thul and Powell (2023) sequentially adapt allocations under uncertainty. Holleran, Martonosi, and Veatch (2023) redistribute doses donated by higher-income countries to recipient countries to anticipate emerging variants. Rey, Hammad, and Saberi (2023) adjust allocation policies based on new observations (updated data on deaths and infections).

In this study, the terminology "equitable allocation of vaccines" was used to denote fairness in the allocation stage, ensuring equitable access to vaccines while minimizing deaths. Equity is addressed through constraints in the mathematical model using two equity policies: (1) proportional to the population size, and (2) proportional to the population weighted by the Social Vulnerability Index (IVS, from the Portuguese acronym for Índice de Vulnerabilidade Social) (IPEA, 2025). The first equity policy allocates doses proportional to each region's population, while the second policy, besides addressing the population proportion, also incorporate the social vulnerability of regions. Finally, a dynamic model was used to incorporate changes associated with the epidemiological characteristics of diseases and the consequent necessary adjustments in the allocation and distribution of vaccines over time.

3 METHODS

This chapter describes the problem addressed and proposes an approach to jointly address the Vaccine Allocation and Distribution Problems. First, the Vaccine Allocation Problem (VAP) addresses the allocation of a variety of emergency and routine vaccines. The Vaccine Distribution Problem (VDP) is then carried out to ensure the distribution of the allocated vaccines in the vaccine supply chain.

3.1. Problem Description

Vaccines are divided into emergency and routine vaccines. Emergency vaccines control highly contagious outbreaks and require rapid and widespread distribution, such as in epidemic situations. Routine vaccines protect against common and predictable diseases as part of regular immunization schedules indicated for specific populations. Conversely, emergency vaccines are recommended for use in the general population or specific exposed or compromised groups. The availability of emergency vaccines may initially be limited if the vaccine has not been developed or produced (Ndeffo Mbah et al., 2014), as was the case with Covid-19. In contrast, routine vaccines have a more stable and predictable supply, influenced mainly by demographic changes and management decisions (Chen et al., 2014).

Each country must determine the routine and emergency vaccines to include in its immunization plan to face specific situations in a region or in the entire country. The types and quantities of vaccines in the immunization plans are based on different epidemiological profiles and resource constraints and vary significantly from country to country. For example, while Brazil incorporates 31 vaccines into its immunization schedule (Brazil, 2021), Haiti administers 12 vaccines (WHO, 2023b).

Countries also must develop methods to generate these storage and distribution tactical plans in alignment with their public health policies. These policies define the set of routine vaccines included in the national immunization program, as well as their target coverage levels by age group. They also define emergency vaccine requirements based on the epidemiological dynamics of the disease and demand during outbreaks (OPAS, 2023).

Tactical planning determines the allocation and distribution of vaccines within the Storage and Distribution echelon of the VSCs. This echelon uses central, regional, and local warehouses (see Figure 3). In vaccine allocation, different methods should be used to estimate the amount of routine and emergency vaccines that should be available in regional and local warehouses.

Routine vaccines are estimated based on specific population coverage targets, while emergency vaccines are estimated based on the number of available doses at the time of planning. We assume that the estimated vaccines are available at a central warehouse on the first day of the planning horizon. From there, they are distributed to regional warehouses, which then distribute them to their associated local warehouses.

Figure 3 - Storage and Distribution echelon flow

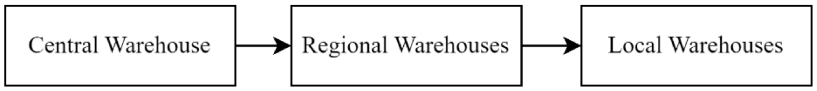

Immunization plans must be adaptable to face the constant re-evaluation required (tactical decision). In this sense, developing an approach to systematically allocate and distribute vaccines that is flexible enough to accommodate different routine and emergency vaccines in a variety of demand scenarios is essential. Tactical planning in the Storage and Distribution echelon may consider the entire echelon (including central, regional, and local warehouses) or any subset of the echelon (central and regional warehouses and regional and local warehouses).

To address this challenge, we present a novel approach that combines allocation and distribution decisions, jointly solving the VAP and the VDP. This approach determines the quantity of vaccines for each site and defines the logistics for distribution. The details of this approach are presented in Section 3.2.

3.2. Vaccine Allocation and Distribution Problem

The immunization planning must contain vaccination strategies for the joint allocation and distribution of routine vaccines and, if necessary, emergency vaccines in the Storage and Distribution echelon of VSCs. At this echelon, vaccines should be allocated and distributed from the central warehouse to regional warehouses, and then from regional warehouses to local warehouses. Figure 4 presents the schematic diagram for the Vaccine Allocation and Distribution Problem addressed in this study.

Figure 4 - Vaccine Allocation and Distribution Problem

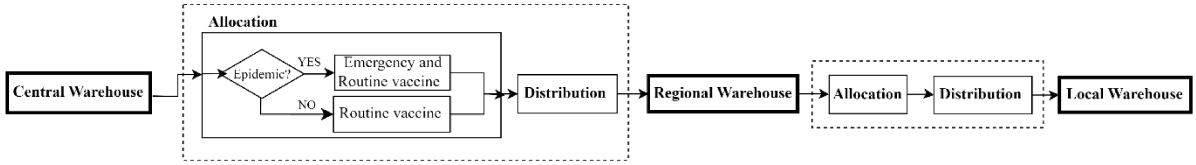

Initially, emergency and routine vaccines are selected to be included in the immunization plan, i.e., the immunization plan is designed for both epidemic and non-epidemic scenarios. In epidemic situations, emergency and routine vaccines are administered, while in non-epidemic situations, only routine vaccines are included. Once the vaccines for the immunization plan have been selected, it is necessary to employ different methods to allocate emergency and routine vaccines.

In the allocation phase, we separately address the Emergency Vaccine Allocation Problem using a non-linear mathematical model and an iterative solution technique (Section 3.2.1) and the Routine Vaccine Allocation Problem (Section 3.2.2) to allocate vaccines from the central warehouse to the regional warehouses. As a result, this phase provides the quantities of each emergency and routine vaccine allocated to each regional warehouse, balancing public health requirements with available supply based on the epidemiological scenario and vaccine coverage. Following allocation, vaccines are distributed to the regional warehouses using a distribution model (Section 3.2.3).

Subsequently, each regional warehouse must allocate vaccines to the associated local warehouses. In contrast to the previous allocation from central to regional warehouses, the allocation of emergency vaccines from regional to local warehouses is now proportional to the population size of each local warehouse. The change in emergency vaccine allocation was necessary due to the lack of detailed epidemiological data on the populations served by each local warehouse. On the other hand, routine vaccines are also allocated from regional warehouses to local ones, as described in Section 3.2.2. The allocation of vaccines in each regional warehouse is carried out independently of the other regional warehouses. Finally, vaccines are then distributed from each regional warehouse to the associated local warehouses using the same distribution model (Section 3.2.3).

3.2.1. Emergency vaccine allocation problem

To address the emergency vaccine allocation problem, we developed our model to operate independently for each type of emergency vaccine. In this case, the model must be run separately

for each vaccine, ensuring that the epidemiological characteristics of each epidemic are adequately addressed. To do this, we formulate an SEIRS-based nonlinear model. Our formulation embeds the SEIRS model (Figure 5) in an optimization model to address the infectious disease dynamics.

The SEIRS model is a compartmental epidemic modeling introduced by Cooke and Van Den Driessche (1996) as an extension of the SEIR (susceptible-exposed-infected-recovered). These models are based on the SIR (susceptible-infected-recovered) framework developed by Kermack and McKendrick (1927). The SEIRS model is governed by a system of ordinary differential equations, and a SEIRS formulation can be found in McGee (2020).

Figure 5 - Susceptible-exposed-infected-recovered-susceptible diagram

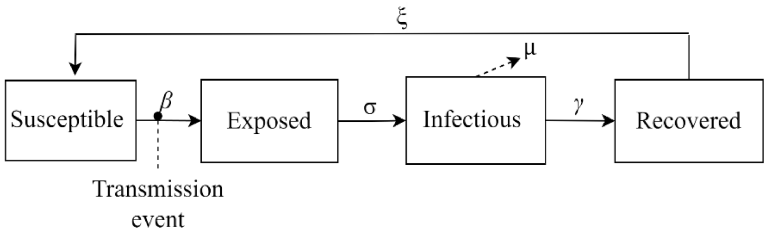

For each vaccine, the model requires the initial values of the transmissibility rate (β_{0l}), infection rate (σ_{0l}), recovered rate (γ_{0l}), ressusceptibility rate (ξ_{0l}), mortality rate (μ_{0l}) and historical data on infection cases, vaccination records, and the available quantities of vaccines. A calibration process (Section 3.2.1.2) was carried out to obtain the initial values of the SEIRS rates ($\beta_{0l}, \sigma_{0l}, \gamma_{0l}, \mu_{0l},$ and ξ_{0l}). Therefore, $\beta_{0l}, \sigma_{0l}, \gamma_{0l}, \mu_{0l}$ and ξ_{0l} are model parameters, while $\beta_{dl}, \sigma_{dl}, \gamma_{dl}, \mu_{dl}$ and ξ_{dl} are variables. As output, the model defines the quantity of vaccines that will be destined to location l on day d (v_{dl}^{c}). We define the sets, parameters, and decision variables.

Sets

L	Set of locations l
D	Set of days d

Parameters

φ_l	Vaccine storage efficiency rate in location l (%)
$\eta^{\blacksquare}$	Effect on vaccine-related ■ rate ($\beta, \sigma, \gamma, \xi, \mu$) (%)
η^{dist}	Effect of distancing on the transmissibility rate (%)

t	Time (continuous) (days)
Δt	Time interval used in the discretization of the differential equations
S_l'	Initial number of susceptible in location l
E_l'	Initial number of exposed in location l
I_l'	Initial number of infected in location l
R_l'	Initial number of recovered in location l
F_l'	Initial number of deaths in location l
V_d	Total vaccines available per day in location l
T_l	Vaccine delivery time in location l
M_l	Maximum vaccination capacity in location l
V_{dl}^{sMax}	Maximum vaccines stored capacity in location l
N_l^T	Total number of individuals in location l
β_{0l}	Initial transmissibility rate in location l (%)
σ_{0l}	Initial infection rate in location l (%)
γ_{0l}	Initial recovered rate in location l (%)
ξ_{0l}	Initial ressusceptibility rate in location l (%)
μ_{dl}	Initial mortality rate in location l (%)
Variables	
β_{dl}	Transmissibility rate on day d in location l (%)
σ_{dl}	Infection rate on day d in location l (%)
γ_{dl}	Recovered rate on day d in location l (%)
ξ_{dl}	Ressusceptibility rate on day d in location l (%)
μ_{dl}	Mortality rate on day d in location l (%)
α_{dl}	Percentage of vaccines that will be destinated to location l on day d (%)
v_{dl}^c	Number of vaccines that will be destinated to location l on day d
v_{dl}^a	Number of vaccines administered in location l on day d
v_{dl}^s	Number of vaccines stored in location l on day d
n_{dl}^{vc}	Number of people vaccinated in location l on day d
f_{dl}	Number of deaths in location l on day d
s_{dl}	Number of people susceptible in location l on day d
e_{dl}	Number of people exposed in location l on day d
i_{dl}	Number of people infected in location l on day d

r_{dl} Number of people recovered in location l on day d

The emergency vaccine allocation is then formulated in Equations (1)-(22).

$$min \sum_{d} \sum_{l} f_{dl} \tag{1}$$

$$\frac{\partial s_{dl}}{\partial t} = -\frac{\eta^{dist} \beta_{dl} s_{dl} i_{dl}}{N_l^T} + \xi_{dl} r_{dl} \qquad \forall d, \forall l \tag{2}$$

$$\frac{\partial e_{dl}}{\partial t} = \frac{\eta^{dist} \beta_{dl} s_{dl} i_{dl}}{N_l^T} - \sigma_{dl} e_{dl} \qquad \forall d, \forall l \tag{3}$$

$$\frac{\partial i_{dl}}{\partial t} = \sigma_{dl} e_{dl} - \gamma_{dl} i_{dl} - \mu_{dl} i_{dl} \qquad \forall d, \forall l \tag{4}$$

$$\frac{\partial r_{dl}}{\partial t} = \gamma_{dl} i_{dl} - \xi_{dl} r_{dl} \qquad \forall d, \forall l \tag{5}$$

$$\frac{\partial f_{dl}}{\partial t} = \mu_{dl} i_{dl} \qquad \forall d, \forall l \tag{6}$$

$$N_l^T = s_{dl} + e_{dl} + i_{dl} + r_{dl} - f_{dl} \qquad \forall d, \forall l \tag{7}$$

$$s_{0l} = S_l', e_{0l} = E_l', i_{0l} = I_l', r_{0l} = R_l', f_{0l} = F_l' \qquad \forall l \tag{8}$$

$$v_{dl}^c = \alpha_{(d-T_l),l} V_{(d-T_l)} \qquad \forall d, \forall l \tag{9}$$

$$\sum_{l} \alpha_{dl} = 1 \qquad \forall d, \forall l \tag{10}$$

$$v_{dl}^a \leq min\left(v_{d-1,l}^s, M_l\right) \qquad \forall d, \forall l \tag{11}$$

$$n_{dl}^{vc} = n_{(d-1),l}^{vc} + v_{dl}^a \qquad \forall d, \forall l \tag{12}$$

$$n_{dl}^{vc} \leq N_l^T - f_{dl} \qquad \forall d, \forall l \tag{13}$$

$$v_{dl}^s = \varphi_l v_{(d-1),l}^s + v_{dl}^c - v_{dl}^a \qquad \forall d, \forall l \tag{14}$$

$$v_{dl}^s \leq V_{dl}^{sMax} \qquad \forall d, \forall l \tag{15}$$

$$\beta_{dl} = \beta_{0l}(1 - n_{dl}^{vc}/N_l^T) + \beta_{0l} \eta^{\beta} n_{dl}^{vc}/N_l^T \qquad \forall d, \forall l \tag{16}$$

$$\sigma_{dl} = \sigma_{0l}(1 - n_{dl}^{vc}/N_l^T) + \sigma_{0l} \eta^{\sigma} n_{dl}^{vc}/N_l^T \qquad \forall d, \forall l \tag{17}$$

$$\gamma_{dl} = \gamma_{0l}(1 - n_{dl}^{vc}/N_l^T) + \gamma_{0l}\eta^{\gamma} n_{dl}^{vc}/N_l^T \qquad \forall d, \forall l \qquad (18)$$

$$\mu_{dl} = \mu_{0l}(1 - n_{dl}^{vc}/N_l^T) + \mu_{0l}\eta^{\mu} n_{dl}^{vc}/N_l^T \qquad \forall d, \forall l \qquad (19)$$

$$\xi_{dl} = \xi_{0l}(1 - n_{dl}^{vc}/N_l^T) + \xi_{0l}\eta^{\xi} n_{dl}^{vc}/N_l^T \qquad \forall d, \forall l \qquad (20)$$

$$\beta_{dl}, \sigma_{dl}, \gamma_{dl}, \mu_{dl}, \xi_{dl}, \alpha_{dl} \in \mathbb{R}_{[0,1]} \qquad \forall d, \forall l \qquad (21)$$

$$v_{dl}^{c}, v_{dl}^{a}, v_{dl}^{s}, n_{dl}^{vc}, f_{dl}, s_{dl}, e_{dl}, i_{dl,} r_{dl} \in \mathbb{Z}^{+} \qquad \forall d, \forall l \qquad (22)$$

The objective (1) is to minimize the number of deaths. Equations (2)-(6) are used to estimate the number of susceptible, exposed, infected, recovered, and dead individuals and are based on the SEIRS model presented by McGee (2020). However, our formulation incorporates the effect of social distancing (η^{dist}) when calculating the number of susceptible and infected individuals (Equations (2)-(3)). The virus transmission rate (β_{dl}) is important in determining how quickly the disease can spread through the population during the early stages. Its estimation is inherently challenging because reported cases are likely to be a smaller fraction of the real cases (Paes; Ferreira; Moura, 2023), and the real number of cases and their changes over time are unknown. In this thesis, β_{dl} is estimated using the calibration process described in Section 3.2.1.2. The total population is obtained from Equation (7). The set of equations in (8) represents the initial number of susceptible, exposed, infected, recovered, and dead individuals. Equation (9) shows that the amount of vaccine at the localities depends on the amount sent out T_l days ago. Equation (10) ensures that all vaccines are allocated. Constraint (11) guarantees that the quantity of vaccine administered does not exceed the minimum value between the available stock and the vaccination capacity. Equation (12) shows that the number of individuals vaccinated until the day is equal to the number of individuals vaccinated on the previous day plus the number of vaccines administered on the day. Constraint (13) guarantees that the vaccinated population is smaller than the living population. Inventory constraints (14)-(15) ensure that the inventory respects the storage capacity. Equations (16)-(20) represent the effect of vaccination on transmissibility, infection, recovered, deaths, and ressusceptibility rates based on the percentage of the population vaccinated. The effect of the vaccine is on the total vaccinated population. Therefore, vaccines administered in one day generate a prolonged effect of reducing infections and deaths. Finally, Constraints (21)-(22) represent the domain of variables.

As the constraints associated with the SEIRS model are non-linear (Equations (2)-(6)), the proposed model (Equations (1)-(22)) is a non-linear mathematical model. Solving this model

involves addressing a combination of discrete decisions that evolve over time and differential equations. To test this model, we use a scenario based on the Brazilian National System, considering the allocation and distribution from the central to the regional warehouses. This scenario achieved 15,394 constraints and 16,849 variables (13,609 continuous and 3,240 integer variables). The Gurobi 10.0 solver (Gurobi, 2025) was not able to solve it with a 10-hour time limit (36,000 s), even using a relaxed version of the model, removing the integrality constraint (linear relaxation). Therefore, we developed an iterative solution technique to enable its solution in a reasonable processing time.

3.2.1.1. Iterative solution technique

To solve the emergency vaccine allocation problem, we developed an iterative solution technique that combines an epidemiological SEIRS model with a mathematical programming model.

In an epidemic scenario, using existing data to project long-term epidemic trends is not recommended (Zhang; Long; Li, 2023). Then, we run the model for different time buckets, allowing us to make short-term forecasts as the model parameters are readjusted with updated data. For each time bucket, the model specifies the initial day, the last day of the time bucket, and the days corresponding to the decision horizon.

Within each time bucket, the solution technique alternates between two stages: **(1) Simulation Stage:** simulate the dynamics of the epidemic for a given vaccine allocation, and **(2) Optimizing Stage:** Optimize the vaccine allocation given the projected dynamics of infections and deaths. The optimization stage is reduced to a mixed integer linear programming (MILP) model. Using the resulting vaccine allocation, the simulation stage re-estimates the infected population and the number of deaths. We iterate between the Simulation and Optimization stages until the tolerance level (ε) for the percentage deviation in the number of deaths between the stages is reached. The next time bucket is then initialized, and the whole process (Simulation Stage and Optimizing Stage) is repeated. This procedure continues until the end of the epidemic. The flowchart of the iterative solution technique is shown in Figure 6.

Figure 6 - Iterative solution technique

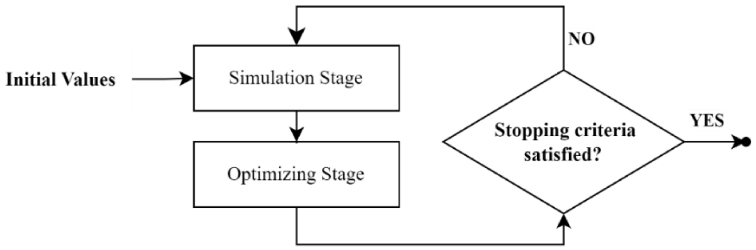

In the first run of the simulation stage, initial parameters are defined based on available data (Initial Values). Section 3.2.1.2 describes the calibration process used to estimate the initial SEIRS rate parameters ($\beta_{0l}, \sigma_{0l}, \gamma_{0l}, \mu_{0l}$, and ξ_{0l}). Then, the simulation stage is solved for each location using these initial conditions and without the influence of the optimization stage.

Simulation Stage: Equations (23)-(29), adapted from the SEIRS formulation presented by McGee (2020), are used to estimate the number of infected people ($\hat{\imath}_{dl}$) considering the vaccine allocation offered by the optimization stage. The rates of transmission (β_{dl}), infection (σ_{dl}), recovery (γ_{dl}), ressusceptibility (ξ_{dl}) and mortality (μ_{dl}) are variables of the model described by Equations (1)-(22); however, using the iterative solution technique, these rates are parameters used in the model (23)-(29) and calculated at each step using (31)-(47). To indicate that the rates are decision variables in the optimization stage, and parameters in the simulation stage, we use $\beta_{dl}, \sigma_{dl}, \gamma_{dl}, \mu_{dl}$ and ξ_{dl} and $\bar{\beta}_{dl}, \bar{\sigma}_{dl}, \bar{\gamma}_{dl}, \bar{\mu}_{dl}$ and $\bar{\xi}_{dl}$, respectively.

$$\frac{\partial s_{dl}}{\partial t} = -\frac{\eta^{dist}\bar{\beta}_{dl}s_{dl}i_{dl}}{N_l^T} + \bar{\xi}_{dl}r_{dl} \qquad \forall d, \forall l \qquad (23)$$

$$\frac{\partial e_{dl}}{\partial t} = \frac{\eta^{dist}\bar{\beta}_{dl}s_{dl}i_{dl}}{N_l^T} - \bar{\sigma}_{dl}e_{dl} \qquad \forall d, \forall l \qquad (24)$$

$$\frac{\partial i_{dl}}{\partial t} = \bar{\sigma}_{dl}e_{dl} - \bar{\gamma}_{dl}i_{dl} - \bar{\mu}_{dl}i_{dl} \qquad \forall d, \forall l \qquad (25)$$

$$\frac{\partial r_{dl}}{\partial t} = \bar{\gamma}_{dl}i_{dl} - \bar{\xi}_{dl}r_{dl} \qquad \forall d, \forall l \qquad (26)$$

$$\frac{\partial f_{dl}}{\partial t} = \bar{\mu}_{dl}i_{dl} \qquad \forall d, \forall l \qquad (27)$$

$$N_l^T = s_{dl} + e_{dl} + i_{dl} + r_{dl} - f_{dl} \qquad \forall d, \forall l \qquad (28)$$

$$s_{0l} = S_l', e_{0l} = E_l', i_{0l} = I_l', r_{0l} = R_l', f_{0l} = F_l' \qquad \forall l \qquad (29)$$

The SEIRS model (Simulation Stage) is governed by a system of ordinary differential equations (Equations (23)-(29)) that are used to estimate the number of susceptible, exposed, infected, recovered, and dead individuals. As noted previously, this formulation was based on McGee (2020) and introduced the effect of social distancing (η^{dist}) into the calculation of the number of susceptible and infected individuals (Equations ((23)-(24)).

The number of deaths at this stage (d_SIM) is defined in Equation (30).

$$d\_SIM = \sum_d \sum_l f_{dl} \qquad (30)$$

Optimizing Stage: Given the estimated infections in the simulation stage ($\hat{\imath}_{dl}$), the vaccine allocation problem is solved, providing the vaccine allocation that minimizes the number of deaths. Equations (31)-(48) represent the MILP model.

$$min \sum_d \sum_l f_{dl} \qquad (31)$$

$$\frac{f_{dl} - f_{(d-1),l}}{\Delta t} = \mu_{dl} \hat{\imath}_{dl} \qquad \forall d, \forall l \qquad (32)$$

$$f_{dl} \leq N_l^T \qquad \forall d, \forall l \qquad (33)$$

$$v_{dl}^c = \alpha_{(d-T_l),l} V_{(d-T_l)} \qquad \forall d, \forall l \qquad (34)$$

$$\sum_l \alpha_{d,l} = 1 \qquad \forall d, \forall l \qquad (35)$$

$$v_{dl}^a \leq \min\left(v_{d-1,l}^s, M_l\right) \qquad \forall d, \forall l \qquad (36)$$

$$n_{dl}^{vc} = n_{(d-1),l}^{vc} + v_{dl}^a \qquad \forall d, \forall l \qquad (37)$$

$$n_{dl}^{vc} \leq N_l^T - f_{dl} \qquad \forall d, \forall l \qquad (38)$$

$$v_{dl}^{s} = \varphi v_{(d-1),l}^{s} + v_{dl}^{c} - v_{dl}^{a} \qquad \forall d, \forall l \qquad (39)$$

$$v_{dl}^{s} \leq V_{dl}^{sMax} \qquad \forall d, \forall l \qquad (40)$$

$$\beta_{dl} = \beta_{0l}(1 - n_{dl}^{vc}/N_l^T) + \beta_{0l}\eta^{\beta} n_{dl}^{vc}/N_l^T \qquad \forall d, \forall l \qquad (41)$$

$$\sigma_{dl} = \sigma_{0l}(1 - n_{dl}^{vc}/N_l^T) + \sigma_{0l}\eta^{\sigma} n_{dl}^{vc}/N_l^T \qquad \forall d, \forall l \qquad (42)$$

$$\gamma_{dl} = \gamma_{0l}(1 - n_{dl}^{vc}/N_l^T) + \gamma_{0l}\eta^{\gamma} n_{dl}^{vc}/N_l^T \qquad \forall d, \forall l \qquad (43)$$

$$\mu_{dl} = \mu_{0l}(1 - n_{dl}^{vc}/N_l^T) + \mu_{0l}\eta^{\mu} n_{dl}^{vc}/N_l^T \qquad \forall d, \forall l \qquad (44)$$

$$\xi_{dl} = \xi_{0l}(1 - n_{dl}^{vc}/N_l^T) + \xi_{0l}\eta^{\xi} n_{dl}^{vc}/N_l^T \qquad \forall d, \forall l \qquad (45)$$

$$\mu_{dl}\hat{\imath}_{dl} \leq \mu_{wdl}\hat{\imath}_{wdl} \qquad \forall d, \forall l, \forall w \qquad (46)$$

$$n_{dl}^{vc} \in \mathbb{Z}^{+} \qquad \forall d, \forall l \qquad (47)$$

$$\beta_{dl}, \sigma_{dl}, \gamma_{dl}, \mu_{dl}, \xi_{dl}, \alpha_{dl} \in \mathbb{R}_{[0,1]} \qquad \forall d, \forall l \qquad (48)$$

The objective function (31) minimizes the number of deaths. Equation (32) estimates the number of deaths and Constraint (33) guarantees that the number of deaths is less than or equal to the living population. Constraints (34)-(45) of this stage (Optimizing Stage) correspond to Equations (9)-(20). Constraint (46) avoids vaccine allocations with the same number of deaths, which improves model convergence. Constraints (47)-(48) represent the domain of variables.

The number of deaths estimated at the Optimization Stage (d_OPT) is defined in the Equation (49).

$$d\_OPT = \sum_{d}\sum_{l} f_{dl} \qquad (49)$$

We iterate between the Simulation and Optimization stages until the percentage deviation in the number of deaths between the stages is lower than the specified tolerance level (ε); otherwise, the process continues to the next iteration. The percentage deviation between the Optimizing and Simulation stages is measured using Equation (50).

$$\frac{d\_OPT - d\_SIM}{d\_SIM} \leq \varepsilon \qquad (50)$$

Upon reaching the tolerance level, the quantity of emergency vaccines for each state (v_{dl}^{c}) is an input for the subsequent procedure in the integrated framework (Figure 4), the distribution of vaccines.

The Iterative Solution Technique was implemented in Python (Python, 2025) to enable interaction between the Simulation Stage and the Optimization Stage. The Simulation Stage used the Initial Value Problem (solve_ivp) numerical solver from the SciPy library (SciPy, 2025) to solve the system of ordinary differential equations and obtain the number of people susceptible (s_{dl}), exposed (e_{dl}), infected ($\hat{\imath}_{dl}$), and recovered (r_{dl}). The number of infected ($\hat{\imath}_{dl}$), obtained in the Simulation Stage, is used as a parameter in the Optimization Stage (Equations (31)-(48)) which is solved with Gurobi solver (Gurobi, 2025) to determine vaccine allocation.

To test this technique, we use a scenario based on the allocation from the central warehouse to regional warehouses in the Brazilian National System (see detailed description in Section 4). This scenario achieved 8,941 constraints and 8,101 variables (7,291 continuous and 810 integer variables). The model is solved in 19 seconds, confirming the efficiency of the proposed technique.

3.2.1.2. Parameters Calibration

In the SEIRS model, calibration is a fundamental process to adjust the theoretical parameters to the observed conditions. In this work, we calibrated the parameters using data on infection cases, deaths, and vaccination to estimate the epidemiological parameters of transmissibility (β_{0l}), infection (σ_{0l}), recovery (γ_{0l}), mortality (μ_{0l}), and reinfection (ξ_{0l}) rates for the Covid-19 and Influenza epidemics. The calibration processes for these parameters were previously reported in Araújo et al. (2023) and Araújo et al. (2024), and are summarized below.

To use the SEIRS model in our work and the available data, we assume all individuals in the region have the same epidemiological parameters and are equally likely to interact with all other individuals. The model also assumes that the population is evenly distributed across a geographic area of the region, although urban centers with a higher concentration of population may have a higher probability of infection than areas with a smaller number of people.

For the Covid-19 epidemic, we use daily historical data from each Brazilian state for the number of cases (infections), deaths (absolute number of deaths), and number of vaccinated individuals

available at https://github.com/wcota/covid19br, which aggregates data from at least two sources: the Ministry of Health and Brasil.IO. Previous works use the same data source in their analysis (see, for example, Aragão et al., 2022; Araújo et al., 2023; Badr et al., 2023; Cassão et al., 2023; De Almeida et al., 2022). We used data from 18 January 2021 to 14 November 2021 from the 26 Brazilian states and the Federal District (DF) to calibrate the parameter of the SEIRS model for Covid-19 (Figure 7 and Figure 8).

Figure 7- Infections by Covid-19 in Brazil

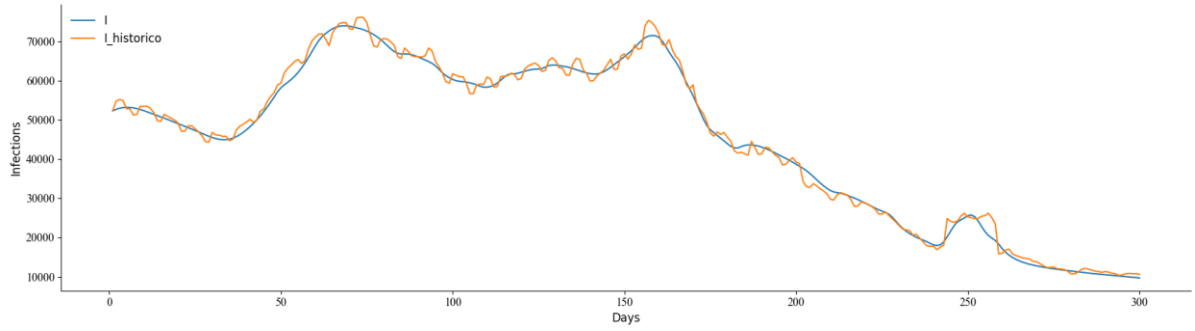

Figure 8 - Deaths by Covid-19 in Brazil

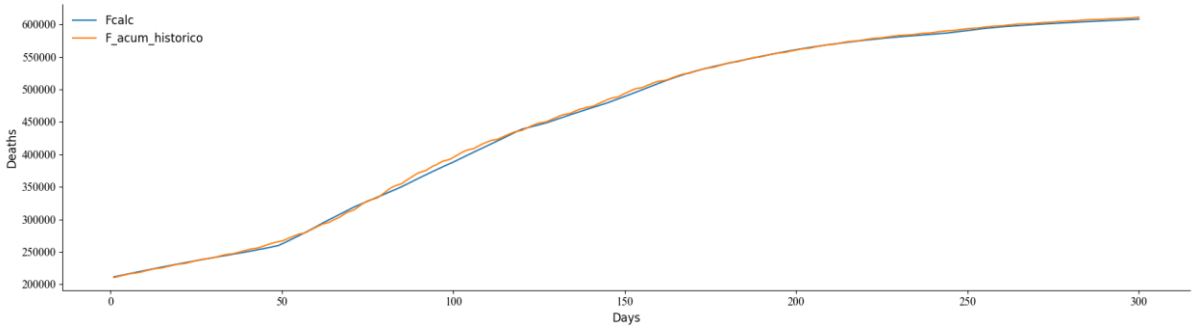

The infection and death curves for all 27 Brazilian states are presented in detail in Araújo et al. (2023). This paper estimated curves for three possible scenarios of vaccination programs and non-pharmaceutical interventions (NPIs) in 819 days of the Covid-19 epidemic (from March 8, 2020, to June 5, 2022).

For the influenza epidemic (H1N1), we use data from March 2010 to November 2010 from the 26 Brazilian states and the Federal District (DF) for the number of cases (infections), deaths (absolute number of deaths), and number of vaccinated individuals available at the official database of the Brazilian health system (see https://opendatasus.saude.gov.br/dataset/srag-2009-2012). Figure 9 and Figure 10 show the estimates of the cases of infection and deaths caused by influenza in Brazil.

Figure 9 - Infections by Influenza in Brazil

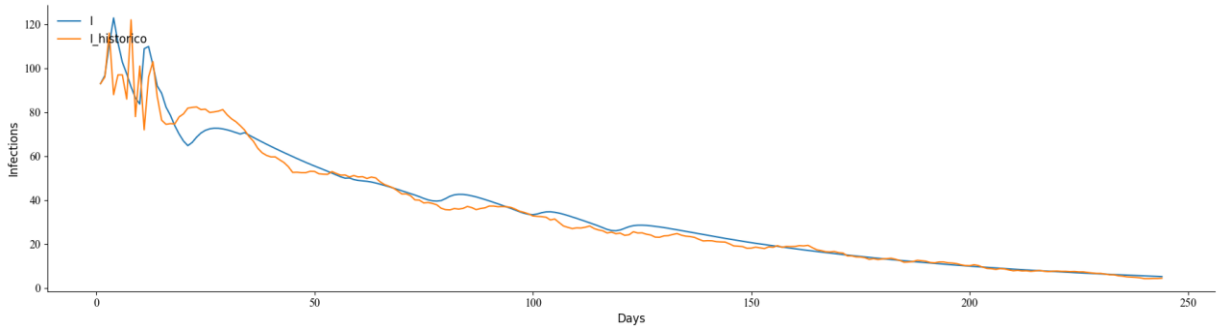

Figure 10 - Deaths by Influenza in Brazil

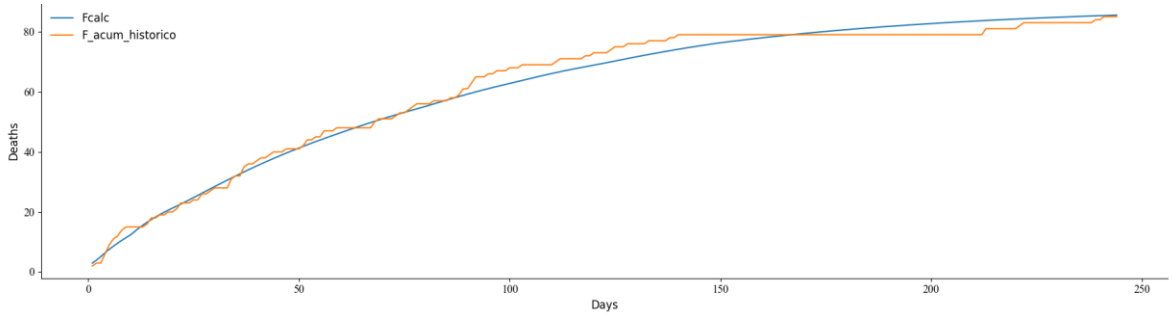

After obtaining the disease-specific parameters (β_{0l}, σ_{0l}, γ_{0l}, μ_{0l}, and ξ_{0l}) in the calibration process for Covid-19 and Influenza, these parameters are used as Initial Values in the a SEIRS-based nonlinear model described in Section 3.2.1 and in the Simulation Stage of the Iterative Solution Technique (Section 3.2.1.1).

The calibration process must be performed separately for each disease, in our case Covid-19 and Influenza, and may be revised or adjusted as new data becomes available. In addition, the model is flexible for use in a variety of epidemiological scenarios, as it can be calibrated to represent the behavior of different diseases over time.

3.2.1.3. Equity Policies

The emergency vaccine allocation problem addressed previously incorporates the epidemiological behavior of diseases using an efficiency-oriented SEIRS-based nonlinear model and an iterative solution technique. Although the objective of both models (nonlinear and iterative solution technique) is to minimize the number of deaths, immunization plans must also consider equity policies.

The incorporation of equity imposes fairness constraints that restrict the feasible solution set, which may redirect doses across regions in ways that do not minimize national deaths. This can be interpreted as a price of fairness (Bertsimas; Farias; Trichakis, 2011). Conversely, these policies prioritize social objectives by mitigating disparities associated with economic conditions, regional development, and inequitable access to health services.

In countries with extensive geographical areas, the health conditions and access of each region can vary considerably. This highlights the necessity for implementing equity policies, ensuring that regions with sparse populations and limited access to healthcare are not disadvantaged compared to areas with larger populations, greater access to healthcare, and improved infrastructure.

As previously presented in Section 2.2.1, equity in VSC can be addressed either in the objective function or through constraints. In this work, we propose two distinct equity policies to be incorporated as constraints in the emergency vaccine allocation problem, in both the nonlinear model and the iterative solution technique.

The equity constraints (Equations (51) and (52)) incorporate the proportion of the population by ensuring the difference between the allocation of vaccines between each pair of regional warehouses is smaller than an established tolerance (ψ). Additionally, Equation (52) also incorporates the IVS by weighting the population using the IVS values. By using the IVS as a criterion for prioritizing vaccine allocation, we prioritize economically vulnerable regions with inadequate infrastructure and restricted access to healthcare. Other equity policies can be incorporated accordingly.

$$\frac{\left(\sum_d V_d\left(\frac{N_l^T}{\sum_{\bar{l}\in L} N_{\bar{l}}^T}\right) - v_{dl}^c\right)}{\sum_d V_d\left(\frac{N_l^T}{\sum_{\bar{l}\in L} N_{\bar{l}}^T}\right)} - \frac{\left(\sum_d V_d\left(\frac{N_{l`}^T}{\sum_{\bar{l}\in L} N_{\bar{l}}^T}\right) - v_{dl`}^c\right)}{\sum_d V_d\left(\frac{N_{l`}^T}{\sum_{\bar{l}\in L} N_{\bar{l}}^T}\right)} \leq \psi \qquad \forall (l, l`) \in (L\ x\ L) \qquad (51)$$

$$\frac{\left(\sum_d V_d\left(\frac{\theta_l N_l^T}{\sum_{\bar{l}\in L} \theta_{\bar{l}} N_{\bar{l}}^T}\right) - v_{dl}^c\right)}{\sum_d V_d\left(\frac{\theta_l N_l^T}{\sum_{\bar{l}\in L} \theta_{\bar{l}} N_{\bar{l}}^T}\right)} - \frac{\left(\sum_d V_d\left(\frac{\theta_l N_{l`}^T}{\sum_{\bar{l}\in L} \theta_{\bar{l}} N_{\bar{l}}^T}\right) - v_{dl`}^c\right)}{\sum_d V_d\left(\frac{\theta_l N_{l`}^T}{\sum_{\bar{l}\in L} \theta_{\bar{l}} N_{\bar{l}}^T}\right)} \leq \psi \qquad \forall (l, l`) \in (L\ x\ L) \qquad (52)$$

3.2.2. Routine vaccine allocation problem

The routine vaccine allocation (v_{rl}^r) is calculated for each vaccine r at each location l based on the immunization coverage, the number of doses each person should receive of that vaccine, and

the population of each state. The population of each state was divided into specific age groups for each type of vaccine. Formally, we define the sets, parameters, and variables.

Sets

L	Set of locations l
V	Set of routine vaccines r

Parameters

P_{rl}	Population of specific age group in state l for each vaccine r
G_r	Target vaccination coverage for vaccine r (%)
H	Planning horizon (days)
M_r	Number of doses of vaccine r

Variables

v_{rl}^r	Number of routine vaccines r destinated to location l

The routine vaccine required is then formulated in Equation (53).

$$v_{rl}^r = \frac{H * M_r * G_r * P_{rl}}{365} \tag{53}$$

3.2.3. Vaccine distribution problem

The VDP addressed in this thesis consists of distributing vaccines from the central warehouse to regional and local warehouses, based on allocation decisions of emergency (Section 3.2.1) and routine (Section 3.2.2) vaccines. At this stage, the objective is to determine how the allocated quantities of routine and emergency vaccines should be transported while minimizing total transportation costs, subject to constraints such as vehicle capacity, travel time, and resource availability.

The VDP encompasses a fleet of vehicles that may make multiple trips within a single period. Each trip starts and ends at a warehouse, and vehicles are subject to both capacity constraints and maximum allowable times. When multiple transportation modes are available between origin and destination locations, the least-cost alternative based on mode-specific cost and travel time matrices is selected.

In the literature, distribution problems with these characteristics are commonly associated with the vehicle routing problem (VRP). Classical VRP formulations, however, assume that each vehicle executes a single route within the planning horizon (Cattaruzza; Absi; Feillet, 2018; Toth; Vigo, 2002). This assumption does not adequately reflect many real-world logistics systems, in which vehicles are often reused and make several trips during the same planning period (Brandão; Mercer, 1998; Cattaruzza; Absi; Feillet, 2018; Fleischmann, 1990; Şen; Bülbül, 2008). To address this limitation, the multi-trip vehicle routing problem (MTVRP) was introduced by Fleischmann (1990), initially referred to as the Vehicle Routing Problem with Multiple Use of Vehicles (Cattaruzza; Absi; Feillet, 2018; Mingozzi; Roberti; Toth, 2013; Neira et al., 2020). Since then, the problem has been addressed in the literature under various denominations, such as multitrip VRP (Prins, 2002), VRP with multiple routes (Azi; Gendreau; Potvin, 2007), VRP with multiple trips (Olivera; Viera, 2007), and VRP with multiple depots returns (Tsirimpas et al., 2008). Despite these different terminologies, the problem definition remains the same, and the literature addressing this class of problems is still limited (Cattaruzza; Absi; Feillet, 2018).

The MTVRP consists of determining a set of routes and an assigning each route to a vehicle, such that each route starts and ends at the warehouse; the sum of the demands of customers in any route does not exceed vehicles capacity and the total duration of the routes assigned to the same vehicle does not exceed planning period (Cattaruzza; Absi; Feillet, 2018; Fleischmann, 1990).

Given that vehicles may make multiple trips within the planning horizon, returning to the warehouse after each route, and are subject to capacity and time constraints, the VDP addressed in this work can be classified as an MTVRP. Therefore, the VDP is formulated as an MTVRP, integrating routing decisions, vaccine quantities, and temporal constraints.

VDP formulation is presented in Equations (54)-(66). We define the sets, parameters, and decision variables.

Sets

K	Set of vehicles k
L	Set of locations l ($L = L^{no} U L^{o}$)
L^{no}	Subset of locations l that are not origin
L^{o}	Subset of locations l that are origin
V^{t}	Set of vaccines v (emergency and routine vaccines)

J	Set of trips j
LxL	Set of 2 by 2 combination of locations (origin-destination combinations)

Parameters

V_{vl}^{C}	Demand for vaccines type v at location l
V_{vl}^{F}	Supply of vaccines type v available at location l
$C_{kll'}^{j}$	Transportation cost for vehicle k for a trip j between locations l and l', regardless of the quantity of vaccines transported (R$)
C_{k}^{v}	Transportation cost per vaccine v (R$)
$T_{kll'}$	Transportation time for vehicle k between locations l and l' (hours)
M_{k}^{K}	Total transport capacity of vehicle k
M_{kv}^{KV}	Capacity transport for vaccine v in vehicle k
Q_{k}	Quantity of available vehicles of type k
H_{k}^{K}	Number of hours that vehicle k is available to work within the planning horizon (hours)
H_{k}^{J}	Maximum operating hours for vehicle k during trip j (hours)
L_{k}^{K}	Origin location of vehicle k

Variables

$b_{jkll'}$	Binary variable indicating if vehicle k travels from l to l' on trip j
$u_{vjkll'}$	Quantity of vaccines v transported by vehicle k between locations l and l' on trip j
y_{vjkl}	Total number of vaccines entering (if positive) or leaving (if negative) a location l

The vaccine distribution is then formulated in Equations (54)-(66). We formulate the VDP addressed in this thesis, adapting the four-index formulation described and presented in Cattaruzza et al. (2018). In this formulation, the key multi-trip characteristic is enforced by a vehicle-level time limit. Specifically, Equations (54)-(62) were inspired by Cattaruzza et al. (2018) formulation.

$$min \sum_{j\in J}\sum_{k\in K}\sum_{(l,l')\in LxL} b_{jkll'}C_{kll'}^{j} + \sum_{v\in V^{t}}\sum_{j\in J}\sum_{k\in K}\sum_{(l,l')\in LxL} u_{vjkll'}C_{k}^{v} \tag{54}$$

$$\sum_{j\in J}\sum_{k\in K} y_{vjkl} + V_{vl}^{F} = V_{vl}^{C} \qquad \forall v, \forall l \tag{55}$$

$$y_{vjkl} = \sum_{l' \in L} u_{vjkl'l} - \sum_{l' \in L} u_{vjkll'} \qquad \forall j, \forall, \forall k, \forall l \qquad (56)$$

$$y_{vjkl} \geq 0 \qquad \forall v, \forall j, \forall k, \forall l \in L^{no} \qquad (57)$$

$$\sum_{j \in J} \sum_{k \in K} \sum_{l' \in L} u_{vjkll'} \leq V_{vl}^{F} + \sum_{j \in J} \sum_{k \in K} \sum_{l' \in L} u_{vjkl'l} \qquad \forall v, \forall l \qquad (58)$$

$$\sum_{v \in V^t} u_{vjkll'} \leq b_{jkll'} M_k^K \qquad \forall j, \forall k, \forall (l, l') \in LxL \qquad (59)$$

$$\sum_{l' \in L} b_{jkll'} \leq 1 \qquad \forall j, \forall k, \forall l \in L^o \qquad (60)$$

$$\sum_{l' \in L} b_{jkll'} = \sum_{l' \in L} b_{jkl'l} \qquad \forall j, \forall k, \forall l \qquad (61)$$

$$\sum_{j \in J} \sum_{(l,l') \in LxL} b_{jkll'} T_{kll'} \leq H_k^K \qquad \forall k \qquad (62)$$

$$\sum_{(l,l') \in LxL} b_{jkll'} T_{kll'} \leq H_k^J \qquad \forall j, \forall k \qquad (63)$$

$$b_{jkll'} \in \{0,1\} \qquad \forall j, \forall k, \forall l \qquad (64)$$

$$u_{vjkll'} \in \mathbb{Z}^+ \qquad \forall v, \forall j, \forall k, \forall l \qquad (65)$$

$$y_{vjkl} \in \mathbb{Z}^+ \qquad \forall v, \forall j, \forall k, \forall l \qquad (66)$$

The objective function (54)) minimizes the total transportation cost by considering both the costs of trips j (first summation) and the cost associated with the quantity of vaccine v transported (second summation). This adapts the formulation objective function to immunization logistics by combining arc-activation costs with vaccine-dependent flow costs.

While the four-index MTVRP ensures customer demand satisfaction through visit-coverage constraints, the VDP achieves this via multi-vaccine flow balance constraints ((55)-(58)). In particular, Equation (55) ensures that the demand for each location l is equal to the sum of the vaccine supply and the balance of input and output of the vaccines. Equation (56) calculates the resulting amount of vaccine at the location l for each trip j using a vehicle k. Constraint (57)

ensures that vaccines are not withdrawn from locations that are not origins (subset L^{no}). Constraint (58) guarantees that the quantity of vaccines v departing the location l does not exceed the local supply plus the total amount of vaccines that have arrived at the location l.

Constraint (59) shows that the total quantity of vaccines transported by each vehicle k in each trip j must not exceed the vehicle capacity and corresponds to the capacity constraints in the four-index formulation for the MTVRP. Constraint (60) guarantees that each trip j can only depart from the origin once and Equation (61) ensures that a vehicle k that arrives at a location l also departs from that location. Constraints (60)-(61) correspond to the flow-conservation constraints of the four-index vehicle-flow formulation. Constraint (62) shows that the total transportation time for a vehicle k must not exceed its maximum operational hours within the planning horizon and directly corresponds to the multi-trip constraint in the four-index MTVRP formulation, which limits the total duration of each vehicle's time. Constraint (63) guarantees that the travel time for vehicle k on each trip j does not exceed the maximum travel time. Finally, Constraints (64)-(66) represent the domain of variables.

This formulation is used in both distribution stages, differing only in the input data. In the central-to-regional distribution stage, the model generates 610,179 constraints and 397,881 variables (383,671 continuous and 14,210 integer) and is solved with Gurobi 10.0 within 600 seconds. In the regional-to-local distribution stage, the model generates 23,199 constraints and 16,969 variables (16,363 continuous and 606 integer), requiring about 12,600 seconds (approximately 3.5 hours) of CPU time in Gurobi 10.0. These results suggest that the availability of modes of transportation (air and road) and fleet size provides flexibility in routing in the central-to-regional distribution while in the regional-to-local stage, distribution relies on a limited fleet using a single transportation mode (road). The results for both distribution stages are presented in Chapter 4.

4 RESULTS

This chapter presents the results considering the input data used in this work and a comparison between the predictions and the historical data of Covid-19. The chapter then presents a toy problem, a scenario analysis and vaccine allocation and distribution results.

4.1. Data Sources

This study uses vaccination data from the PNI to demonstrate the proposed method's (Chapter 3) applicability in a real-world setting. Established in 1973, the PNI is coordinated by the Ministry of Health in collaboration with state and municipal health departments. Through PNI, Brazil is one of the countries that provides the highest range of free vaccines (Butantan Institute, 2023; Domingues et al., 2020). As a result of high immunization coverage and the PNI expansion, the country eradicated poliovirus and rubella circulation (Brazil, 2015; OPAS, 2023) and reduced the infections and deaths from vaccine-preventable diseases such as diphtheria, tetanus, and whooping cough (Butantan Institute, 2023). Successful interventions in the past, including vaccinating more than 15 million children in just one day in the 1980s and 50 million children aged 9 months to 14 years in four weeks in 1992 (Domingues et al., 2020), were crucial to eradicating these diseases.

The PNI defines the configuration of the Storage and Distribution echelon of Brazilian Public VSC. At the tactical level, the PNI establishes coverage targets and allocation criteria, determines shipment periodicity, and establishes rules for vaccine transport (Brazil., 2021; Brazil, 2025b; Domingues et al., 2020).

In the Storage and Distribution echelon of the Brazilian VSC, we address the allocation and distribution from the central to regional warehouses and from regional to local warehouses. The allocation and distribution from the central to regional warehouses is carried out from the central warehouse in São Paulo, which supplies 27 regional warehouses. In turn, the allocation and distribution from the regional to local warehouses is carried out in Minas Gerais state, where the regional warehouse in Belo Horizonte supplies 28 local warehouses. Minas Gerais is the state with the largest number of municipalities in Brazil, and has a vulnerability index (IVS) configuration similar to the national IVS. The North and Northeast regions are more vulnerable than the Southeast and South regions (IPEA, 2025). Accordingly, the allocation and distribution from other regional warehouses to the local one can be carried out using the appropriate regional data.

Figure 11 represents the flow from the central warehouse in São Paulo to the 27 regional warehouses located in state capitals (central to regional warehouses) and the flow from the regional warehouse in Belo Horizonte (Minas Gerais) to the 28 local warehouses (regional to local warehouses).

Figure 11 - Allocation and Distribution flows of the Brazilian VSC

The input data for the emergency vaccine allocation problem (Section 3.2.1) includes daily historical records of cases (infections), deaths, and vaccinations at the state level for each disease (Covid-19 and Influenza), as well as demographic data, vaccine availability, and vaccination and storage capacity. Table 3 and Table 4 present the input data and references. The dataset on Covid-19 includes the period from January to November 2021, and the dataset on influenza starts on March 8 and ends on November 30, 2010.

Table 3 - Emergency vaccines input data

Data	Description	Reference
Historical Records	Daily history of infections and deaths by state	Influenza (Brazil, 2012) Covid-19 (Cota, 2023a)
	People vaccinated by state	Influenza (Brazil, 2010) Covid-19 (Cota, 2023b)
Population	Population of each Brazilian state Population of each MG municipalities	IBGE (2022)
Social Vulnerability Index (IVS)	IVS of each Brazilian state	IPEA (2025)
Regional Warehouse	Location	Regional warehouse manager, personal communication
Local Warehouse	Location and municipalities served by each local warehouse	MG_GOV (2025)

Table 4 - Vaccine arrivals dates

Covid-19*		Influenza**	
Dates	Quantity of vaccines	Dates	Quantity of vaccines
18/01/2021	6,542,208	08/03/2010	26,578,450
01/02/2021	11,203,530	05/04/2010	42,958,920
01/03/2021	13,951,063	10/05/2010	32,023,790
01/04/2021	14,631,379		
01/05/2021	28,196,818		
01/06/2021	26,268,963		
01/07/2021	30,683,671		
01/08/2021	15,187,286		
01/09/2021	8,085,410		
01/10/2021	3,318,334		
01/11/2021	1,733,524		

Source: Brazil (2010)**; Cota (2023b)*

In Brazil, routine vaccines offered as part of regular immunization campaigns are shown in Table 5. We use as inputs to calculate the quantity of routine vaccines (Section 3.2.2) the number of doses each individual should receive of each vaccine (M_r), the vaccination coverage target for each vaccine (G_r), and the number of individuals who should receive each vaccine (P_{rl}) (IBGE, 2018).

Table 5 - Routine vaccines data

Vaccine*	Doses (M_r)*	Vaccination coverage target (G_r)**
Bacille Calmette-Guérin (BCG)	Single dose at birth	90%
Bacterial triple pregnant women (dTpa)	Single dose	95%
Diphtheria and tetanus (dT - adult bacterial duo)	One dose from the age of 7 every 10 years	95%
Diphtheria and tetanus pregnant women (dT)	Three doses	95%
Diphtheria, tetanus and pertussis (dtp)	One dose at 15 months	95%
Diphtheria, tetanus and pertussis (dtp) (booster dose)	One dose at 4 years of age	95%
Diphtheria, Tetanus, Whooping Cough, Haemophilus influenzae B and Hepatitis B (Penta)	Three doses: 2, 4 and 6 months	95%
Hepatitis A	One dose at 15 months	95%
Hepatitis B	Single dose at birth	95%
Hepatitis B pregnant women	Three doses	95%
Measles, mumps, rubella (MMR)	One dose at 12 months	95%
Measles, Mumps, Rubella and Chickenpox (Viral Tetra)	One dose at 15 months	95%
Meningococcal C	Two doses: 3 and 5 months	95%
Meningococcal C (booster dose)	One dose at 12 months	95%
Papillomavirus	Two doses for boys and girls between 9 and 14 years	95%
Pneumococcal	Two doses: 2 and 4 months	95%
Pneumococcal (booster dose)	One dose at 12 months	95%
Polio	Three doses: 2, 4 and 6 months	95%
Rotavirus	Three doses: 1, 2 and 4 months	95%
Varicella	One dose at 4 years of age	95%
Yellow fever	Single dose at 9 months	95%
Yellow fever (booster dose)	One dose at 4 years of age	95%

Source: Brazil (2024a*, 2024b**)

The input data used in the distribution model (Section 3.2.3) includes vehicle specifications, such as the quantity of available vehicles of type k (Q_k) (air or road), total transport capacity of vehicle k (M_k^K), transportation cost for vehicle k for a trip j between locations l and l', regardless of the quantity of vaccines transported ($C_{kll'}^j$), number of hours that vehicle k is available to work within the planning horizon(H_k^K), and maximum operating hours for vehicle k during trip j (H_k^J). H_k^K is calculaded considering the time horizon and the number of hours worked daily. The same model is used to distribute vaccines from central to regional warehouses and from regional to local warehouses.

From central to regional warehouses, the vaccine is distributed by an outsourced company. This company does not have a dedicated fleet to distribute the vaccine; however, the distribution is carried out in available refrigerated trucks and commercial flights for air transport. Due to this, we assume the quantities and capacities of vehicles described in Table 6. On the other hand, the

vaccines are distributed from regional to local warehouses using state-owned refrigerated trucks in Minas Gerais state. There are two trucks available to distribute vaccines from the regional warehouse in Belo Horizonte to the local warehouses.

The total transport capacity of each vehicle (M_k^K) was calculated based on the technical specifications available in the vehicle manual (Facchini, 2025). For air transportation, the total transport capacity of the airplane was calculated based on the technical specifications provided in the vehicle manual (Ana, 2025). Since vaccines compete for space with passenger baggage, we assume that approximately 10% of the available capacity cargo can be used to transport vaccines (Casagrande, 2021). Transportation costs were defined based on reference values for refrigerated road transport (ANTT, 2025) and air cargo rates from Brazilian commercial flights (Viracopos, 2025). All monetary values are presented in Brazilian reais (BRL) and converted to U.S. dollars (USD) using the Central Bank of Brazil's (Banco Central do Brasil, 2026) closing selling rate from 27 January 2026 (1 USD = 5.2392 BRL). The operational rules adopted by regional warehouses managers were the basis for determining available working days, daily working hours, and maximum travel time per trip data. Table 6 presents the inputs used in the distribution model. Detailed travel times and cost matrices between all routes are also considered (see Annex B).

Table 6 - Distribution model data

	CW → RW		RW → LW
	Airplane	Truck	Truck
Quantity of available vehicles of type k (Q_k)	26	10	2
Total transport capacity of vehicle k (M_k^K)	500,000	1,500,000	800,000
Transportation cost ($C_{kll'}^j$)	US$1,33 /km	US$ 0.95/km	US$ 0.95/km
Number of hours that vehicle k is available (hours) (H_k^K)	-	360	360
Maximum travel time (hours) (H_k^J)	-	60	72

Note: CW: Central Warehouse, RW: Regional Warehouse. LW: Local Warehouse.

4.2. Comparison between predictions and historical data for Covid-19

To demonstrate the ability of the proposed technique (Section 3.2.1.1) to estimate the number of deaths and infections during an epidemic, we utilize historical vaccination data and epidemiological parameters from the Covid-19 epidemic. The EQ_POP equity policy was chosen because it best aligns with the allocation strategy outlined by the state managers in the interviews. Figures (12)-(13) show monthly projections of deaths and infections due to Covid-19 and historical observations over seven months of the 2021 epidemic.

Figure 12 - Cumulative projections of deaths by Covid-19 in the Brazil

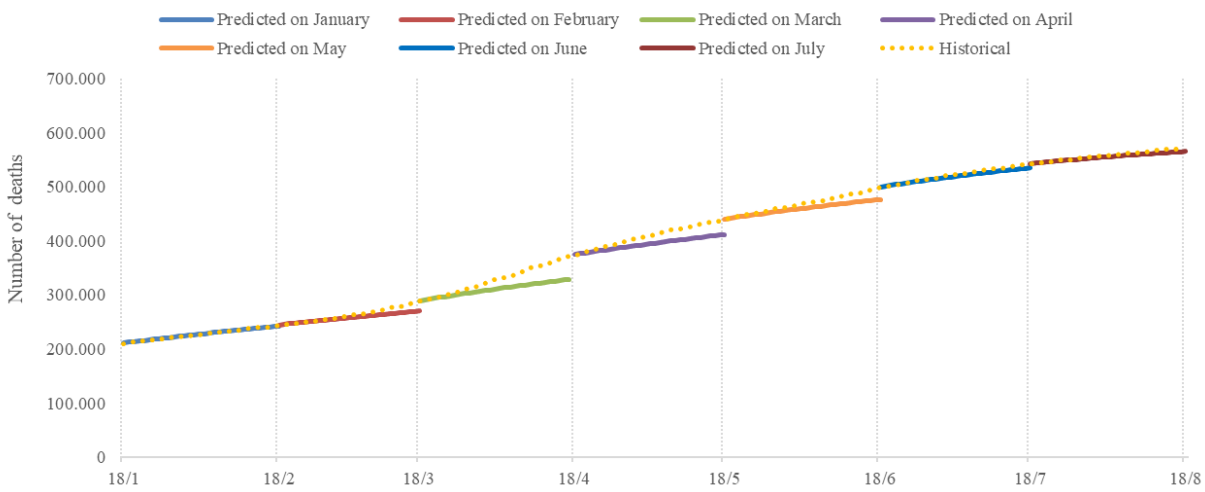

Figure 13 - Projections of infections by Covid-19 in the Brazil

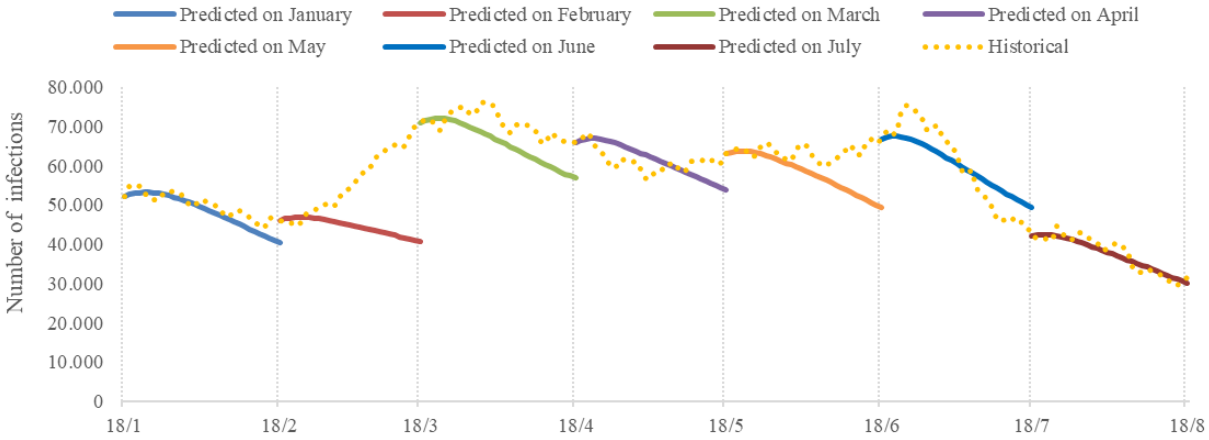

The criterion used to evaluate the predictive performance of the proposed technique was the mean absolute percentage error (MAPE). MAPE was calculated using Equation (67), where P_t is the predicted value at time t, Z_t is the observed value at time t and T is the number of predictions. Table 7 presents the MAPE for the number of deaths and infections. The MAPE was calculated for each time bucket for all of Brazil, suggesting good accuracy in predicting epidemic diseases based on the results of Zhang et al. (2014).

$$MAPE = \frac{1}{T}\sum_{t=1}^{T}\left|\frac{(P_t - Z_t}{Z_t}\right| \quad (67)$$

Table 7 - MAPE for deaths and infections from Covid-19

	January	February	March	April	May	June	July
Deaths	0%	2%	5%	4%	2%	1%	1%
Infections	4%	18%	7%	6%	9%	8%	4%

Table 7 shows the increase in infections in February (MAPE = 18%), indicating the difficulty in capturing the rapid increase in the number of cases due to the Gamma (P.1) variant. Figure 13 illustrates the increase in new infections between February 18 and March 18, 2021, after the variant was first detected in Manaus in December 2020 (Michelon, 2021) and has a greater ability to spread, leading to a rapid increase in infections (PAHO, 2021).

4.3. Toy Problem

The proposed formulation presented in Section 3.2.1 is a non-linear mathematical model (Equations (1)-(22)) with constraints (2)-(8) associated with the SEIRS epidemiological model. Specifically, Equations (2)-(3) use bilinear terms associated with the number of new infections results from the interactions between susceptible and infected populations (a main characteristic of SEIR-based compartmental models). The bilinear terms result in highly challenging optimization models (Bertsimas et al., 2022).

As discussed in Section 3.2.1, under a 10-hour time limit (36,000 s), the non-linear formulation could not solve the allocation problem between the central and regional warehouses of the Brazilian National System. Due to this, we develop an iterative solution technique. However, to validate this technique, we created a small instance (toy problem) to compare them. The toy problem was based on the Brazilian National System. However, we use only the four states of Brazil's Southeast region (Minas Gerais, São Paulo, Rio de Janeiro, and Espírito Santo) and a 30-day planning horizon. All other inputs and parameters were the same as those described in Section 4.1.

Both the non-linear model and the proposed iterative solution technique were then used to solve this toy problem using Gurobi 10.0 (Gurobi, 2025). In the non-linear model, Gurobi 10.0 solves the formulation described in Equations (1)-(22), including Equations (2)-(8) regarding the SEIRS epidemiological dynamics. In turn, the iterative solution technique obtains a solution by alternating between the Simulation and Optimization stages (Section 3.2.1.1). In this technique, the SEIRS model is solved in the Simulation Stage outside the Gurobi 10.0, and Gurobi 10.0 is used only to solve the Optimization Stage. Therefore, the constraints and variables for the

iterative solution technique shown in Table 8 refer to the Optimization Stage solved by Gurobi 10.0. The toy problem was solved under the EQ_POP equity policy. The same analysis could also be carried out under EQ_POP_IVS and NO_EQ allocation strategies.

We compared the total number of deaths obtained by the non-linear model and the iterative solution technique (Table 8). The non-linear model yields 107,745 deaths, while the proposed iterative solution technique yields 107,804 deaths, corresponding to a relative difference of 0.0548%. Regarding CPU time, the iterative solution technique solves the toy instance in 7.5 seconds, whereas the non-linear model requires 75 seconds, representing a 90% reduction in runtime. The mathematical models in both approaches achieved optimal solutions (Gap = 0.0%) and the iterative technique decreased the number of constraints and variables compared with the non-linear model. These results indicate that the proposed iterative solution technique can solve this problem within a reasonable computation time.

Table 8 - Computational results for the small instance

	Number of Deaths	CPU time	Constraints	Variables		Gap
				Continuous	Integer	
Non-Linear model	107,745	75s	2,659	2013	480	0.0%
Iterative Solution Technique	107,804	7.5s	1,487	1081	120	0.0%
Percentage difference	0.0548%	90%	-	-		-

4.4. Scenarios analysis

Four scenarios were employed to address different epidemiological behaviors of diseases using the proposed technique. Each scenario delineates a combination of routine and emergency vaccines in both epidemic and non-epidemic settings. Each scenario addresses the allocation and distribution of vaccines from the central warehouse in São Paulo to regional warehouses in state capitals. At the state level, Minas Gerais was chosen to demonstrate the allocation and distribution of the vaccine from the regional warehouse in Belo Horizonte to each local warehouse in the state.

- Scenario 1 [Routine vaccines]: Only routine vaccines are allocated and distributed (in the absence of an epidemic).
- Scenario 2 [Routine and Covid-19 vaccines]: Routine immunization is maintained, with the addition of emergency Covid-19 vaccine allocation and distribution (single epidemic).

- Scenario 3 [Routine and Influenza vaccines]: Routine immunization is maintained, with the addition of emergency Influenza vaccine allocation and distribution (single epidemic).
- Scenario 4 [Routine, Covid-19, and Influenza vaccines]: Routine immunization is maintained, with the addition of emergency influenza and Covid-19 vaccine allocation and distribution, i.e., in the event of a simultaneous Covid-19 and influenza epidemics. In this case, we assume independence between the epidemics, in which the epidemiological parameters of one disease do not influence those of the other disease.

Scenarios 2, 3, and 4 were evaluated using the two equity policies for the allocation of emergency vaccines, as defined in Section 3.2.1.3 (EQ_POP and EQ_POP_IVS). The same scenarios were also evaluated without incorporating equity constraints (NO_EQ) using the same mathematical modelling.

4.5. Allocation and Distribution Results

The results for each scenario presented in this section were obtained for the allocation of emergency (Section 3.3.1.1) and routine (Section 3.2.2) vaccines using equity policies described in Section 3.2.1.3. The distribution of vaccines, in turn, used the model described in Section 3.2.3. The input data detailed in Section 4.1 were also used in these methods to obtain the allocation and distribution plans for each addressed scenario.

4.5.1 Scenario 1 [Routine vaccines]

Allocation from the central warehouse to the regional warehouses: Table 9 shows the monthly allocation of routine vaccines to ensure vaccination coverage (Table 5). As the coverage target is the same for all states, routine vaccines are allocated proportionally to each state's population, with the most populous states receiving larger quantities. Appendix A provides the specific quantities allocated of each vaccine. This scenario is important since maintaining routine immunization is essential to prevent setbacks in diseases already under control (UNICEF, 2022; WHO, 2021a).

Table 9 - Vaccine allocation from central to regional warehouses in Scenario 1

Regional Warehouse	Quantity of vaccines	Regional Warehouse	Quantity of vaccines
AC	54,231	PB	194,067
AL	170,018	PE	455,740
AM	262,636	PI	162,310
AP	52,211	PR	518,221
BA	676,910	RJ	723,967
CE	432,733	RN	159,328
DF	144,143	RO	90,490
ES	189,452	RR	42,997
GO	327,231	RS	467,704
MA	380,478	SC	336,104
MG	895,259	SE	112,640
MS	145,709	SP	1,980,215
MT	192,321	TO	82,863
PA	473,464		

Distribution from the central warehouse to regional warehouses: Figure 14 presents a map of Brazil in which the intensity of the red shading reflects the total volume of vaccine doses allocated to each regional warehouse. The states with darker-shaded regions (e.g., São Paulo, Minas Gerais, Bahia, Paraná, and Rio de Janeiro) receive the highest vaccine volumes. The results show that vaccines allocated further away from the central warehouse are distributed by air, while vaccines allocated to states closer to São Paulo are, in general, transported by road.

Table 10 shows that road distribution is realized using three truck trips, corresponding to 30% utilization of the available road fleet. Trips' durations range from 22.90 to 30.46 hours, representing 38.17%-50.77% of the maximum travel-time limit per trip H_k^J. Transported quantities range from 913,419 to 1,366,649 doses, corresponding to 60.89%-91.11% of truck capacity M_k^K. In this scenario, the quantity of vaccines remains constant over time, and the same routes are used.

Table 10 - Road routes from central to regional warehouses in Scenario 1

Vehicle	Number of trips	Route	Time (hours)	Transported vaccines
Truck 1	1	SP → RJ → ES → SP	22.90	1,366,649
Truck 2	1	SP → PR → RS → SC → SP	28.75	913,419
Truck 3	1	SP → MG → DF → GO → SP	30.46	1,322,029

Figure 14 - Multimodal distribution from central to regional warehouses in Scenario 1

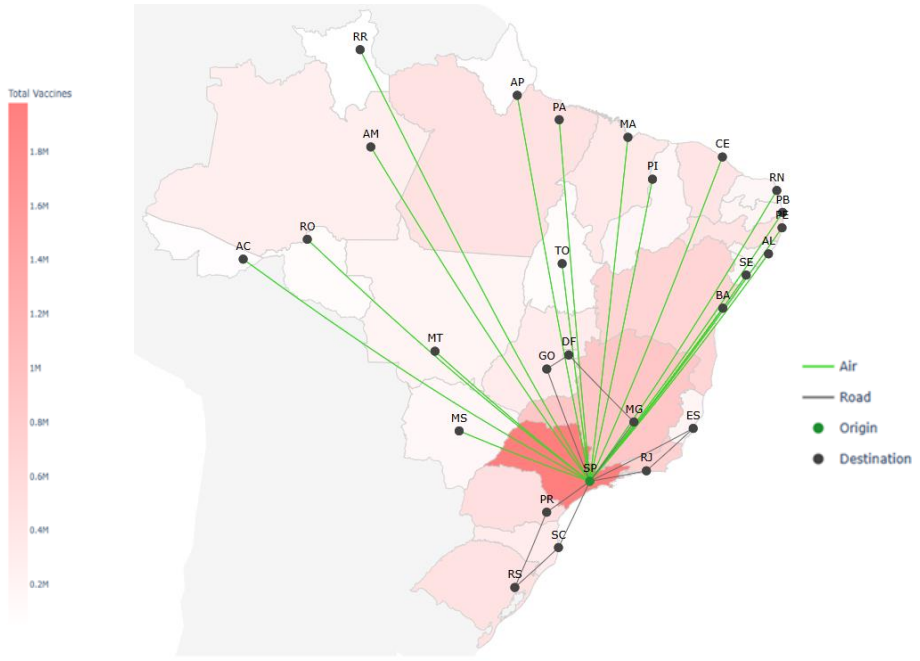

Table 11 shows the quantity of vaccines transported by mode of transportation for each regional warehouse. Each regional warehouse is served by only one mode of transportation. For the São Paulo regional warehouse, we assume that the regional warehouse is co-located with the central warehouse in Guarulhos. Therefore, there is no need for transport from the central warehouse to the regional warehouse. Consequently, doses allocated to the São Paulo regional warehouse, which account for approximately 20% of the total quantity in this stage, do not incur in transportation costs in the central-to-regional distribution in our model. Under these conditions, the monthly distribution cost reported in Table 12 (US$ 146,663) reflects only the transport to the remaining regional warehouses using air and road transport. Despite transporting a similar quantity of doses, the total cost is concentrated in air transport, which correspond to 95.73% of the total monthly cost, whereas road transport represents only 4.27%. Air transport is used to supply regional warehouses that are, in general, farther away, while road transport is designated for states closer to São Paulo. It is important to note that the results of the study do not indicate that road transport is more efficient (cost per unit). The results indicated that for routes with proximity to the central warehouse, road transport is the preferable option. Table 12 reports a month of the planning horizon, as the distribution pattern remains unchanged across months.

Table 11 - Vaccines transported by modal from central to regional warehouses in Scenario 1

Regional Warehouse	Air	Road	Regional Warehouse	Air	Road
AC	54,231	-	PB	194,067	-
AL	170,018	-	PE	455,740	-
AM	262,636	-	PI	162,310	-
AP	52,211	-	PR	-	518,221
BA	676,910	-	RJ	-	723,967
CE	432,733	-	RN	159,328	-
DF	-	144,143	RO	90,490	-
ES	-	189,452	RR	42,997	-
GO	-	327,231	RS	-	467,704
MA	380,478	-	SC	-	336,104
MG	-	895,259	SE	112,640	-
MS	145,709	-	*SP	-	-
MT	192,321	-	TO	82,863	-
PA	473,464	-			

*Vaccines stored in the regional warehouse in São Paulo = 1,980,215 vaccines

Table 12 - Vaccines distributed by modal from central to regional warehouses in Scenario 1

Mode	Vaccines	Percentage of vaccines	Cost by mode (US$)	Cost per unit (US$ /vaccine)
Air	4,141,146	53.48 %	140,394	0.0339
Road	3,602,097	46.52 %	6,269	0.0017
	7,743,243	100 %	146,663	0.0189

Allocation from the regional warehouse to local warehouses: Table 13 shows the monthly allocation of routine vaccines to ensure vaccination coverage (Table 5) in the municipalities attended by each local warehouse. The routine vaccines are allocated proportionally to the population served by each local warehouse. Belo Horizonte local warehouse receives 233,166 doses, constituting approximately 26% of the total monthly volume allocated at this level. The four local warehouses with the highest allocation of vaccines (Divinópolis, Uberlândia, Montes Claros, and Pouso Alegre) besides Belo Horizonte, together account for approximately 48% of the total allocation. Pirapora and Ituiutaba warehouses, on the other hand, receive less than 1% of the monthly volume of vaccines each.

Table 13 - Vaccine Allocation from regional to local warehouses in Scenario 1

Local Warehouse	Quantity of vaccines	Local Warehouse	Quantity of vaccines
Alfenas	18,692	Passos	19,888
Barbacena	23,147	Patos de Minas	19,295
Belo Horizonte	233,166	Pedra Azul	12,927
Coronel Fabriciano	34,301	Pirapora	5,757
Diamantina	16,574	Ponte Nova	14,716
Divinópolis	56,368	Pouso Alegre	44,185
Governador Valadares	27,694	São João Del Rei	10,275
Itabira	19,788	Sete Lagoas	26,561
Ituiutaba	8,137	Teófilo Otoni	20,272
Januária	16,677	Ubá	20,159
Juiz de Fora	34,140	Uberaba	34,506
Leopoldina	9,561	Uberlândia	49,894
Manhuaçu	20,622	Unaí	11,853
Montes Claros	47,396	Varginha	38,708

Distribution from the regional warehouse to local warehouses: Figure 15 presents a map of Minas Gerais state that shows the road vaccine distribution configuration from the regional warehouse in Belo Horizonte to the 27 local warehouses. In the regional to local distribution, as only road transport is permitted, all deliveries are made by truck.

For the Belo Horizonte local warehouse, we assume that the municipalities supplied by this local warehouse collect their allocated quantities directly at the regional warehouse in Belo Horizonte. Under this assumption, no transportation is required between the regional and local warehouses in Belo Horizonte, and no distribution costs are accounted for. Consequently, Table 14 presents only the vehicles and trips required to supply the remaining local warehouses with the vaccines present in Table 13.

Figure 15 - Distribution from regional to local warehouses in Scenario 1

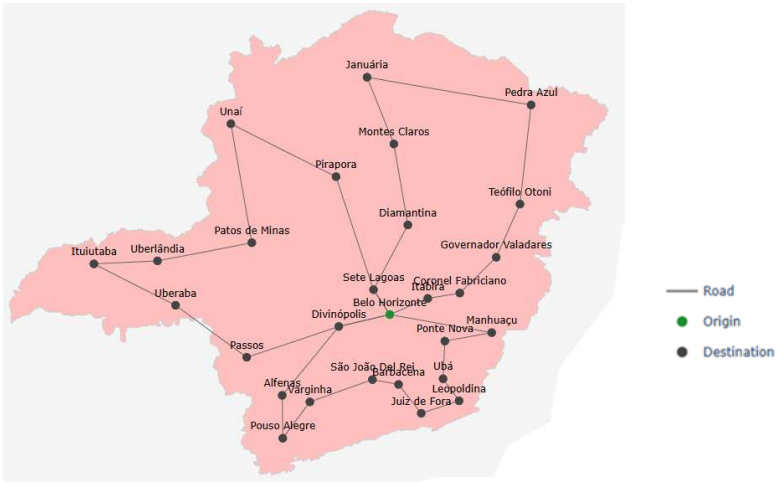

Table 14 - Routes from regional to local warehouses in Scenario 1

Vehicle	Number of trips	Route	Time (hours)	Transported vaccines
Truck 1	1	Belo Horizonte → Manhuaçu → Ponte Nova → Ubá → Leopoldina → Juiz de Fora → Barbacena → São João Del Rei → Varginha → Pouso Alegre → Alfenas → Divinópolis → Belo Horizonte	20,71	206,274
Truck 2	1	Belo Horizonte → Divinópolis → Passos → Uberaba → Ituiutaba → Uberlândia → Patos de Minas → Unaí → Pirapora → Sete Lagoas → Belo Horizonte	27.83	173,410
Truck 2	2	Belo Horizonte → Itabira → Coronel Fabriciano → Governador Valadares → Teófilo Otoni → Pedra Azul → Januária → Montes Claros → Diamantina → Sete Lagoas → Belo Horizonte	24,18	266,567

As presented in Table 14, three trips are required to supply the 27 local warehouses, all departing from and returning to the Belo Horizonte regional warehouse, using the available trucks. In this scenario, the trucks exhibit relatively low-capacity utilization, with transported quantities ranging from 173,410 to 266,567 doses, corresponding to 21.68%-33.32% of M_k^K (Table 6). Similarly, trip durations range from 20.71 to 27.83 hours, representing 28.76%-38.65% of the maximum travel-time limit per trip (H_k^J). These results indicate that the distribution routes are not constrained by vehicle capacity or trip-time limitations. Instead, the results suggest that the routes are influenced by the spatial configuration of local warehouses and the beginning and ending of routes at the regional warehouse in Belo Horizonte. Divinópolis and Sete Lagoas appear in more than one route, as show in Figure 15 and Table 14. These cities are located in two main roads of Minas Gerais state used in transportation routes from Belo Horizonte to the interior of the state.

In this scenario, the monthly cost of routine vaccine transportation is US$5,553, with an average cost of US$ 0.0083 per unit.

4.5.2 Scenario 2 [Routine and Covid-19 vaccines]

Allocation from the central warehouse to the regional warehouses: Figure 16 shows the emergency vaccine allocation under two equity policies (EQ_POP and EQ_POP_IVS) and the baseline reference (NO_EQ), as well as the corresponding predicted cumulative deaths under each strategy. The routine vaccine allocation is also presented in Figure 16.

In this scenario, we assume that the vaccination against Covid-19 begins almost one year after the start of the epidemic, due to the need to develop a vaccine. Consequently, the number of deaths on the first day of immunization is already high. The predicted number of deaths from Covid-19 curves, in turn, was obtained using the epidemiological parameters recorded on the first day of vaccination, for each allocation strategy.

The Covid-19 vaccine availability over time is the same under NO_EQ, EQ_POP, and EQ_POP_IVS, as indicated by the Covid-19 vaccine line in red in Figure 16. The three strategies differ only in how these vaccine quantities are allocated among regional warehouses. Consequently, the predicted cumulative death curves, shown by the three dashed lines, vary across strategies. As expected, NO_EQ yields the lowest number of deaths, since it prioritizes allocations that maximize mortality reduction. EQ_POP and EQ_POP_IVS equity policies, in turn, impose fairness constraints in allocation, resulting in increased cumulative deaths compared to NO_EQ, representing the price of fairness.

Additionally, under equity metrics-based strategies, allocations are constrained by fairness criteria, ensuring proportional vaccine allocation across states by limiting the maximum allocation deviation ψ. Therefore, a regional-warehouse analysis is required to describe the resulting allocation patterns and to compare the predicted deaths across the regional warehouse under each strategy.

Figure 16 - Cumulative Vaccine Allocation from central warehouse to regional warehouses in Scenario 2

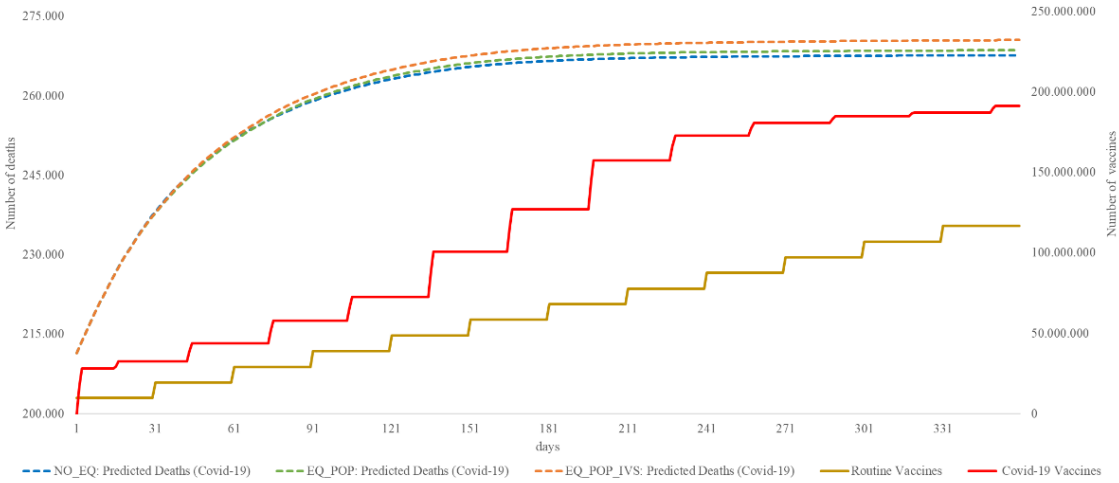

To evaluate the equity policies effects across states, Figures 17, 18, 19, and 20 present vaccine allocations and predicted deaths for Minas Gerais, São Paulo, Acre, and Alagoas, respectively. These states were selected to represent contrasting profiles regarding population size and vulnerability (IVS), including populous and less vulnerable states (São Paulo and Minas Gerais), as well as less populous and more vulnerable states (Acre and Alagoas). Under the NO_EQ strategy, allocations are driven by efficiency, i.e., doses are directed to the states where they yield a large reduction in deaths. Consequently, São Paulo receives a larger quantity of vaccines, whereas less populous states such as Acre and Alagoas receive fewer vaccines and later allocations. In the EQ_POP policy, allocation considers a population-proportional metric, whereas EQ_POP_IVS incorporates vulnerability by prioritizing states with higher IVS values. As a result, São Paulo receives fewer vaccines than under NO_EQ, while Acre and Alagoas receive earlier and larger allocations. These equity policies decrease predicted deaths in the more vulnerable states relative to NO_EQ, illustrating the efficiency–equity trade-off at the national level.

Figure 17 - Cumulative Vaccine Allocation in Minas Gerais state in Scenario 2

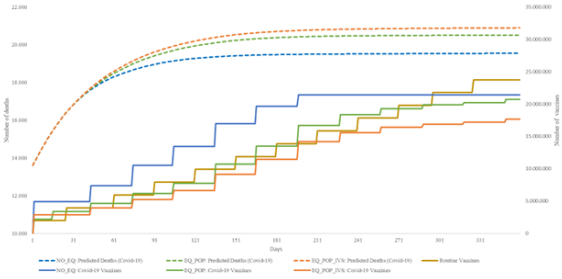

Figure 18 - Cumulative Vaccine Allocation in São Paulo state in Scenario 2

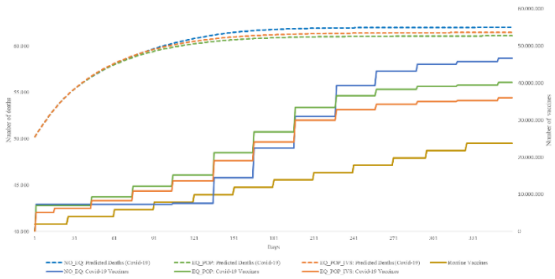

Figure 19 - Cumulative Vaccine Allocation in Acre state in Scenario 2

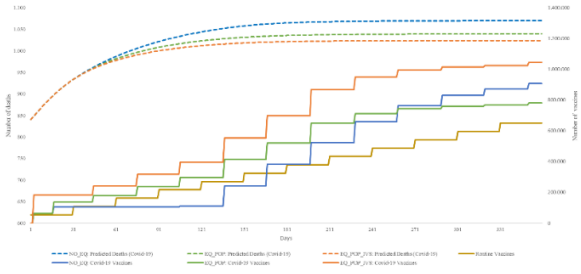

Figure 20 - Cumulative Vaccine Allocation in Alagoas state in Scenario 2

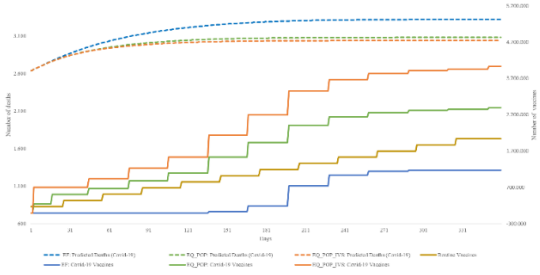

Figure 21 presents the monthly quantities of routine and emergency vaccines allocated to be used as input in the distribution model. Note that the amount of routine vaccine is the same throughout the year (Table 9); however, the initial monthly amounts of Covid-19 vaccine were small and increased as production capacity increased. However, from the seventh month, the monthly allocation of Covid-19 vaccines begins to decline, corresponding to stabilization of the death curve shown in Figure 16.

Figure 21 - Monthly Vaccine Allocation from central to regional warehouses in Scenario 2

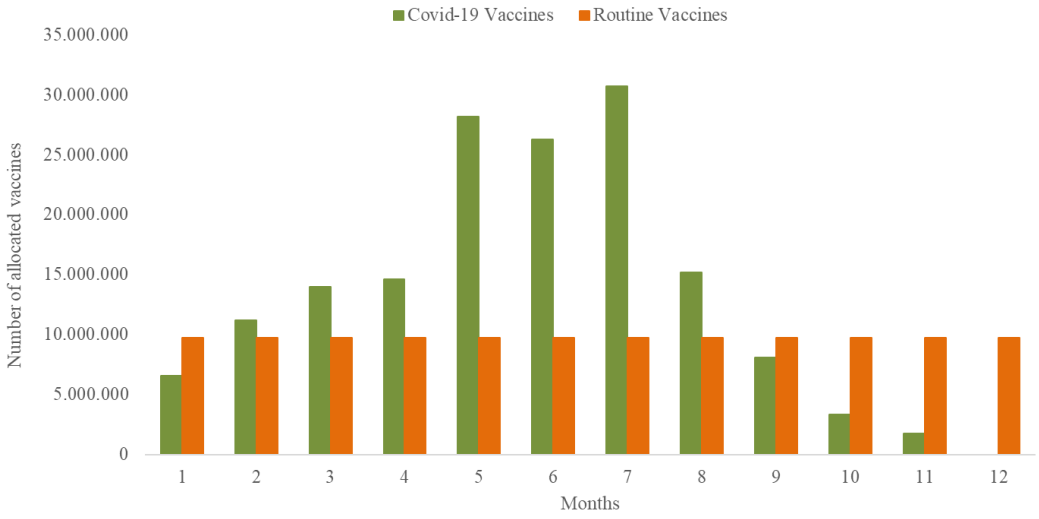

Distribution from the central warehouse to regional warehouses: Figure 22 shows the distribution of vaccines (Covid-19 and routine) by transport modal from the central warehouse to regional warehouses during the seventh distribution month (the month corresponding to the highest volume of vaccine, see Figure 21) under EQ_POP_IVS equity policy. This policy was selected because it better represents equity by prioritizing vulnerable regions. The application of the vaccine distribution model using NO_EQ and EQ_POP is straightforward. However, the allocation of quantities in regional warehouses varies across policies. As in Scenario 1, we assume that the São Paulo regional warehouse is co-located with the central warehouse in Guarulhos and, consequently, transport is not required in the central-to-regional stage.

Table 15 also shows the routes used by each truck in road transportation. Compared with Scenario 1, the number of trucks used increases from three to ten, as the total distributed quantity increased from 7.7 million to 32.4 million doses. In Scenario 2, half of the trips are made with trucks operating at maximum capacity (1,500,000 vaccines), while the remaining trips operate at least at 55% to 71% of capacity. Trip times range from 10.20 to 30.77 hours, which corresponds to 17.00% to 51.28% of the maximum travel time limit per trip (H_k^J). Therefore, the results suggest that the capacity of the trucks in high volume scenario, as Scenario 2, affect most routes.

Figure 22 - Multimodal distribution from central to regional warehouses in Scenario 2

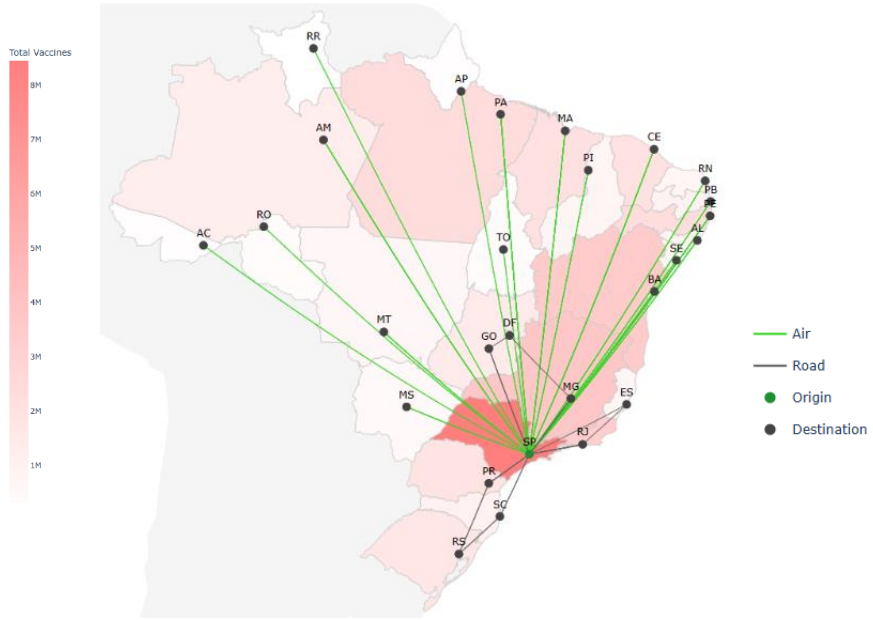

Table 15 - Road routes from central to regional warehouses in Scenario 2

Vehicle	Number of trips	Route	Time (hours)	Transported vaccines
Truck 1	1	SP → SC → RS → PR → SP	28.75	1,500,000
Truck 2	1	SP → MG → SP	14,.65	1,500,000
Truck 3	1	SP → SC → RS → PR → SP	28.75	1,371,750
Truck 4	1	SP → RJ → SP	10.72	1,500,000
Truck 5	1	SP → GO → SP	23.15	1,353,983
Truck 6	1	SP → PR → SP	10.20	1,353,983
Truck 7	1	SP → RJ → SP	10.72	830,779
Truck 8	1	SP → MG → SP	14.65	1,500,000
Truck 9	1	SP → RJ → ES →SP	22.90	1,500,000
Truck 10	1	SP → GO → DF → MG → SP	30.77	1,060,075

Table 16 shows the quantity of vaccines transported by transport mode. As in Scenario 1, each regional warehouse is supplied by a single mode (air or road). In the seventh month, 57.98% of vaccines were distributed by air, while 42.02% were distributed by road (Table 17). Although air transport accounts for 57.98% of the transported doses, it represents approximately 96.0% of the total transportation cost, whereas road transport accounts for 42.02% of the doses but only about 4.0% of the total cost. The cost per unit decreases 35% while the transported volume increases approximately 418% in Scenario 2 compared to Scenario 1, due to trucks higher loading levels. Transporting more vaccines per trip spreads these route-based costs over a larger quantity of vaccines, since, as can be seen in Table 15, several trips with trucks operating close to capacity (1,500,000).

Table 16 - Vaccines transported by modal from central to regional warehouses in Scenario 2

Regional Warehouse	Air	Road	Regional Warehouse	Air	Road
AC	227,157	-	PB	866,864	-
AL	837,807	-	PE	2,179,789	-
AM	1,159,558	-	PI	732,888	-
AP	204,824	-	PR	-	1,788,832
BA	3,276,337	-	RJ	-	3,151,906
CE	1,936,217	-	RN	701,942	-
DF	-	539,657	RO	339,744	-
ES	-	678,873	RR	145,825	-
GO	-	1,353,983	RS	-	1,634,245
MA	1,984,645	-	SC	-	948,673
MG	-	3,520,433	SE	508,219	-
MS	502,439	-	SP*	-	-
MT	621,916	-	TO	315,330	-
PA	2,245,338	-			

*Vaccines stored in the regional warehouse in São Paulo = 8,003,705 vaccines

Table 17 - Vaccines distributed by modal from central to regional warehouses in Scenario 2

Mode	Doses transported	Percentage of vaccines	Cost by mode (US$)	Cost per unit (US$/vaccine)
Air	18,786,839	57.98%	359,646	0.0191
Road	13,616,587	42.02%	14,909	0.0011
	32,403,426	100 %	374,555	0.0116

Allocation from the regional warehouse to local warehouses: Table 18 presents the quantities of the vaccine allocated to the 28 local warehouses. As in Scenario 1, allocations across local warehouses are proportional to population size; however, the number of vaccines allocated was 393.2% higher than in Scenario 1.

Table 18 - Vaccine Allocation from regional to local warehouses in Scenario 2

Local Warehouse	Quantity of vaccines	Local Warehouse	Quantity of vaccines
Alfenas	59,327	Passos	63,377
Barbacena	92,017	Patos de Minas	68,532
Belo Horizonte	979,232	Pedra Azul	79,328
Coronel Fabriciano	128,420	Pirapora	29,138
Diamantina	90,863	Ponte Nova	58,639
Divinópolis	166,255	Pouso Alegre	131,243
Governador Valadares	125,518	São João Del Rei	34,493
Itabira	82,844	Sete Lagoas	101,977
Ituiutaba	29,051	Teófilo Otoni	115,257
Januária	104,494	Ubá	66,911
Juiz de Fora	123,243	Uberaba	110,995
Leopoldina	30,893	Uberlândia	162,037
Manhuaçu	88,328	Unaí	52,517
Montes Claros	219,534	Varginha	126,011

Distribution from the regional warehouse to local warehouses: Figure 23 shows the road vaccine distribution configuration from the regional warehouse in Belo Horizonte to the 27 local warehouses. As in scenario 1, we assume no transportation is required between the regional and local warehouse in Belo Horizonte. The vehicles and trips required to transport the vaccines listed in Table 18 are described in Table 19.

Figure 23 - Distribution from regional to local warehouses in Scenario 2

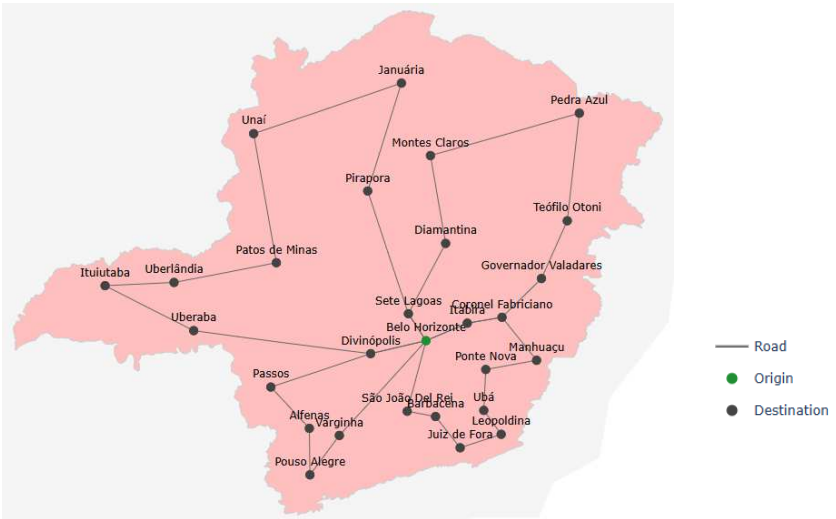

Table 19 - Routes from regional to local warehouses in Scenario 2

Vehicle	Number of trips	Route	Time (hours)	Transported vaccines
Truck 1	1	Belo Horizonte → Divinópolis → Uberaba → Ituiutaba → Uberlândia → Patos de Minas → Unaí → Januária → Pirapora → Sete Lagoas → Belo Horizonte	30.88	723,008
Truck 2	1	Belo Horizonte → Itabira → Coronel Fabriciano → Manhuaçu → Ponte Nova→ Ubá → Leopoldina → Juiz de Fora → Barbacena→ São João Del Rei → Belo Horizonte	14.30	705,777
Truck 2	2	Belo Horizonte → Varginha → Pouso Alegre → Alfenas → Passos → Divinópolis → Belo Horizonte	12.85	379,952
Truck 2	3	Belo Horizonte → Sete Lagoas → Diamantina → Montes Claros → Pedra Azul →Teófilo Otoni → Governador Valadares → Coronel Fabriciano → Itabira → Belo Horizonte	20.01	732,464

In this scenario, four truck trips are required to supply the 27 local warehouses, with Truck 1 making one trip and Truck 2 making three trips. The MTVRP formulation allows vehicles to be used in multiple trips within the planning horizon, thereby meeting demand with the same fleet size and without requiring additional vehicles.

Transported quantities range from 379,952 to 732,464 doses, corresponding to 47.49%-91.56% of the truck capacity. Three trips operate at high loading levels, between 88.22% and 91.56% of capacity, while one tour operates at 47.49%. Trips durations range from 12.85 to 30.88 hours, corresponding to 17.85%-42.89% of the maximum travel-time limit per trip. As mentioned before, the number of transported doses increased 383.8% while adding only one additional trip and increasing truck utilization. In Scenario 2, besides Divinópolis and Sete Lagoas, Coronel Fabriciano and Itabira also appear on more than one route possible due to its location near the main roads used for transportation from Belo Horizonte to various locations in Minas Gerais.

In this scenario, the monthly cost of local vaccine distribution is US$ 7,757, with a cost per unit of US$0.0030. Compared with Scenario 1, the total cost increases due to the larger distributed quantity; however, the cost per unit decreases. This reduction is associated with the increase in the number of doses transported per trip (truck loads) observed in Table 19, since road transportation costs are incurred per trip and route.

4.5.3 Scenario 3 [Routine and Influenza vaccines]

Allocation from the central warehouse to the regional warehouses: Figure 24 shows the allocation of the emergency influenza vaccine according to two equity policies (EQ_POP and EQ_POP_IVS) and the baseline reference (NO_EQ), as well as the routine vaccines. The corresponding predicted cumulative deaths under each strategy are also presented in Figure 24.

In this scenario, we also assume that the vaccination against influenza begins almost one year after the start of the epidemic, due to the need to develop a vaccine. We use the epidemiological parameters recorded on the first day of vaccination to predict cumulative deaths under each allocation strategy using the epidemiological model. As described in Scenario 2, equity policies were modeled using two equity policies to ensure proportional vaccine allocation across states by limiting the maximum deviation in allocation (ψ).

The influenza vaccine availability over time is the same under NO_EQ, EQ_POP, and EQ_POP_IVS, as indicated by the influenza vaccine line in black in Figure 24. The three strategies differ only in how these vaccine quantities are allocated among regional warehouses. In the influenza epidemic, the number of deaths is low under all three strategies; therefore, the predicted cumulative-death curves, represented by the dashed lines, exhibit small differences across policies, specifically when compared with Scenario 2. As expected, the NO_EQ strategy results in the lowest number of deaths. Routine vaccine monthly quantities remain fixed at the values defined in Table 9 and do not change across strategies.

Figure 24 - Cumulative Vaccine Allocation from central warehouse to regional warehouses in Scenario 3

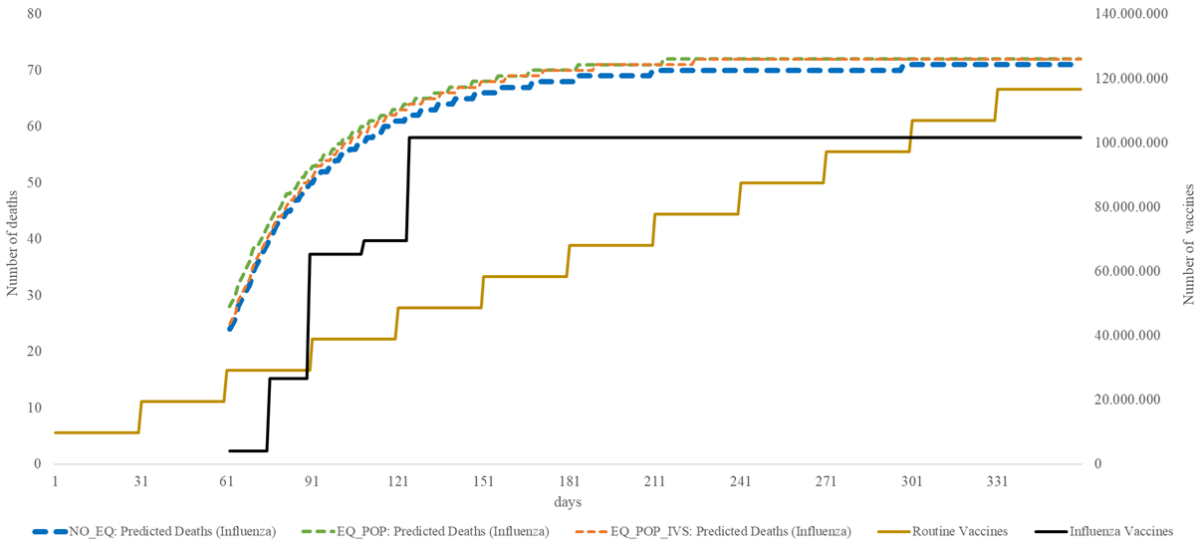

Figures 25-28 present the vaccine allocations and predicted deaths for Minas Gerais, São Paulo, Acre, and Alagoas, respectively. As in previous scenarios, populous and less vulnerable states, such as São Paulo, receive smaller amounts in the EQ_POP_IVS policy, whereas more vulnerable states, Acre and Alagoas, benefit from larger allocations when vulnerability is addressed.

However, in this scenario, influenza vaccination yields comparatively limited reductions in deaths, which is reflected in a smaller allocation under NO_EQ in the Minas Gerais regional warehouse. This contrasts with Scenario 2, where Covid-19 vaccination produces larger mortality reductions, and NO_EQ therefore assigns substantial quantities to populous states such as Minas Gerais.

Under EQ_POP and EQ_POP_IVS policies, allocations must ensure the proportionality constraints in Equations (51)-(52). As a result, Minas Gerais receives a larger allocation in this scenario, corresponding to its population share under EQ_POP and its IVS-weighted population share under EQ_POP_IVS, regardless of the comparatively low influenza mortality. This differs from Scenario 2, where NO_EQ already assigns substantial Covid-19 allocations to populous states such as Minas Gerais.

As in Scenario 2, in São Paulo state, the EQ_POP_IVS policy allocates fewer doses than NO_EQ and EQ_POP, whereas Acre and Alagoas receive earlier and larger allocations when vulnerability is incorporated. Despite these allocation differences, predicted influenza deaths remain very low across all four states, and the mortality curves show only minor variation across strategies.

Figure 25 - Cumulative Vaccine Allocation in Minas Gerais state in Scenario 3

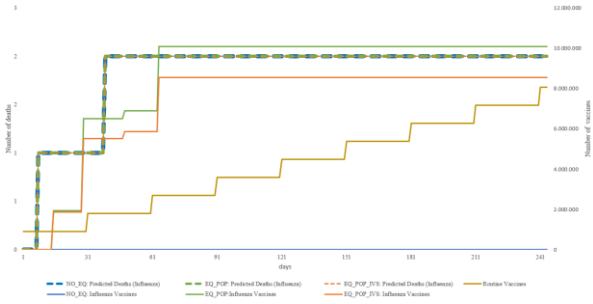

Figure 26 - Cumulative Vaccine Allocation in São Paulo state in Scenario 3

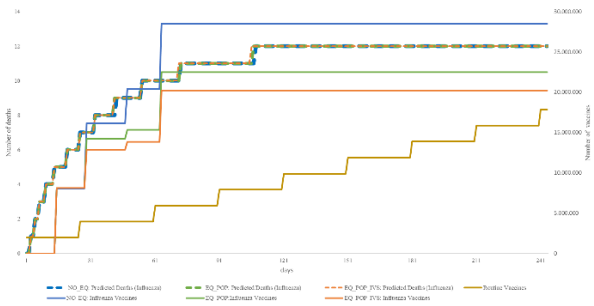

Figure 27 - Cumulative Vaccine Allocation in Acre state in Scenario 3

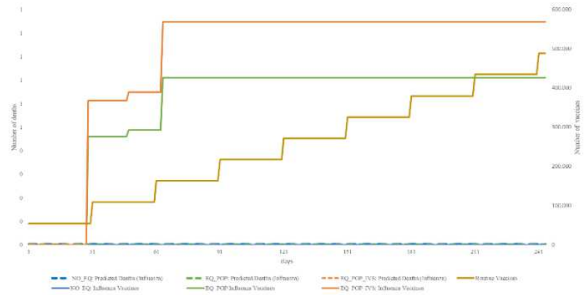

Figure 28 - Cumulative Vaccine Allocation in Alagoas state in Scenario 3

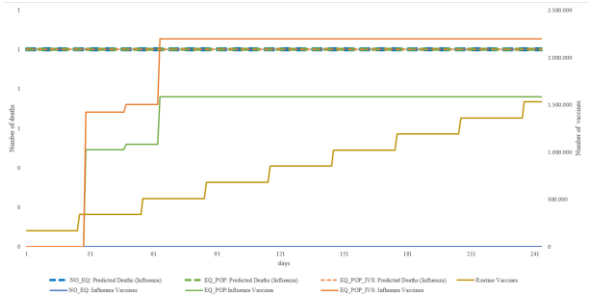

Figure 29 shows the monthly quantities of routine and emergency influenza vaccines allocated to be used as input in the distribution model. Routine vaccine quantities remain constant over time (Table 9), whereas influenza vaccine availability is concentrated in three months, generating significant monthly peaks in the total distributed quantity.

Figure 29 - Monthly Vaccine Allocation from central to regional warehouses in Scenario 3

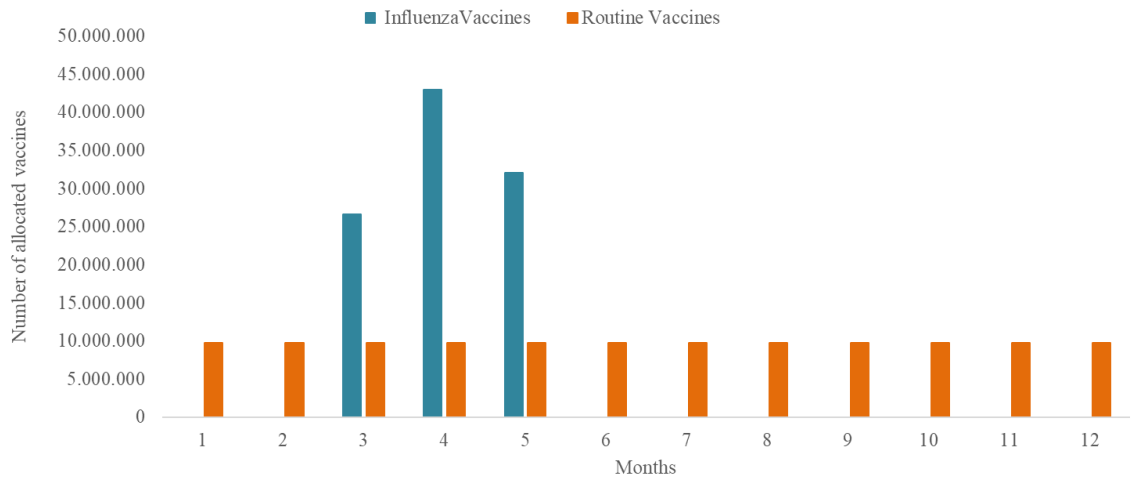

Distribution from the central warehouse to regional warehouses: Figure 30 presents the multimodal distribution of routine and emergency influenza vaccines from the central warehouse to regional warehouses in the fourth distribution month, which corresponds to the highest transported quantity in Scenario 3 (Figure 29) under the EQ_POP_IVS equity policy. Table 20 also presents the road routes for this month. As in the previous scenarios, no transportation is required for the São Paulo regional warehouse in the central-to-regional stage.

Compared with Scenarios 1 and 2, this scenario shows higher road fleet utilization. A total of 13 trips are executed by 9 trucks, including the use of 4 vehicles across two trips. Capacity usage remains high, with 61.5% of trips operating at the maximum capacity (1,500,000 doses). Transported quantities range from 872,209 to 1,500,000 doses, corresponding to 58.15%-100.00% of truck capacity, and 9 of the 13 trips operate at high loading levels (≥90% of capacity). Trip times range from 10.20 to 30.78 hours, corresponding to 17.0%-51.3% of the maximum trip time limit. The results indicate that, in this high quantity distribution scenario, vehicle capacity (M_k^K) is the main determinant in the number of trips and vehicle use, while ensuring trip times are satisfied for all trips.

Figure 30 - Multimodal distribution from central to regional warehouses in Scenario 3

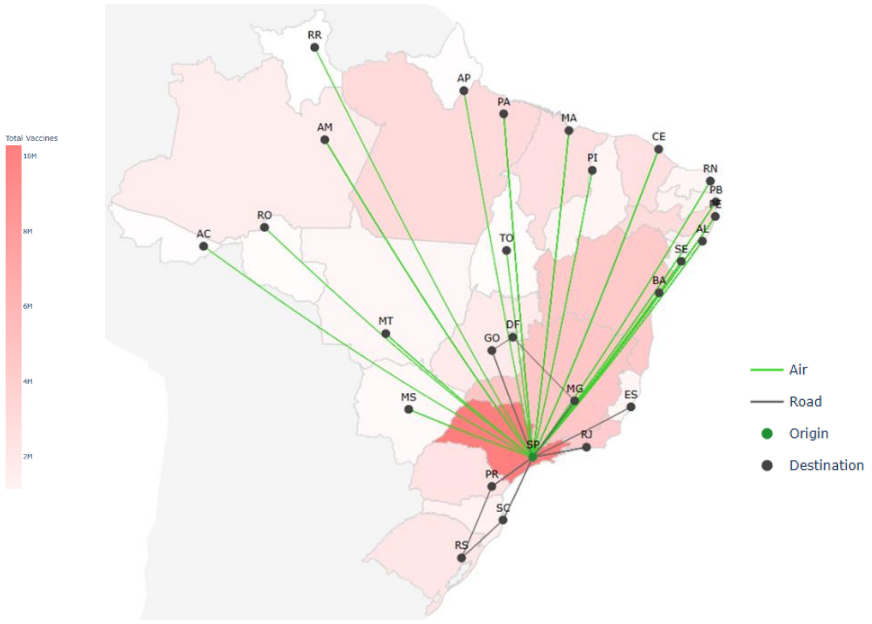

Table 20 - Road routes from central to regional warehouses in Scenario 3

Vehicle	Number of trips	Route	Time (hour)	Transported vaccines
Truck 1	1	SP → MG → SP	14,65	1,500,000
Truck 1	2	SP → GO → SP	23,15	1,027,293
Truck 2	1	SP → PR → SP	10,20	1,385,827
Truck 3	1	SP → RJ → SP	10,72	1,500,000
Truck 3	2	SP → GO → DF → MG → SP	30,77	1,500,000
Truck 4	1	SP → PR → RS →SC →SP	28,75	1,500,000
Truck 5	1	SP → MG → SP	14,65	1,500,000
Truck 5	2	SP → RJ → SP	10,72	1,145,036
Truck 6	1	SP → MG → SP	14,65	1,500,000
Truck 7	1	SP → RJ → SP	10,72	1,500,000
Truck 8	1	SP → SC → SP	17,62	1,190,657
Truck 9	1	SP → PR → RS →SC →SP	28,75	1,500,000
Truck 9	2	SP → ES →SP	22,05	872,209

Table 21 presents the quantity of vaccines distributed by transport mode, and shows that, as in previous scenarios, each regional warehouse is supplied by a single mode (air or road). In the fourth month, 42,383,071 vaccines are transported, representing a 547.4% increase relative to Scenario 1 and a 30.8% increase relative to Scenario 2. Although air transport accounts for 58.42% of the transported doses, it represents 95.9% of the total transportation cost, whereas road transport accounts for 41.58% of the doses and 4.1% of the total cost. The total transportation cost is US$439,359, which corresponds to 299.6% of the Scenario 1 cost and 117.3% of the Scenario 2 cost. The cost per unit in this scenario is US$0.0104, which is 10.3%

lower than in Scenario 2 (US$0.0116). This decrease is associated with the increase in the number of vaccines transported and load of vehicles.

Table 21 - Vaccines transported by modal from central to regional warehouses in Scenario 3

Regional Warehouse	Air	Road	Regional Warehouse	Air	Road
AC	297,891	-	PB	1,142,067	-
AL	1,110,960	-	PE	2,884,999	-
AM	1,526,438	-	PI	966,278	-
AP	267,249	-	PR	-	2,290,764
BA	4,339,613	-	RJ	-	4,145,036
CE	2,551,205	-	RN	919,411	-
DF	-	695,896	RO	441,699	-
ES	-	872,209	RR	187,866	-
GO	-	1,773,968	RS	-	2,095,063
MA	2,640,817	-	SC	-	1,190,657
MG	-	4,557,426	SE	670,027	-
MS	643,359	-	SP*	-	-
MT	791,619	-	TO	410,419	-
PA	2,970,112	-			

*Vaccines stored in the regional warehouse in São Paulo = 10,299,306 vaccines

Table 22 - Vaccines distributed by modal from central to regional warehouses in Scenario 3

Mode	Vaccines transported	Percentage of vaccines	Cost by mode (US$)	Cost per unit (US$/vaccine)
Air	24,762,049	58.42%	421,232	0.0170
Road	17,621,022	41.58%	18,127	0.0010
	42,383,071	100 %	439,359	0.0104

Allocation from the regional warehouse to local warehouses: Table 23 presents the allocation of vaccines across 28 local warehouses. In this scenario, the total quantity of vaccines allocated increases by 30.79% compared to Scenario 2, and by 547.35% compared to Scenario 1. The distribution pattern among the local warehouses remains the same across the scenarios, as the proportional population size is used in allocation.

Table 23 - Vaccine Allocation from regional to local warehouses in Scenario 3

Local Warehouse	Quantity of vaccines	Local Warehouse	Quantity of vaccines
Alfenas	76,802	Passos	82,045
Barbacena	119,120	Patos de Minas	88,720
Belo Horizonte	1,267,665	Pedra Azul	102,694
Coronel Fabriciano	166,245	Pirapora	37,719
Diamantina	117,626	Ponte Nova	75,911
Divinópolis	215,224	Pouso Alegre	169,898
Governador Valadares	162,490	São João Del Rei	44,653
Itabira	107,245	Sete Lagoas	132,014
Ituiutaba	37,609	Teófilo Otoni	149,208
Januária	135,273	Ubá	86,619
Juiz de Fora	159,545	Uberaba	143,690
Leopoldina	39,991	Uberlândia	209,765
Manhuaçu	114,345	Unaí	67,986
Montes Claros	284,197	Varginha	163,127

Distribution from the regional warehouse to local warehouses: Figure 31 show the road vaccine distribution configuration from the regional warehouse in Belo Horizonte to the 27 local warehouses. As in previous scenarios, vaccine transport to the Belo Horizonte local warehouse is not included in this regional-to-local distribution stage. The vehicles and trips required to transport the vaccines listed in Table 23 are described in Table 24.

Figure 31 - Distribution from regional to local warehouses in Scenario 3

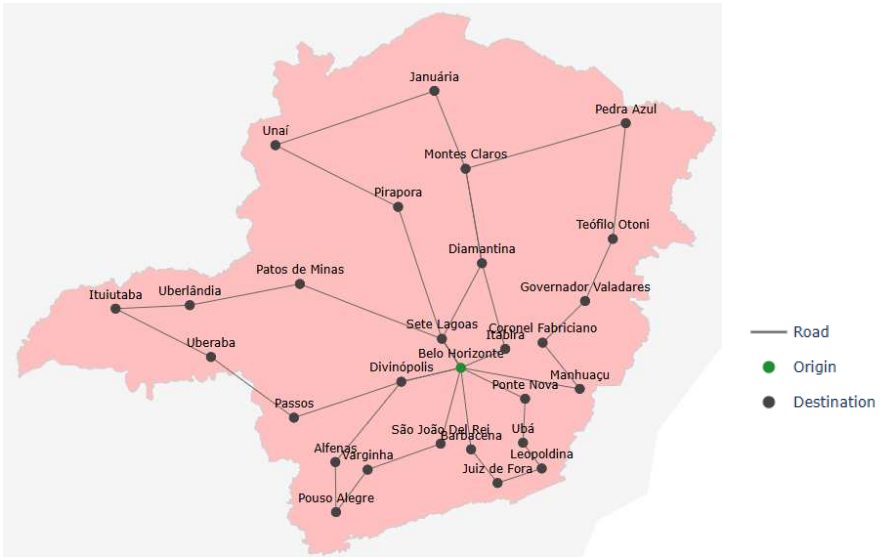

Table 24 - Routes from regional to local warehouses in Scenario 3

Vehicle	Number of trips	Route	Time (hours)	Transported vaccines
Truck 1	1	Belo Horizonte → Manhuaçu → Coronel Fabriciano → Governador Valadares→ Teófilo Otoni → Pedra Azul→ Montes Claros → Diamantina → Sete Lagoas → Belo Horizonte	23.42	795,176
Truck 1	2	Belo Horizonte → Itabira → Diamantina → Montes Claros → Januária → Unaí → Pirapora → Sete Lagoas → Belo Horizonte	24.50	649,852
Truck 1	3	Belo Horizonte → Sete Lagoas → Patos de Minas → Uberlândia → Ituiutaba → Uberaba → Passos→ Divinópolis → Belo Horizonte	20.45	693,843
Truck 2	1	Belo Horizonte → Divinópolis → Alfenas → Pouso Alegre → Varginha→ São João Del Rei → Belo Horizonte	12.50	669,704
Truck 2	2	Belo Horizonte → Barbacena → Juiz de Fora → Leopoldina → Ubá→ Ponte Nova → Belo Horizonte	9.18	481,186

Table 24 shows five trips were used to transport the vaccines, with Truck 1 responsible for three trips and Truck 2 for two trips. Transported quantities range from 481,186 to 795,176 vaccines, corresponding to 60.19%-99.40% of the vehicle capacity. Trip durations range from 9.18 to 24.50 hours, corresponding to 12.76%-34.03% of the trip time limit.

Scenario 3 transports 3,289,761 doses within Minas Gerais, representing a 29.5% increase relative to Scenario 2 and a 409.1% increase relative to Scenario 1. In this scenario, with the increase in number of trips, local warehouses of Montes Claros and Diamantina, more distant of Belo Horizonte are also included in two trips

The monthly cost for local vaccine distribution is US$ 8,785, with a road cost per unit of US$ 0.0026. Compared to Scenario 2, this represents a 12.6% reduction in unit cost, and relative to Scenario 1, a 58.1% reduction, consistent with higher doses transported per trip spreading route-based costs over a larger delivered volume.

4.5.4. Scenario 4 [Routine, Covid-19 and Influenza vaccines]

Allocation from the central warehouse to the regional warehouses: Figure 32 presents the allocation of Covid-19 (Scenario 2) and influenza (Scenario 3) vaccines combined into a single joint allocation plan, according to two equity policies (EQ_POP and EQ_POP_IVS) and the baseline reference (NO_EQ), along with routine vaccines. In addition, Figure 32 shows the corresponding predicted cumulative deaths under each strategy. As in the previous scenarios, the monthly routine vaccine allocations remain fixed at the quantities defined in Table 9.

The Covid-19 vaccine is allocated throughout the year, with monthly availability changing over the full planning horizon, whereas the influenza vaccine allocation is concentrated in a short period of three months. As in Scenarios 2 and 3, emergency vaccine availability is identical across strategies, and the only difference is in how doses are allocated across regional

warehouses. Consequently, differences across strategies are reflected in the predicted-death curves, with Covid-19 accounting for most of the variation, while influenza deaths remain comparatively small and present only minor differences across policies.

As in Scenarios 2 and 3, the NO_EQ strategy is associated with lower cumulative Covid-19 and Influenza deaths, indicating its efficiency-oriented allocation. In contrast, EQ_POP and EQ_POP_IVS policies lead to higher deaths. For influenza, death curves are very similar across policies, since the number of influenza-related deaths is low compared to Covid-19.

Figure 32 - Cumulative Vaccine Allocation from central warehouse to regional warehouses in Scenario 4

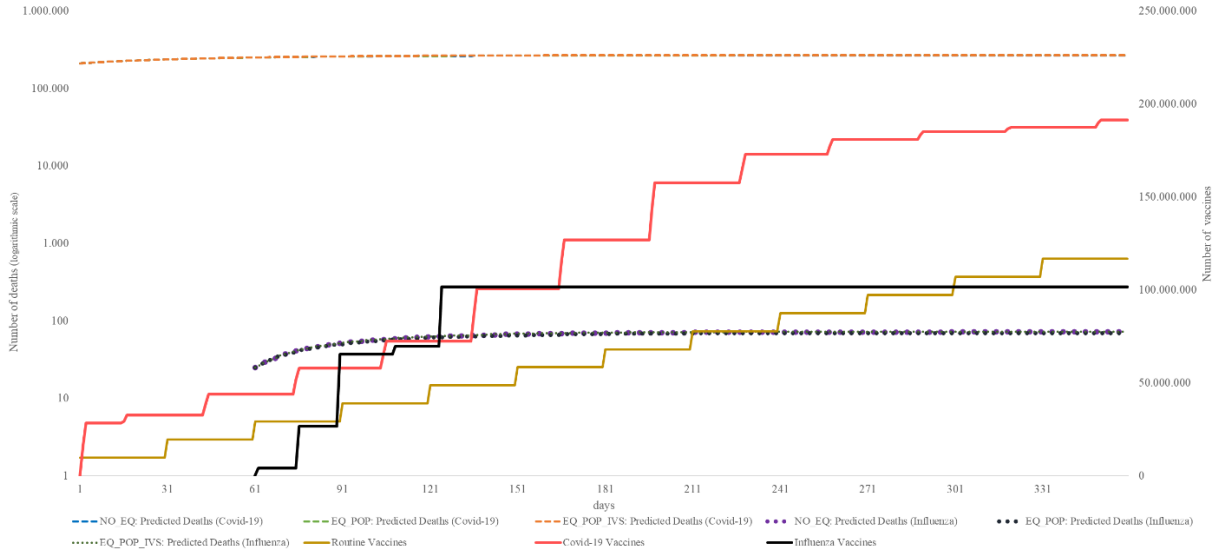

Figure 33 shows the monthly quantities of routine and emergency vaccines allocated to be used as input in the distribution model. The total amount of vaccine allocated each month varies widely over the twelve months, from about 16 million doses in the first month to 69 million doses in the fifth month and gradually declines as emergency immunization is reduced.

Figure 33 - Monthly Vaccine Allocation from central to regional warehouses in Scenario 4

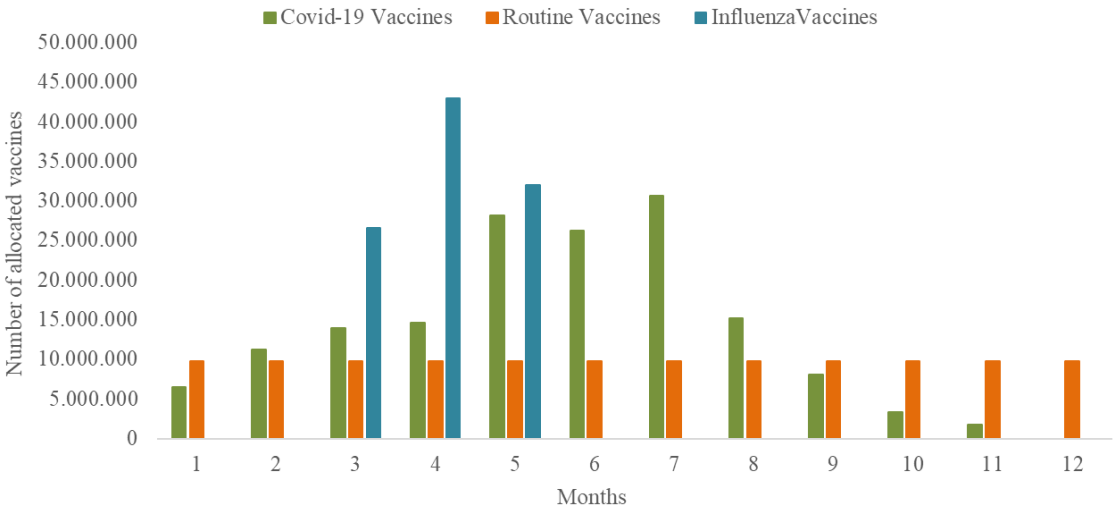

Distribution from the central warehouse to regional warehouses: Figure 34 shows the distribution of vaccines (Covid-19, Influenza and routine) by transport modal from the central warehouse to regional warehouses during the fifth distribution month, under EQ_POP_IVS equity policy. As in previous scenarios, we assume that transport is not required to São Paulo regional warehouse.

Figure 34 - Multimodal distribution from central to regional warehouses in Scenario 4

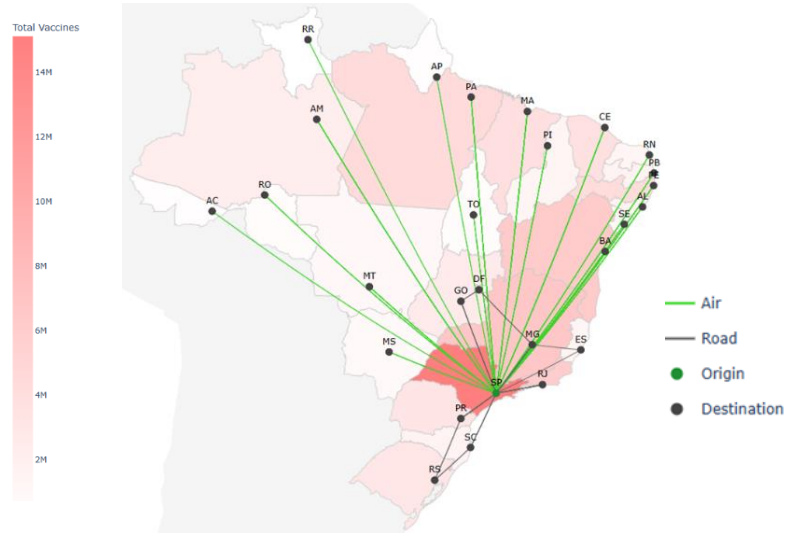

Table 25 - Road routes from central to regional warehouses in Scenario 4

Vehicle	Number of trips	Route	Time (hours)	Transported vaccines
Truck 1	1	SP → SC → RS →PR →SP	28.75	1,500,000
Truck 1	2	SP → MG → SP	14.65	1,500,000
Truck 2	1	SP → RJ → SP	10.72	1,455,175
Truck 2	2	SP → GO → DF → MG → SP	30.77	1,463,709
Truck 3	1	SP → GO → SP	23.15	1,500,000
Truck 3	2	SP → PR → RS →SC →SP	28.75	1,485,796
Truck 4	1	SP → RJ → SP	10.72	1,500,000
Truck 4	1	SP → PR → SP	10.20	1,317,620
Truck 5	1	SP → RJ → SP	10.72	1,500,000
Truck 5	2	SP → SC → SP	17.62	1,482,888
Truck 6	1	SP → PR → SP	10.20	1,500,000
Truck 6	2	SP → MG → SP	14.65	1,498,592
Truck 7	1	SP → MG → DF → GO → SP	30.46	1,496,514
Truck 8	1	SP → MG → SP	14.65	1,499,566
Truck 8	2	SP → ES → MG → SP	24.90	1,490,179
Truck 9	1	SP → RJ → SP	10,72	1,042,343

As present in Table 25, the utilization of nine trucks results in sixteen trips, with seven of the nine trucks making two trips. In Scenario 4, trip times range from 10.20 to 30.77 hours, which corresponds to 17.00% to 51.28% of the maximum travel-time limit per trip. Transported quantities range from 1,042,343 to 1,500,000 doses, corresponding to 69.49%-100.00% of truck capacity; moreover, 14 of the 16 trips operate at high loading levels (≥90% of capacity), including 6 trips at full capacity. Compared to previous scenarios, Scenario 4 increases road operations through additional trips and vehicle capacity utilization.

Table 26 shows the quantities transported in each transport mode from the central warehouse to each regional warehouse. As in the previous scenarios, each regional warehouse is served by a single transport mode, with air transport assigned to longer-distance regional warehouses and road transport concentrated in states closer to the São Paulo central warehouse. In accordance with the assumption adopted, the 13,760,232 doses allocated to São Paulo regional warehouse do not require central-to-regional transportation. Thus, 56,183,834 (Table 27) vaccines are transported, at a total transportation cost US$ 563,958, yielding a cost of US$0.0100 per transported dose.

Table 26 - Vaccines transported by modal from central to regional warehouses in Scenario 4

Regional Warehouse	Air	Road	Regional Warehouse	Air	Road
AC	396,032	-	PB	1,516,848	-
AL	1,489,952	-	PE	3,845,380	-
AM	2,026,068	-	PI	1,290,100	-
AP	352,262	-	PR	-	3,003,128
BA	5,787,624	-	RJ	-	5,497,518
CE	3,388,721	-	RN	1,225,556	-
DF	-	921,746	RO	582,846	-
ES	-	1,151,683	RR	246,244	-
GO	-	2,345,919	RS	-	2,749,083
MA	3,534,418	-	SC	-	1,534,093
MG	-	6,029,212	SE	890,384	-
MS	847,061	-	SP*	-	-
MT	1,032,471	-	TO	542,352	-
PA	3,957,133	-			

*Vaccines stored in the regional warehouse in São Paulo = 13,760,232 vaccines

Table 27 - Vaccines distributed by modal from central to regional warehouses in Scenario 4

Mode	Doses transported	Percentage of vaccines	Cost by mode (US$)	Cost per unit (US$/vaccine)
Air	32,951,452	58.65 %	541,690	0.0164
Road	23,232,382	41.35 %	22,268	0.0009
	56,183,834	100 %	563,958	0.0100

Allocation from the regional warehouse to local warehouses: Table 28 presents the quantities of the vaccine allocated to the 28 local warehouses. The total quantity allocated within Minas Gerais is 6.03 million vaccines, representing an increase of 71.3% relative to Scenario 2 and 32.3% relative to Scenario 3.

Table 28 - Vaccine Allocation from regional to local warehouses in Scenario 4

Local Warehouse	Quantity of Vaccines	Local Warehouse	Quantity of Vaccines
Alfenas	101,605	Passos	108,542
Barbacena	157,589	Patos de Minas	117,372
Belo Horizonte	1,677,046	Pedra Azul	135,859
Coronel Fabriciano	219,932	Pirapora	49,900
Diamantina	155,612	Ponte Nova	100,426
Divinópolis	284,727	Pouso Alegre	224,764
Governador Valadares	214,965	São João Del Rei	59,074
Itabira	141,876	Sete Lagoas	174,648
Ituiutaba	49,755	Teófilo Otoni	197,396
Januária	178,959	Ubá	114,592
Juiz de Fora	211,070	Uberaba	190,094
Leopoldina	52,906	Uberlândia	277,506
Manhuaçu	151,271	Unaí	89,941
Montes Claros	375,977	Varginha	215,808

Distribution from the regional warehouse to local warehouses: Figure 35 show the road vaccine distribution configuration from the regional warehouse in Belo Horizonte to the 27 local warehouses. As in the previous scenarios, we assume that there is no transportation to the Belo Horizonte local warehouse. The vehicles and trips required to transport the vaccines listed in Table 28 are described in Table 29.

Figure 35 - Distribution from regional to local warehouses in Scenario 4

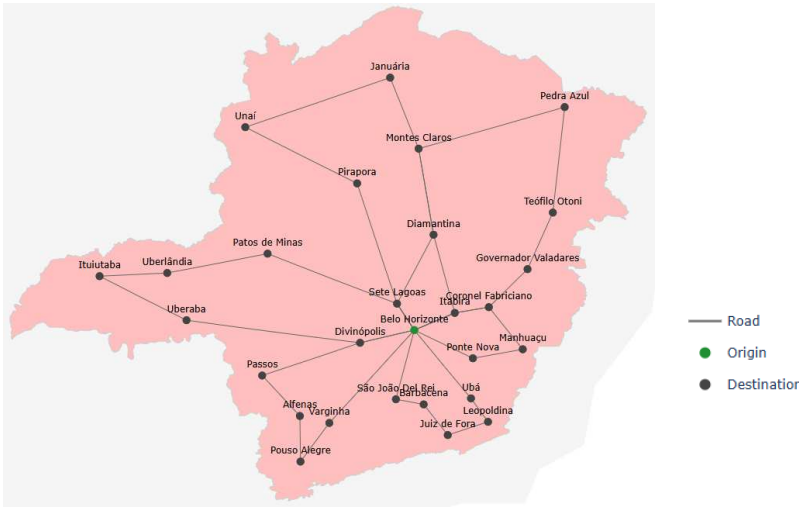

Table 29 - Routes from regional to local warehouses in Scenario 4

Vehicle	Number of trips	Route	Time (hours)	Transported vaccines
Truck 1	1	Belo Horizonte → Ubá → Leopoldina → Juiz De Fora→ Barbacena → São João del Rei→ Belo Horizonte	9.55	595,231
Truck 1	2	Belo Horizonte → Itabira → Diamantina → Montes Claros → Januária → Unaí → Pirapora → Sete Lagoas → Belo Horizonte	24.50	781,094
Truck 1	3	Belo Horizonte → Divinópolis → Uberaba → Ituiutaba → Uberlândia → Patos De Minas → Sete Lagoas → Belo Horizonte	19.68	800,000
Truck 2	1	Belo Horizonte → Sete Lagoas → Diamantina → Montes Claros → Pedra Azul→ Teófilo Otoni → Governador Valadares → Coronel Fabriciano → Itabira → Belo Horizonte	20.01	799,750
Truck 2	2	Belo Horizonte → Varginha → Pouso Alegre → Alfenas → Passos → Divinópolis → Belo Horizonte	12.85	770,173
Truck 2	3	Belo Horizonte → Itabira → Coronel Fabriciano → Manhuaçu → Ponte Nova → Belo Horizonte	8.72	605,918

Table 29 presents the same two-truck fleet as the previous scenarios, making six trips, with each truck responsible for three trips. All scenarios use the two trucks available; however, they use different numbers of trips. Truck loads range from 595,231 to 800,000 doses, corresponding to 74.40%-100.00% of the truck capacity (M_k^K), with four of the six trips operating at or above 96.27% utilization. Trip durations vary from 8.72 to 24.50 hours, representing 12.11%-34.03% of the maximum travel-time limit per trip (H_k^J). In this scenario, the monthly cost of local vaccine transportation is US$ 9,866 with a transportation cost per unit of US$ 0.0022.

4.5.5. Comparison of distribution results across scenarios

Table 30 presents a comparison of the central-to-regional distribution results across scenarios. The modal division changes minimally across scenarios, with air responsible for 53.48% to 58.65% of transported doses and road accounting for 41.35% to 46.52%. The decrease in cost per unit is consistent with the increase in the vaccines transported. As quantity increases, the trucks operate closer to vehicle capacity, spreading route-based costs over more vaccines and reducing the cost per unit.

Table 30 - Vaccines distributed by modal from central to regional warehouses in scenarios

Scenario	Air (%)	Air cost per unit (US$/dose)	Road (%)	Road cost per unit (US$/dose)	Average cost per unit (US$/dose)	Total doses	Total cost (US$)
1	53.48%	0.0339	46.52%	0.0017	0.0189	7.7 million	146,663
2	57.98%	0.0191	42.02%	0.0011	0.0116	32.4 million	374,555
3	58.42%	0.0170	41.58%	0.0010	0.0104	42.3 million	439,359
4	58.65 %	0.0164	41.35 %	0.0009	0.0100	56.1 million	563,958

Table 31 compares the regional-to-local distribution across scenarios, showing the increase in quantities and cost across scenarios in the distribution in Minas Gerais. However, despite the increase in total cost, the average cost per unit decreases. This behavior indicates scale effects in the regional-to-local stage, as higher quantities are distributed without increasing the fleet. The reduction in unit cost is associated with higher loading levels and number of trips per vehicle.

Table 31 - Vaccines distributed from regional to local warehouses in scenarios

Scenario	Average cost per unit (US$/dose)	Total doses	Total cost (US$)
1	0.0083	662,093	5,553
2	0.0030	2,541,201	7,757
3	0.0026	3,289,761	8,785
4	0.0022	4,352,166	9,866

5 CONCLUSIONS AND FUTURE PERSPECTIVES

The expansion of immunization programs is associated with the growing number of vaccine-preventable diseases and the concomitant existence of routine vaccination and epidemic outbreaks. In this context, this work focused on challenges regarding equity objectives, epidemiological dynamics, and logistical limitations.

This thesis addressed the Vaccine Allocation and Distribution Problem at the tactical level of the VSC by coupling a SEIRS-based epidemiological allocation model with an optimization distribution model for routine and emergency vaccines. In the allocation stage, the proposed technique embeds the SEIRS model in an optimization model to minimize deaths, while enforcing equity policies through proportionality constraints based on population size and IVS-weighted population size. Following allocation, an optimization model is used to develop multimodal distribution plans that minimize transportation costs, subject to vehicle capacity and trip time constraints.

The results show that the proposed framework generates allocation and distribution plans under distinct epidemiological scenarios. Across the four scenarios, allocation decisions are carried out at two levels (central-to-regional and regional-to-local), and the resulting allocated vaccines are subsequently included in distribution plans at the same two levels. The central-to-regional allocation uses a one-year planning horizon, while for the distribution plans, the month with the highest transported quantity was selected in each scenario. Due to this, the regional-to-local allocation and distribution plans also use the same peak month. Routine vaccines are allocated to ensure coverage targets, while emergency allocations vary with the epidemiological outbreak and the equity policy. The allocation plans allow for comparison of how equity policies change the allocation across regional warehouses of emergency vaccines and the associated epidemiological outcomes across strategies.

In the Covid-19 epidemic, the allocation results illustrate an efficiency–equity trade-off. Equity policies allocate more vaccines to less populous and more vulnerable states, resulting in a higher cumulative mortality compared to efficiency-oriented allocations. For influenza epidemics, allocations also vary across equity policies. However, the impact on mortality is limited due to the low predicted deaths, resulting in small differences in mortality across allocation strategies.

At the distribution stage, the multimodal distribution plans satisfy vehicle capacity and trip time constraints. To evaluate the logistics performance of each scenario, we use the distribution problem to develop distribution plans for the peak month. In these months, transported volumes

range in the central-to-regional stage from 7.7 million to 56.1 million doses, while the transportation cost per dose decreases from US$0.0189 to US$0.0100. In turn, transported quantities in the regional-to-local stage range from 662,093 to 4,352,166 doses, and the average road-transport cost per dose decreases from US$0.0083 to US$0.0022 as truck loading increases. The framework supports tactical immunization planning by providing a quantitative tool to evaluate trade-offs among equity and efficiency. Combining policy decisions with vaccine allocation and logistics plans might help health authorities evaluate the impacts of equity policies and develop feasible response strategies for addressing both non-epidemic and epidemic settings. Moreover, the framework supports transportation planning by identifying the transportation modes and road routes used to supply each warehouse.

This thesis contributes to the VSC literature by proposing, to the best of our knowledge, an integrated tactical planning framework that jointly addresses vaccine allocation and distribution for both non-epidemic and epidemic scenarios. Most previous approaches model allocation or distribution in isolation and do not simultaneously combine routine and emergency vaccines with epidemiological dynamics, equity constraints, and multi-trip distribution planning.

Several directions for future research arise from this work. An interesting future research direction is to use other objectives in the formulations to address epidemics with different epidemiological behavior. Multi-objective formulations may also be developed to incorporate multiple performance metrics simultaneously. Additional research may also improve the calibration of SEIRS epidemiological parameters using Machine Learning methods. Future improvements could also incorporate detailed population structure to enable prioritization of key groups such as the elderly and healthcare workers. We also intend to incorporate the production and vaccination echelons of VSC by extending the framework to address the entire VSC (horizontal integration). Finally, applying the framework to other countries, regions, and vaccine-preventable diseases would help assess generalizability and identify context-specific operational trade-offs.

REFERENCES

ABBASI, B. et al. Modeling Vaccine Allocations in the COVID-19 Pandemic: A Case Study in Australia. **SSRN**, p. 34, 2020.

ALEM, D.; CAUNHYE, A. M.; MORENO, A. Revisiting Gini for equitable humanitarian logistics. **Socio-Economic Planning Sciences**, v. 82, n. PB, p. 101312, 2022.

ALMARAJ, I. I. et al. A multi-objective integrated supply chain model under dynamic allocation of temporary vaccine centers and uncertain demand. **Applied Mathematical Modelling**, v. 150, n. PA, p. 116328, 2026.

ANA. **ANA Crago Specification**. Disponível em: <https://www.anacargo.jp/en/int/specification/a320.html>. Acesso em: 14 apr. 2025.

ANTT. **Tabelas de Frete**. Disponível em: <https://agenciabrasil.ebc.com.br/sites/default/files/atoms/files/tabelas.pdf?>.

ANVISA. **Câmara de Regulação do Mercado de Medicamentos - CMED**. Disponível em: <https://www.gov.br/anvisa/pt-br/assuntos/medicamentos/cmed>. Acesso em: 9 mar. 2026.

ARAGÃO, D. P. et al. Multivariate data driven prediction of COVID-19 dynamics: Towards new results with temperature, humidity and air quality data. **Environmental Research**, v. 204, n. November 2021, 2022.

ARAÚJO, S. R. DE et al. Evaluating Influenza Vaccine Allocation Strategies Through Seirs Modeling in Brazilian States. 2024.

ARAÚJO, J. L. B. et al. Unveiling the paths of COVID-19 in a large city based on public transportation data. **Scientific Reports**, v. 13, n. 1, p. 1–11, 2023.

AZI, N.; GENDREAU, M.; POTVIN, J. Y. An exact algorithm for a single-vehicle routing problem with time windows and multiple routes. **European Journal of Operational Research**, v. 178, n. 3, p. 755–766, 2007.

BADR, H. S. et al. Unified real-time environmental-epidemiological data for multiscale modeling of the COVID-19 pandemic. **Scientific Data**, v. 10, n. 1, p. 1–14, 2023.

BANCO CENTRAL DO BRASIL. **Banco Central do Brasil**. Disponível em: <https://www.bcb.gov.br/conversao>. Acesso em: 27 jan. 2026.

BÉLAND, D. et al. **The Oxford Handbook of The Welfare State**. Second Edi ed. Oxford University Press, 2021.

BERTSIMAS, D. et al. Optimizing Vaccine Allocation to Combat the COVID-19 Pandemic. **medRxiv**, p. 2020.11.17.20233213, 2020.

BERTSIMAS, D. et al. Where to locate COVID-19 mass vaccination facilities? **Naval Research Logistics**, v. 69, n. 2, p. 179–200, 2022.

BERTSIMAS, D.; FARIAS, V. F.; TRICHAKIS, N. The price of fairness. **Operations Research**, v. 59, n. 1, p. 17–31, 2011.

BRANDÃO, J.; MERCER, A. The multi-trip vehicle routing problem. **Journal of the Operational Research Society**, v. 49, n. 8, p. 799–805, 1998.

BRAZIL. **Conheça a força do PNI e a importância da vacinação para o enfrentamento de doenças**. Disponível em: <https://www.gov.br/saude/pt-br/assuntos/noticias/2021/junho/conheca-a-forca-do-pni-e-a-importancia-da-vacinacao-para-o-enfrentamento-de-doencas>. Acesso em: 21 oct. 2024.

BRAZIL. **Estratégia Nacional de Vacinação Contra o Vírus Influenza Pandêmico (H1N1) 2009**. Disponível em: <https://bvsms.saude.gov.br/bvs/publicacoes/estrategia_nacional_vacinacao_influenza.pdf>.

BRAZIL. **SRAG 2009 a 2012 - Banco de Dados de Síndroma Respiratória Aguda Grave**. Disponível em: <https://opendatasus.saude.gov.br/dataset/srag-2009-2012>. Acesso em: 2 mar. 2024.

BRAZIL. **Manual de Rede de Frio do Programa Nacional de Imunizações**. Disponível em: <https://www.gov.br/saude/pt-br/vacinacao/rede-de-frio/publicacoes/manual-de-rede-de-frio-do-programa-nacional-de-imunizacoes-5-ed/view>. Acesso em: 3 mar. 2024.

BRAZIL. **Manual de Rede de Frio do Programa Nacional de Imunizações**. Disponível em: <https://www.gov.br/saude/pt-br/vacinacao/rede-de-frio/publicacoes/manual-de-rede-de-frio-do-programa-nacional-de-imunizacoes-5-ed/view>. Acesso em: 24 apr. 2023.

BRAZIL. **Desinformação afasta pessoas de vacinação**. Disponível em: <https://www.gov.br/secom/pt-br/fatos/brasil-contra-fake/noticias/2023/3/desinformacao-afasta-pessoas-de-vacinacao>. Acesso em: 3 jan. 2024.

BRAZIL. **Calendário Técnico Nacional de Vacinação**. Disponível em: <https://www.gov.br/saude/pt-br/vacinacao/calendario-tecnico>. Acesso em: 3 apr. 2024a.

BRAZIL. **Cobertura Vacinal - Ocorrência**. Disponível em: <https://infoms.saude.gov.br/extensions/SEIDIGI_DEMAS_VACINACAO_CALENDARIO_NACIONAL_COBERTURA_OCORRENCIA/SEIDIGI_DEMAS_VACINACAO_CALENDARIO_NACIONAL_COBERTURA_OCORRENCIA.html>. Acesso em: 17 dec. 2024b.

BRAZIL. **Equidade em Saúde**. Disponível em: <https://www.gov.br/saude/pt-br/composicao/saps/equidade-em-saude>. Acesso em: 7 jul. 2025a.

BRAZIL. **Programa Nacional de Imunização (PNI)**. Disponível em: <https://www.gov.br/saude/pt-br/vacinacao>.

BROWN, S. T. et al. The benefits of redesigning Benin's vaccine supply chain. **Vaccine**, v. 32, n. 32, p. 4097–4103, 2014.

BUHAT, C. A. H. et al. Using Constrained Optimization for the Allocation of COVID-19 Vaccines in the Philippines. **Applied Health Economics and Health Policy**, v. 19, n. 5, p. 699–708, 2021.

BUTANTAN INSTITUTE. **Queda nas taxas de vacinação no Brasil ameaça a saúde das crianças**. Disponível em: <https://butantan.gov.br/noticias/queda-nas-taxas-de-vacinacao-no-brasil-ameaca-a-saude-das-criancas>. Acesso em: 3 jan. 2024.

CALANAN, R. M. et al. **CDC's Guiding Principles to Promote an Equity-Centered Approach to Public Health Communication**. Disponível em: <https://www.cdc.gov/pcd/issues/2023/23_0061.htm>. Acesso em: 1 aug. 2025.

CASAGRANDE, V. **Como companhias aéreas se preparam para transporte de vacina pelo Brasil?** Disponível em: <https://economia.uol.com.br/todos-a-bordo/2021/01/16/companhias-aereas-vacina-covid-19.htm>. Acesso em: 10 apr. 2025.

CASSÃO, V. et al. Unsupervised analysis of COVID-19 pandemic evolution in brazilian states: Vaccination Scenario. **Procedia Computer Science**, v. 219, n. 2022, p. 1453–1461, 2023.

CATTARUZZA, D.; ABSI, N.; FEILLET, D. Vehicle routing problems with multiple trips. **Annals of Operations Research**, v. 271, n. 1, p. 127–159, 2018.

CDC. **Vaccine Storage and Handling Toolkit**. Disponível em: <https://www.cdc.gov/vaccines/hcp/downloads/storage-handling-toolkit.pdf?>. Acesso em: 16 apr. 2025.

CHEN, S. I. et al. A planning model for the WHO-EPI vaccine distribution network in developing countries. **IIE Transactions (Institute of Industrial Engineers)**, v. 46, n. 8, p. 853–865, 2014.

CHICK, S. E.; MAMANI, H.; SIMCHI-LEVI, D. Supply chain coordination and influenza vaccination. **Operations Research**, v. 56, n. 6, p. 1493–1506, 2008.

CHOWDHURY, N. R. et al. Modeling a sustainable vaccine supply chain for a healthcare system. **Journal of Cleaner Production**, v. 370, n. July, p. 133423, 2022.

COTA, W. **Número de casos confirmados de COVID-19 no Brasil**. Disponível em: <https://covid19br.wcota.me/>.

COTA, W. **Monitoring the number of COVID-19 cases and deaths in Brazil at municipal and federative units level**. Disponível em: <https://preprints.scielo.org/index.php/scielo/preprint/view/362/444>.

DE ALMEIDA, L. et al. Quantifying political influence on COVID-19 fatality in Brazil. **PLoS ONE**, v. 17, n. 7 July, p. 1–11, 2022.

DE ARAÚJO, S. R. et al. Preventable COVID-19 cases and deaths by alternative vaccination and non-pharmacological intervention policies in Brazil | Casos e mortes evitáveis de COVID-19 por políticas de vacinação alternativas e intervenções não farmacológicas no Brasil. **Revista Brasileira de Epidemiologia**, v. 26, p. 1–9, 2023.

DEY, S. et al. Optimization modeling for pandemic vaccine supply chain management: A review and future research opportunities. **Naval Research Logistics**, p. 1–62, 2024.

DOMINGUES, C. M. A. S. et al. The Brazilian National Immunization Program: 46 years of achievements and challenges. **Cadernos de Saude Publica**, v. 36, 2020.

DUIJZER, L. E.; VAN JAARSVELD, W.; DEKKER, R. Literature review: The vaccine supply chain. **European Journal of Operational Research**, v. 268, n. 1, p. 174–192, 2018.

ENAYATI, S.; ÖZALTIN, O. Y. Optimal influenza vaccine distribution with equity. **European Journal of Operational Research**, v. 283, n. 2, p. 714–725, 2020.

FACCHINI. **Especificações Técnicas Furgão Refrigerado**. Disponível em: <https://www.facchini.com.br/clic?arquivo=fur_fr-br.pdf&area=produtos>.

FIOCRUZ. **Eqüidade em Saúde**. Disponível em: <https://www.sites.epsjv.fiocruz.br/dicionario/verbetes/equsau.html>. Acesso em: 17 jul. 2025.

FLEISCHMANN, B. The vehicle routing problem with multiple use of vehicles The vehicle routing

problem with multiple use of the vehicles Scope and Purpose. n. June, 1990.

FRUGOLI, A. G. et al. Vaccine fake news: an analysis under the World Health Organization's 3Cs model. **Revista da Escola de Enfermagem**, v. 55, p. 1–8, 2021.

GENG, H.; SHI, C. M. Health policy, price regulation, and innovation: Evidence from China's vaccine industry. **Journal of Development Economics**, v. 167, n. July 2023, p. 103229, 2024.

GEORGIADIS, G. P.; GEORGIADIS, M. C. Optimal planning of the COVID-19 vaccine supply chain. **Vaccine**, v. 39, n. 37, p. 5302–5312, 2021.

GILANI, H.; SAHEBI, H. A data-driven robust optimization model by cutting hyperplanes on vaccine access uncertainty in COVID-19 vaccine supply chain. **Omega (United Kingdom)**, v. 110, p. 102637, 2022.

GOENTZEL, J. et al. Vaccine network design to maximize immunization coverage. **Journal of Humanitarian Logistics and Supply Chain Management**, v. 13, n. 2, p. 140–156, 2023.

GUROBI. **Gurobi Optimization**. 2025. Disponível em: <https://www.gurobi.com/>

HIRSH BAR GAI, D. et al. Evaluating scenarios of locations and capacities for vaccine storage in Nigeria. **Vaccine**, v. 36, n. 24, p. 3505–3512, 2018.

HOGAN, G. et al. Evidence for inequities in the risk of foodborne and waterborne diseases in the Canadian population : a scoping review. **Journal of Health Equity**, v. 2, n. 1, 2025.

HOLLERAN, A.; MARTONOSI, S. E.; VEATCH, M. International Vaccine Allocation: An Optimization Framework. p. 1–32, 2023.

HOVAV, S.; HERBON, A. Prioritizing high-risk sub-groups in a multi-manufacturer vaccine distribution program. **International Journal of Logistics Management**, v. 28, n. 2, p. 311–331, 2017.

HOVAV, S.; TSADIKOVICH, D. A network flow model for inventory management and distribution of influenza vaccines through a healthcare supply chain. **Operations Research for Health Care**, v. 5, p. 49–62, 2015.

HU, MI.; ZHANG, C.; ZHOU, Y. Partial or Full Doses First? Vaccine Allocation Under Limited Supply. **SSRN**, p. 57, 2023.

IBGE. **Projeções da População**. Disponível em:

<https://www.ibge.gov.br/estatisticas/sociais/populacao/9109-projecao-da-populacao.html?edicao=21830>. Acesso em: 7 may. 2024.

IBGE. **Cidades e Estados – Araxá**.

IPEA. **IVS**. Disponível em: <https://ivs.ipea.gov.br/#/>. Acesso em: 3 sep. 2025.

JADIDI, M. M. et al. A two-step vaccination technique to limit COVID-19 spread using mobile data. **Sustainable Cities and Society**, v. 70, n. February, p. 102886, 2021.

JAHED, A.; HADJI MOLANA, S. M.; TAVAKKOLI-MOGHADDAM, R. A sustainable vaccine supply-production-distribution network with heterologous and homologous vaccination strategies: Bi-objective optimization. **Socio-Economic Planning Sciences**, v. 98, n. November 2024, p. 102113, 2025.

JARUMANEEROJ, P. et al. An epidemiology-based model for the operational allocation of COVID-19 vaccines: A case study of Thailand. **Computers and Industrial Engineering**, v. 167, n. February, p. 108031, 2022.

JOHNS HOPKINS MEDICINE. **The Difference Between Health Equity and Equality**. Disponível em: <https://www.hopkinsacg.org/health-equity-equality-and-disparities/>. Acesso em: 1 aug. 2025.

KARGAR, B. et al. Data-driven modeling for designing a sustainable and efficient vaccine supply chain: A COVID-19 case study. **Transportation Research Part E: Logistics and Transportation Review**, v. 184, n. March, p. 103494, 2024.

KERMACK, W. O.; MCKENDRICK, A. G. A contribution to the mathematical theory of epidemics. **Proceedings of the Royal Society of London. Series A, Containing Papers of a Mathematical and Physical Character**, v. 115, n. 772, p. 700–721, 1927.

KHEYBARI, S. et al. Optimizing vaccination facility locations and capacity as a pandemic response: A case study of Mashhad, Iran. **International Journal of Production Economics**, v. 292, n. December 2024, 2025.

LEMMENS, S. et al. A review of integrated supply chain network design models: Key issues for vaccine supply chains. **Chemical Engineering Research and Design**, v. 109, p. 366–384, 2016.

LIGHT, D. W.; ANDRUS, J. K.; WARBURTON, R. N. Estimated research and development costs of rotavirus vaccines. **Vaccine**, v. 27, n. 47, p. 6627–6633, 2009.

LIN, Q.; ZHAO, Q.; LEV, B. Cold chain transportation decision in the vaccine supply chain. **European**

Journal of Operational Research, v. 283, n. 1, p. 182–195, 2020.

LONGINI, I. M.; ACKERMAN, E.; ELVEBACK, L. R. An optimization model for influenza A epidemics. **Mathematical Biosciences**, v. 38, n. 1–2, p. 141–157, 1978.

LOPES, J. M. et al. Optimization methods for large-scale vaccine supply chains: a rapid review. **Annals of Operations Research**, v. 316, n. 1, p. 699–721, 2022.

LOPES, J. M. **Stochastic optimization and machine learning applied in the demand forecast, allocation and distribution of vaccines between Brazilian states**. [s.l.] Universidade Federal de São Paulo, 2022.

MAK, H. Y.; DAI, T.; TANG, C. S. Managing two-dose COVID-19 vaccine rollouts with limited supply: Operations strategies for distributing time-sensitive resources. **Production and Operations Management**, v. 31, n. 12, p. 4424–4442, 2022.

MARMOT, M.; ALLEN, J. J. **Social determinants of health equity**. **American Journal of Public Health**, 2014.

MARTONOSI, S. E.; BEHZAD, B.; CUMMINGS, K. Pricing the COVID-19 vaccine: A mathematical approach. **Omega (United Kingdom)**, v. 103, p. 102451, 2021.

MATRAJT, L.; HALLORAN, M. E.; LONGINI, I. M. Optimal Vaccine Allocation for the Early Mitigation of Pandemic Influenza. **PLoS Computational Biology**, v. 9, n. 3, 2013.

MCGEE, R. S. **SEIRS Model Description**. Disponível em: <https://github.com/ryansmcgee/seirsplus/wiki/SEIRS-Model-Description>. Acesso em: 16 feb. 2023.

MEDLOCK, J.; MEYERS, L.; GALVANI, A. Optimizing allocation for a delayed influenza vaccination campaing. **Plos Currents**, v. 9, 2009.

MG_GOV. **Local Warehouses**. Disponível em: <https://www.saude.mg.gov.br/sobre/institucional/superintendencias-regionais-de-saude/>. Acesso em: 15 sep. 2025.

MICHELON, C. M. Principais variantes do SARS-CoV-2 notificadas no Brasil. **Revista Brasileira de Análises Clínicas**, v. 53(2), p. 109–116, 2021.

MIHIGO, R. M. et al. Investing in life saving vaccines to guarantee life of future generations in Africa. **Vaccine**, v. 34, n. 48, p. 5827–5832, 2016.

MINGOZZI, A.; ROBERTI, R.; TOTH, P. An exact algorithm for the multitrip vehicle routing problem. **INFORMS Journal on Computing**, v. 25, n. 2, p. 193–207, 2013.

MINOZA, J. M. A.; BONGOLAN, V. P.; RAYO, J. F. COVID-19 Agent-Based Model with Multi-objective Optimization for Vaccine Distribution. v. 2, 2021.

MOALLA, N.; BOURAS, A.; NEUBERT, G. A framework to optimize production planning in the vaccine industry. **IFIP International Federation for Information Processing**, v. 246, p. 205–212, 2007.

MOHAMMADI, M. et al. Bi-objective optimization of a stochastic resilient vaccine distribution network in the context of the COVID-19 pandemic. **Omega (United Kingdom)**, v. 113, p. 102725, 2022.

MOORE, S. et al. Retrospectively modeling the effects of increased global vaccine sharing on the COVID-19 pandemic. **Nature Medicine**, v. 28, n. 11, p. 2416–2423, 2022.

MUNGUÍA-LÓPEZ, A. DEL C.; PONCE-ORTEGA, J. M. Fair Allocation of Potential COVID-19 Vaccines Using an Optimization-Based Strategy. **Process Integration and Optimization for Sustainability**, v. 5, n. 1, p. 3–12, 2021.

NATURE. **Vaccination rates are falling, and it's not just the COVID-19 vaccine that people are refusing**. Disponível em: <https://www.nature.com/articles/d41586-022-04341-9>. Acesso em: 3 aug. 2023.

NDEFFO MBAH, M. L. et al. Country- and age-specific optimal allocation of dengue vaccines. **Journal of Theoretical Biology**, v. 342, p. 15–22, 2014.

NEIRA, D. A. et al. New compact integer programming formulations for the multi-trip vehicle routing problem with time windows. **Computers and Industrial Engineering**, v. 144, n. March, p. 106399, 2020.

OLIVERA, A.; VIERA, O. Adaptive memory programming for the vehicle routing problem with multiple trips. **Computers and Operations Research**, v. 34, n. 1, p. 28–47, 2007.

OPAS. **Poliomielite**. Disponível em: <https://www.paho.org/pt/topicos/poliomielite>. Acesso em: 3 nov. 2023.

PAES, N. A.; FERREIRA, A. M. S.; MOURA, L. DE A. Proposta metodológica para avaliação de registros de óbitos por COVID-19. **Cadernos de Saúde Pública**, v. 39, n. 1, p. e00096722, 16 Jan. 2023.

PAHO. **Atualização epidemiológica: Variantes de SARS-CoV-2 nas Américas (26 de janeiro de 2021)**. [s.l: s.n.]. Disponível em: <https://iris.paho.org/handle/10665.2/53234>.

PATEL, R.; LONGINI, I. M.; HALLORAN, M. E. Finding optimal vaccination strategies for pandemic influenza using genetic algorithms. **Journal of Theoretical Biology**, v. 234, n. 2, p. 201–212, 2005.

PRINS, C. Efficient Heuristics for the Heterogeneous Fleet Multitrip VRP with Application to a Large-Scale Real Case. **Journal of Mathematical Modelling and Algorithms**, v. 1, n. 2, p. 135–150, 2002.

PYTHON. **Python**. Disponível em: <https://www.python.org/>. Acesso em: 1 sep. 2025.

RAO, I. J.; BRANDEAU, M. L. Optimal allocation of limited vaccine to control an infectious disease: Simple analytical conditions. **Mathematical Biosciences**, v. 337, n. February, p. 108621, 2021.

RASTEGAR, M. et al. An inventory-location optimization model for equitable influenza vaccine distribution in developing countries during the COVID-19 pandemic. **Vaccine**, v. 39, n. 3, p. 495–504, 2021.

REY, D.; HAMMAD, A. W.; SABERI, M. Vaccine allocation policy optimization and budget sharing mechanism using reinforcement learning. **Omega (United Kingdom)**, v. 115, p. 102783, 2023.

RIBEIRO, D. et al. Design and planning of Vaccine Supply Chains Biomedical Engineering Examination Committee. n. November, 2016.

ROY, S.; DUTTA, R.; GHOSH, P. Optimal time-varying vaccine allocation amid pandemics with uncertain immunity ratios. **IEEE Access**, v. 9, p. 15110–15121, 2021.

SADJADI, S. J.; ZIAEI, Z.; PISHVAEE, M. S. The design of the vaccine supply network under uncertain condition: A robust mathematical programming approach. **Journal of Modelling in Management**, v. 14, n. 4, p. 841–871, 2019.

SAVACHKIN, A.; URIBE, A. Dynamic redistribution of mitigation resources during influenza pandemics. **Socio-Economic Planning Sciences**, v. 46, n. 1, p. 33–45, 2012.

SCIPY. **solve_ivp**. Disponível em: <https://docs.scipy.org/doc/scipy/reference/generated/scipy.integrate.solve_ivp.html>. Acesso em: 20 aug. 2025.

ŞEN, A.; BÜLBÜL, K. A survey on multi trip vehicle routing problem. **International Logistics & Supply Chain Congress**, p. 401–407, 2008.

SOUZA, L. P. D. S. et al. **Vaccine Cold Chain in Brazilian Health System: A Logistics Assessment**. [s.l.] Springer International Publishing, 2019.

SUN, X.; ANDOH, E. A.; YU, H. A simulation-based analysis for effective distribution of COVID-19 vaccines: A case study in Norway. **Transportation Research Interdisciplinary Perspectives**, v. 11, p. 100453, 2021.

TAVANA, M. et al. A mathematical programming approach for equitable COVID-19 vaccine distribution in developing countries. **Annals of Operations Research**, p. 1–34, 2021.

THUL, L.; POWELL, W. Stochastic optimization for vaccine and testing kit allocation for the COVID-19 pandemic. **European Journal of Operational Research**, v. 304, n. 1, p. 325–338, 2023.

TOTH, P.; VIGO, D. The vehicle routing problem. Monographs on discrete mathematics and applications. In: **SIAM**. Philadelphi: [s.n.]. p. 1–26.

TSIRIMPAS, P. et al. Single vehicle routing with a predefined customer sequence and multiple depot returns. **European Journal of Operational Research**, v. 187, n. 2, p. 483–495, 2008.

UNICEF. **Pandemia de covid-19 alimenta o maior retrocesso contínuo nas vacinações em três décadas**. Disponível em: <https://www.unicef.org/brazil/comunicados-de-imprensa/pandemia-de-covid-19-alimenta-o-maior-retrocesso-continuo-nas-vacinacoes-em-tres-decadas>. Acesso em: 19 feb. 2025.

VALIZADEH, J. et al. Designing an optimization model for the vaccine supply chain during the COVID-19 pandemic. **Expert Systems with Applications**, v. 214, n. October 2022, 2023.

VIRACOPOS. **Tabela de Preços Serviços Aéreos**. Disponível em: <https://www.viracopos.com/pt_br/cargo/tabela-de-valores.htm?>.

WANG, D. et al. Supply chains create global benefits from improved vaccine accessibility. **Nature Communications**, v. 14, n. 1, 2023.

WHO. **Pandemia de COVID-19 leva a grande retrocesso na vacinação infantil, mostram novos dados da OMS e UNICEF**. Disponível em: <https://www.paho.org/pt/noticias/15-7-2021-pandemia-covid-19-leva-grande-retrocesso-na-vacinacao-infantil-mostram-novos>. Acesso em: 19 feb. 2025a.

WHO. Implementing the Immunization Agenda 2030. **Who**, p. 1–32, 2021b.

WHO. **Essential Programme on Immunization: Supply chain and logistics**. Disponível em: <https://www.who.int/teams/immunization-vaccines-and-biologicals/essential-programme-on-immunization/supply-chain/>. Acesso em: 3 aug. 2023.

WHO. **Essential Programme on Immunization**. Disponível em:

<https://www.who.int/teams/immunization-vaccines-and-biologicals/essential-programme-on-immunization>. Acesso em: 21 oct. 2024a.

WHO. Immunization agenda 2030: A global strategy to leave no one behind. **Vaccine**, v. 42, p. S5–S14, 2024b.

YANG, T. et al. Comparison of health-oriented cross-regional allocation strategies for the COVID-19 vaccine: a mathematical modelling study. **Annals of Medicine**, v. 54, n. 1, p. 941–952, 2022.

YARMAND, H. et al. Optimal two-phase vaccine allocation to geographically different regions under uncertainty. **European Journal of Operational Research**, v. 233, n. 1, p. 208–219, 2014.

YU, Z. et al. A mixed integer programming model for vaccine pricing within a group purchasing organization. **Vaccine**, v. 42, n. 8, p. 1892–1898, 2024.

ZHANG, J.; LONG, D. Z.; LI, Y. A reliable emergency logistics network for COVID-19 considering the uncertain time-varying demands. **Transportation Research Part E: Logistics and Transportation Review**, v. 172, n. September 2022, p. 103087, 2023.

ZHANG, X. et al. Applications and comparisons of four time series models in epidemiological surveillance data. **PLoS ONE**, v. 9, n. 2, p. 1–16, 2014.

Annex A: Description and References of Models and Solver

Table 32 - Methods description and references

Method description	For reference address
Linear Programming (LP): Linear optimization, also known as linear programming (LP), is a mathematical method used to determine the best possible outcome in a given mathematical model. When the objective function and the constraints are linear equations or inequalities, the problem is classified as a linear optimization problem.	Bertsimas and Tsitsiklis (1997) and Wolsey (1998).
Nonlinear Programming (NLP): class of mathematical optimization problems that aims to minimize (or maximize) a function subject to a constraint, where one of the objective and/or constraints is nonlinear.	Kuhn and Tucker (1951) and Nocedal and Wright (2006).
Mixed Integer Programming (MIP): optimization problem that has continuous variables and integer variables (often binary), which aims to optimize an objective function subject to constraints, which may be linear or non-linear.	Wolsey (1998) and Nemhauser and Wolsey (1988).
Mixed-Integer Linear Programming (MILP): optimization problem in which the objective function and all constraints are linear, with continuous and integer (often binary) decision variables.	Bertsimas and Tsitsiklis (1997) and Wolsey (1998).
Mixed-Integer Nonlinear Programming (MINLP): refers to the class of optimization problems in which the decision variables can be both continuous and integer variables, and the objective function and/or constraints include nonlinear expressions.	Floudas (1995) and Tawarmalani and Sahinidis (2002).
Deterministic Model (DM): analytical or optimization formulation in which the parameters are treated as known and fixed, without explicit randomness.	Bertsimas and Tsitsiklis (1997) and Hillier and Lieberman (2024).
Robust Optimization (RO): optimization under parameter uncertainty, in which uncertain are assumed to belong to a prescribed uncertainty set. The objective is to obtain decisions that remain feasible for all scenarios in the uncertainty set and to optimize worst-case performance.	Bertsimas and Sim (2004) and Ben-Tal and Nemirovski (2000).
Stochastic Optimization (SO): encompasses optimization problems in which uncertainty is explicitly modeled as a random element affecting the objective and/or constraints. Decisions are chosen to optimize a criterion defined over the probability distribution.	Lopes (2022) and Shapiro, Dentcheva, and Ruszczyński (2009).

Stochastic Programming (SP): class of SO that models uncertainty by a scenario-based representation of random parameters and organizes decisions in two-stage or multi-stage structures.	Shapiro, Dentcheva, and Ruszczyński (2009) and Thul and Powell (2023).
Robust Stochastic Programming (RSP): hybrid framework that combines stochastic programming with robust optimization. Instead of assuming that the probability model is fully known, RSP aim decisions that perform well (and remain feasible) under a family of possibles probability distributions, optimizing a worst-case expected criterion.	Shapiro (2017) and Jahed, Molana and Tavakkoli-Moghaddam (2025).
Machine Learning (ML): comprises statistical and computational methods that infer predictive models or decision rules from data by optimizing a learning objective over a hypothesis class.	Lopes (2022) and Bishop (2006).
Particle Swarm Optimization (PSO): population-based metaheuristic inspired by social behavior of swarms. Candidate solutions (particles) move through the search space using velocity updates influenced by individual and global best positions; used for complex, nonconvex tuning and routing variants.	Kennedy and Eberhart (1995) and Yang et al. (2022).
Genetic Algorithms (AG): evolutionary metaheuristics that iteratively improve a population of solutions through selection, crossover, and mutation.	Patel, Longini, and Halloran (2005) and Kheybari et al. (2025).
Simulation (SIM): model-based methodology in which a formal representation of a system (real or proposed) is executed to generate time-ordered behavior and to estimate performance measures under specified operating conditions and decision rules.	Banks et al. (1984) and Fishman (1996).
System Dynamics (DM): methodology for modeling and simulating the behavior of complex systems over time. SD models formalize system structure through compartments (state variables), flows (rates of change), and auxiliary variables linked by feedback loops (reinforcing and balancing), implemented as a set of (often nonlinear) differential equations.	Forrester (1968) and McGee (2023).
Non-Dominated Sorting Genetic Algorithm II (NSGA-II:): multi-objective evolutionary algorithm designed to approximate the Pareto-optimal set for problems with two or more conflicting objectives. NSGA-II maintains a population of candidate solutions and iteratively applies selection, crossover, and mutation, while ranking solutions via fast non-dominated sorting into Pareto fronts (front 1 = nondominated, front two dominated only by front 1, etc.). To preserve solution diversity along the trade-off surface, it uses a crowding-distance measure and performs crowding-comparison during selection.	Jahed, Molana and Tavakkoli-Moghaddam (2025).

Multi-Objective Particle Swarm Optimization (MOPSO): swarm metaheuristic that extends classical PSO to multi-objective optimization, where the goal is to approximate the Pareto front rather than a single optimum. In MOPSO, each particle represents a candidate solution whose position is updated via PSO dynamics, but the notion of "best" is defined through Pareto dominance.	
Multi-Objective Grey Wolf Optimizer (MOGWO): elitist swarm-intelligence metaheuristic for multi-objective optimization that extends the Grey Wolf Optimizer (GWO) by replacing the single "best solution" concept with Pareto dominance and maintaining an approximation of the Pareto front via an external archive of non-dominated solutions.	
Gurobi: type of software known as a solver. Given a model, the Gurobi program executes numerical and combinatorial algorithms to find an optimal solution (or the best available solution within time/tolerance limits) and, when possible, to certify the optimality, infeasibility, or failure of the model.	Gurobi (2025).

Annex B: Travel times and costs matrices

Table 33 - Truck travel times (in hours)

Origin	AC	AL	AM	AP	BA	CE	DF	ES	GO	MA	MG	MS	MT	PA	PB	PE	PI	PR	RJ	RN	RO	RR	RS	SC	SE	SP	TO
AC	0,0	63,0	18,1	55,0	55,7	67,5	39,0	51,4	36,6	62,1	44,8	33,6	24,9	61,6	67,0	65,5	61,3	45,9	50,1	69,2	6,8	27,9	52,5	49,7	59,5	45,1	47,1
AL	63,0	0,0	68,6	44,0	7,9	13,4	24,1	21,1	26,3	20,9	23,2	38,0	38,1	27,2	4,9	3,6	15,5	35,9	26,6	7,2	56,3	78,5	44,7	39,6	3,7	30,7	23,1
AM	18,1	68,6	0,0	37,6	62,6	72,0	43,6	56,0	41,1	66,7	49,4	38,1	29,5	66,2	72,6	71,2	65,8	50,5	54,7	74,8	11,3	9,8	57,0	54,3	65,2	49,6	51,8
AP	55,0	44,0	37,6	0,0	45,2	38,1	22,4	52,6	37,9	29,9	46,2	39,3	30,6	23,8	44,4	44,0	30,7	51,6	54,7	44,8	48,6	28,6	56,9	55,4	44,1	49,6	28,0
BA	55,7	7,9	62,6	45,2	0,0	17,4	18,1	15,0	20,5	20,0	17,2	32,1	32,1	26,3	11,9	10,5	14,5	29,8	20,6	14,1	50,3	71,9	38,6	33,5	4,5	24,5	18,2
CE	67,5	13,4	72,0	38,1	17,4	0,0	27,6	30,0	31,0	13,4	31,6	42,6	42,6	20,1	8,6	10,0	7,9	44,3	35,1	6,7	60,8	81,9	53,0	48,0	14,8	39,1	25,4
DF	39,0	24,1	43,6	22,4	18,1	27,5	0,0	15,5	2,6	27,0	9,3	14,2	14,2	26,8	28,1	26,7	22,4	17,1	14,4	30,3	32,4	53,4	25,3	20,9	20,6	12,7	12,2
ES	51,4	21,1	56,0	52,6	15,0	30,0	15,5	0,0	17,9	32,6	6,6	23,7	26,5	38,9	25,0	23,6	27,1	16,3	6,5	27,2	44,7	65,8	25,0	20,0	17,6	11,0	27,7
GO	36,6	26,6	41,1	37,9	20,5	31,0	2,6	17,9	0,0	25,7	11,3	11,7	11,7	25,2	30,5	29,2	24,8	14,8	16,7	32,7	29,9	51,0	23,1	18,7	23,1	11,6	10,9
MA	62,1	20,9	66,7	29,9	20,0	13,4	27,0	32,6	25,7	0,0	34,2	37,2	37,2	10,1	20,8	19,7	5,6	40,4	37,7	20,1	55,4	76,5	48,6	44,2	19,7	37,1	17,3
MG	44,8	23,2	49,4	46,2	17,2	31,6	9,0	6,6	11,3	34,2	0,0	18,2	19,9	35,3	27,1	25,8	28,8	12,6	5,4	29,4	38,1	59,2	21,4	16,3	19,7	7,3	21,1
MS	33,6	38,0	38,1	39,3	32,1	42,6	14,2	23,7	11,7	37,2	18,2	0,0	8,7	36,8	42,0	40,6	36,4	12,4	18,1	44,2	26,9	48,0	19,0	16,2	34,6	12,7	22,3
MT	24,9	38,1	29,5	30,6	32,1	42,6	14,2	26,5	11,7	37,2	19,9	8,7	0,0	36,8	42,1	40,7	36,4	21,0	25,2	44,3	18,2	39,3	27,6	24,8	34,7	20,2	22,3
PA	61,6	27,2	66,2	23,8	26,3	20,1	26,5	38,9	25,2	10,1	35,3	36,8	36,8	0,0	27,0	25,9	11,8	39,9	40,6	26,4	55,0	76,0	48,2	43,8	26,0	36,7	16,0
PB	67,0	4,9	72,6	44,4	11,9	8,6	28,1	25,0	30,5	20,8	27,1	42,0	42,1	27,0	0,0	1,5	15,3	39,9	30,6	2,3	60,3	81,7	48,6	43,6	7,6	34,6	28,2
PE	65,5	3,6	71,2	44,0	10,5	10,0	26,7	23,6	29,2	19,7	25,8	40,6	40,7	25,9	1,5	0,0	14,2	38,5	29,2	3,7	58,9	81,0	47,2	42,2	6,3	33,3	25,7
PI	61,3	15,5	65,8	30,7	14,5	7,9	22,4	27,1	24,8	5,6	28,8	36,4	36,4	11,8	15,3	14,2	0,0	39,3	32,2	14,6	54,6	75,7	47,6	43,1	14,3	34,9	17,5
PR	45,9	35,9	50,5	51,6	29,8	44,3	17,1	16,3	14,8	40,4	12,6	12,4	21,0	39,9	39,9	38,5	39,3	0,0	10,7	42,1	39,2	60,3	8,9	3,8	32,4	5,1	25,5
RJ	50,1	26,6	54,7	54,7	20,6	35,1	14,4	6,5	16,7	37,7	5,4	18,1	25,2	40,6	30,6	29,2	32,2	10,7	0,0	32,8	43,4	64,5	19,4	14,3	23,2	5,4	26,6
RN	69,2	7,2	74,8	44,8	14,1	6,7	30,3	27,2	32,7	20,1	29,4	44,2	44,3	26,4	2,3	3,7	14,6	42,1	32,8	0,0	62,5	84,6	50,8	45,8	9,9	36,8	29,3
RO	6,8	56,3	11,3	48,6	50,3	60,8	32,4	44,7	29,9	55,4	38,1	26,9	18,2	55,0	60,3	58,9	54,6	39,2	43,4	62,5	0,0	21,1	45,8	43,0	52,9	38,4	40,5
RR	27,9	78,5	9,8	28,6	72,4	81,9	53,4	65,8	51,0	76,5	59,2	48,0	39,3	76,0	82,4	81,0	75,7	60,3	64,5	84,6	21,1	0,0	66,9	64,1	75,0	59,5	61,6
RS	52,5	44,7	57,0	56,9	38,6	53,0	25,3	25,0	23,1	48,6	21,4	19,0	27,6	48,2	48,6	47,2	47,6	8,9	19,4	50,8	45,8	66,9	0,0	6,0	41,2	13,9	34,3
SC	49,7	39,6	55,5	55,4	33,5	48,0	20,9	20,0	18,7	44,2	16,3	16,2	24,8	43,8	43,6	42,2	43,1	3,8	14,3	45,8	43,0	64,1	6,0	0,0	36,2	8,8	29,2
SE	59,5	3,7	65,2	44,1	4,5	14,8	20,7	17,6	23,1	19,7	19,7	34,6	34,7	26,0	7,6	6,3	14,3	32,4	23,2	9,9	52,9	75,0	41,2	36,2	0,0	27,3	20,8
SP	45,1	30,7	49,6	49,6	24,5	39,1	12,7	11,0	11,6	37,1	7,3	12,7	20,2	36,7	34,6	33,3	34,9	5,1	5,4	36,8	38,4	59,5	13,9	8,8	27,4	3,8	22,2
TO	47,1	23,1	51,8	28,0	18,2	25,4	12,2	27,7	10,9	17,3	21,1	22,3	22,3	16,0	28,2	25,7	17,5	25,5	26,6	29,3	40,5	61,6	34,3	29,2	20,8	22,2	0,0

Table 34 - Airplane travel times (in hours)

Origin	AC	AL	AM	AP	BA	CE	DF	ES	GO	MA	MG	MS	MT	PA	PB	PE	PI	PR	RJ	RN	RO	RR	RS	SC	SE	SP	TO
AC	0,0	6,3	1,8	5,5	5,6	6,7	3,9	5,1	3,7	6,2	4,5	3,4	2,5	6,2	6,7	6,6	6,1	4,6	5,0	6,9	0,7	2,8	5,2	5,0	6,0	4,5	4,7
AL	6,3	0,0	6,9	4,4	0,8	1,3	2,4	2,1	2,6	2,1	2,3	3,8	3,8	2,7	0,5	0,4	1,5	3,6	2,7	0,7	5,6	7,8	4,5	4,0	0,4	3,1	2,3
AM	1,8	6,9	0,0	3,8	6,3	7,2	4,4	5,6	4,1	6,7	4,9	3,8	2,9	6,6	7,3	7,1	6,6	5,0	5,5	7,5	1,1	1,0	5,7	5,4	6,5	5,0	5,2
AP	5,5	4,4	3,8	0,0	4,5	3,8	2,2	5,3	3,8	3,0	4,6	3,9	3,1	2,4	4,4	4,4	3,1	5,2	5,5	4,5	4,9	2,9	5,7	5,5	4,4	5,0	2,8
BA	5,6	0,8	6,3	4,5	0,0	1,7	1,8	1,5	2,1	2,0	1,7	3,2	3,2	2,6	1,2	1,0	1,5	3,0	2,1	1,4	5,0	7,2	3,9	3,4	0,4	2,5	1,8
CE	6,7	1,3	7,2	3,8	1,7	0,0	2,8	3,0	3,1	1,3	3,2	4,3	4,3	2,0	0,9	1,0	0,8	4,4	3,5	0,7	6,1	8,2	5,3	4,8	1,5	3,9	2,5
DF	3,9	2,4	4,4	2,2	1,8	2,8	0,0	1,5	0,3	2,7	0,9	1,4	1,4	2,7	2,8	2,7	2,2	1,7	1,4	3,0	3,2	5,3	2,5	2,1	2,1	1,3	1,2
ES	5,1	2,1	5,6	5,3	1,5	3,0	1,5	0,0	1,8	3,3	0,7	2,4	2,6	3,9	2,5	2,4	2,7	1,6	0,7	2,7	4,5	6,6	2,5	2,0	1,8	1,1	2,8
GO	3,7	2,7	4,1	3,8	2,1	3,1	0,3	1,8	0,0	2,6	1,1	1,2	1,2	2,5	3,1	2,9	2,5	1,5	1,7	3,3	3,0	5,1	2,3	1,9	2,3	1,2	1,1
MA	6,2	2,1	6,7	3,0	2,0	1,3	2,7	3,3	2,6	0,0	3,4	3,7	3,7	1,0	2,1	2,0	0,6	4,0	3,8	2,0	5,5	7,7	4,9	4,4	2,0	3,7	1,7
MG	4,5	2,3	4,9	4,6	1,7	3,2	0,9	0,7	1,1	3,4	0,0	1,8	2,0	3,5	2,7	2,6	2,9	1,3	0,5	2,9	3,8	5,9	2,1	1,6	2,0	0,7	2,1
MS	3,4	3,8	3,8	3,9	3,2	4,3	1,4	2,4	1,2	3,7	1,8	0,0	0,9	3,7	4,2	4,1	3,6	1,2	1,8	4,4	2,7	4,8	1,9	1,6	3,5	1,3	2,2
MT	2,5	3,8	2,9	3,1	3,2	4,3	1,4	2,6	1,2	3,7	2,0	0,9	0,0	3,7	4,2	4,1	3,6	2,1	2,5	4,4	1,8	3,9	2,8	2,5	3,5	2,0	2,2
PA	6,2	2,7	6,6	2,4	2,6	2,0	2,7	3,9	2,5	1,0	3,5	3,7	3,7	0,0	2,7	2,6	1,2	4,0	4,1	2,6	5,5	7,6	4,8	4,4	2,6	3,7	1,6
PB	6,7	0,5	7,3	4,4	1,2	0,9	2,8	2,5	3,1	2,1	2,7	4,2	4,2	2,7	0,0	0,2	1,5	4,0	3,1	0,2	6,0	8,2	4,9	4,4	0,8	3,5	2,8
PE	6,6	0,4	7,1	4,4	1,0	1,0	2,7	2,4	2,9	2,0	2,6	4,1	4,1	2,6	0,2	0,0	1,4	3,8	2,9	0,4	5,9	8,1	4,7	4,2	0,6	3,3	2,6
PI	6,1	1,5	6,6	3,1	1,5	0,8	2,2	2,7	2,5	0,6	2,9	3,6	3,6	1,2	1,5	1,4	0,0	3,9	3,2	1,5	5,5	7,6	4,8	4,3	1,4	3,5	1,8
PR	4,6	3,6	5,0	5,2	3,0	4,4	1,7	1,6	1,5	4,0	1,3	1,2	2,1	4,0	4,0	3,8	3,9	0,0	1,1	4,2	3,9	6,0	0,9	0,4	3,2	0,5	2,5
RJ	5,0	2,7	5,5	5,5	2,1	3,5	1,4	0,7	1,7	3,8	0,5	1,8	2,5	4,1	3,1	2,9	3,2	1,1	0,0	3,3	4,3	6,4	1,9	1,4	2,3	0,5	2,7
RN	6,9	0,7	7,5	4,5	1,4	0,7	3,0	2,7	3,3	2,0	2,9	4,4	4,4	2,6	0,2	0,4	1,5	4,2	3,3	0,0	6,2	8,5	5,1	4,6	1,0	3,7	2,9
RO	0,7	5,6	1,1	4,9	5,0	6,1	3,2	4,5	3,0	5,5	3,8	2,7	1,8	5,5	6,0	5,9	5,5	3,9	4,3	6,2	0,0	2,1	4,6	4,3	5,3	3,8	4,1
RR	2,8	7,8	1,0	2,9	7,2	8,2	5,3	6,6	5,1	7,7	5,9	4,8	3,9	7,6	8,2	8,1	7,6	6,0	6,4	8,5	2,1	0,0	6,7	6,4	7,5	5,9	6,2
RS	5,2	4,5	5,7	5,7	3,9	5,3	2,5	2,5	2,3	4,9	2,1	1,9	2,8	4,8	4,9	4,7	4,8	0,9	1,9	5,1	4,6	6,7	0,0	0,6	4,1	1,4	3,4
SC	5,0	4,0	5,6	5,5	3,4	4,8	2,1	2,0	1,9	4,4	1,6	1,6	2,5	4,4	4,4	4,2	4,3	0,4	1,4	4,6	4,3	6,4	0,6	0,0	3,6	0,9	2,9
SE	6,0	0,4	6,5	4,4	0,4	1,5	2,1	1,8	2,3	2,0	2,0	3,5	3,5	2,6	0,8	0,6	1,4	3,2	2,3	1,0	5,3	7,5	4,1	3,6	0,0	2,7	2,1
SP	4,5	3,1	5,0	5,0	2,5	3,9	1,3	1,1	1,2	3,7	0,7	1,3	2,0	3,7	3,5	3,3	3,5	0,5	0,5	3,7	3,8	5,9	1,4	0,9	2,7	0,4	2,2
TO	4,7	2,3	5,2	2,8	1,8	2,5	1,2	2,8	1,1	1,7	2,1	2,2	2,2	1,6	2,8	2,6	1,8	2,5	2,7	2,9	4,1	6,2	3,4	2,9	2,1	2,2	0,0

Table 35 – Cost Matrice (US$)

Vehicle	Origin	AC	AL	AM	AP	BA	CE	DF	ES	GO	MA	MG	MS	MT	PA	PB	PE	PI	PR	RJ	RN	RO	RR	RS	SC	SE	SP	TO
Truck	AC	-	-	-	-	-	-	-	-	-	-	-	-	-	-	-	-	-	-	-	-	519.163	-	-	-	-	-	-
Truck	AL	-	-	-	-	603.146	-	-	-	-	-	-	-	-	-	376.966	271.988	-	-	-	545.885	-	-	-	-	280.577	-	-
Truck	AM	-	-	-	-	-	-	-	-	-	-	-	-	-	-	-	-	-	-	-	-	-	749.160	-	-	-	-	-
Truck	AP	-	-	-	-	-	-	-	-	-	-	-	-	-	-	-	-	-	-	-	-	-	-	-	-	-	-	-
Truck	BA	-	603.146	-	-	-	-	-	-	-	-	-	-	-	-	-	-	-	-	-	-	-	-	-	-	339.747	-	-
Truck	CE	-	-	-	-	-	-	-	-	-	-	-	-	-	-	656.589	763.475	605.054	-	-	512.483	-	-	-	-	-	-	-
Truck	DF	-	-	-	-	-	-	-	-	199.458	-	707.169	-	-	-	-	-	-	-	-	-	-	-	-	-	-	-	-
Truck	ES	-	-	-	-	-	-	-	-	-	-	500.076	-	-	-	-	-	-	-	497.213	-	-	-	-	-	-	841.732	-
Truck	GO	-	-	-	-	-	-	199.458	-	-	-	-	-	-	-	-	-	-	-	-	-	-	-	-	-	-	883.723	-
Truck	MA	-	-	-	-	-	-	-	-	-	-	-	-	-	-	-	-	425.638	-	-	-	-	-	-	-	-	-	-
Truck	MG	-	-	-	-	-	-	683.310	500.076	-	-	-	-	-	-	-	-	-	-	414.185	-	-	-	-	-	-	559.246	-
Truck	MS	-	-	-	-	-	-	-	-	-	-	-	-	662.315	-	-	-	-	-	-	-	-	-	-	-	-	-	-
Truck	MT	-	-	-	-	-	-	-	-	-	-	-	662.315	-	-	-	-	-	-	-	-	-	-	-	-	-	-	-
Truck	PA	-	-	-	-	-	-	-	-	-	-	-	-	-	-	-	-	-	-	-	-	-	-	-	-	-	-	-
Truck	PB	-	376.966	-	-	-	656.589	-	-	-	-	-	-	-	-	-	114.521	-	-	-	176.554	-	-	-	-	583.104	-	-
Truck	PE	-	271.988	-	-	-	763.475	-	-	-	-	-	-	-	-	114.521	-	-	-	-	283.440	-	-	-	-	478.126	-	-
Truck	PI	-	-	-	-	-	605.054	-	-	-	425.638	-	-	-	-	-	-	-	-	-	-	-	-	-	-	-	-	-
Truck	PR	-	-	-	-	-	-	-	-	-	-	-	-	-	-	-	-	-	-	-	-	-	-	678.539	286.303	-	389.372	-
Truck	RJ	-	-	-	-	-	-	-	497.213	-	-	414.185	-	-	-	-	-	-	-	-	-	-	-	-	-	-	409.414	-
Truck	RN	-	545.885	-	-	-	512.483	-	-	-	-	-	-	-	-	176.554	283.440	-	-	-	-	-	-	-	-	752.023	-	-
Truck	RO	519.163	-	-	-	-	-	-	-	-	-	-	-	-	-	-	-	-	-	-	-	-	-	-	-	-	-	-
Truck	RR	-	-	749.160	-	-	-	-	-	-	-	-	-	-	-	-	-	-	-	-	-	-	-	-	-	-	-	-
Truck	RS	-	-	-	-	-	-	-	-	-	-	-	-	-	-	-	-	-	678.539	-	-	-	-	-	454.268	-	-	-
Truck	SC	-	-	-	-	-	-	-	-	-	-	-	-	-	-	-	-	-	286.303	-	-	-	-	454.268	-	-	672.813	-
Truck	SE	-	280.577	-	-	339.747	-	-	-	-	-	-	-	-	-	583.104	478.126	-	-	-	752.023	-	-	-	-	-	-	-
Truck	SP	-	-	-	-	-	-	968.659	841.732	883.723	-	559.246	-	-	-	-	-	-	389.372	409.414	-	-	-	-	672.813	-	286.303	-
Truck	TO	-	-	-	-	-	-	-	-	-	-	-	-	-	-	-	-	-	-	-	-	-	-	-	-	-	-	-
Airplane	AC	-	-	-	-	-	-	-	-	-	-	-	-	-	-	-	-	-	-	-	-	-	-	-	-	-	4815.239	-
Airplane	AL	-	-	-	-	-	-	-	-	-	-	-	-	-	-	-	-	-	-	-	-	-	-	-	-	-	3277.409	-
Airplane	AM	-	-	-	-	-	-	-	-	-	-	-	-	-	-	-	-	-	-	-	-	-	-	-	-	-	5305.581	-
Airplane	AP	-	-	-	-	-	-	-	-	-	-	-	-	-	-	-	-	-	-	-	-	-	-	-	-	-	5305.581	-
Airplane	BA	-	-	-	-	-	-	-	-	-	-	-	-	-	-	-	-	-	-	-	-	-	-	-	-	-	2621.393	-
Airplane	CE	-	-	-	-	-	-	-	-	-	-	-	-	-	-	-	-	-	-	-	-	-	-	-	-	-	4177.928	-
Airplane	DF	-	-	-	-	-	-	-	-	-	-	-	-	-	-	-	-	-	-	-	-	-	-	-	-	-	1356.123	-
Airplane	ES	-	-	-	-	-	-	-	-	-	-	-	-	-	-	-	-	-	-	-	-	-	-	-	-	-	1178.424	-
Airplane	GO	-	-	-	-	-	-	-	-	-	-	-	-	-	-	-	-	-	-	-	-	-	-	-	-	-	1237.212	-
Airplane	MA	-	-	-	-	-	-	-	-	-	-	-	-	-	-	-	-	-	-	-	-	-	-	-	-	-	3968.163	-
Airplane	MG	-	-	-	-	-	-	-	-	-	-	-	-	-	-	-	-	-	-	-	-	-	-	-	-	-	782.944	-
Airplane	MS	-	-	-	-	-	-	-	-	-	-	-	-	-	-	-	-	-	-	-	-	-	-	-	-	-	1354.787	-
Airplane	MT	-	-	-	-	-	-	-	-	-	-	-	-	-	-	-	-	-	-	-	-	-	-	-	-	-	2156.436	-
Airplane	PA	-	-	-	-	-	-	-	-	-	-	-	-	-	-	-	-	-	-	-	-	-	-	-	-	-	3918.728	-
Airplane	PB	-	-	-	-	-	-	-	-	-	-	-	-	-	-	-	-	-	-	-	-	-	-	-	-	-	3700.947	-
Airplane	PE	-	-	-	-	-	-	-	-	-	-	-	-	-	-	-	-	-	-	-	-	-	-	-	-	-	3553.978	-
Airplane	PI	-	-	-	-	-	-	-	-	-	-	-	-	-	-	-	-	-	-	-	-	-	-	-	-	-	3730.341	-
Airplane	PR	-	-	-	-	-	-	-	-	-	-	-	-	-	-	-	-	-	-	-	-	-	-	-	-	-	545.121	-
Airplane	RJ	-	-	-	-	-	-	-	-	-	-	-	-	-	-	-	-	-	-	-	-	-	-	-	-	-	573.179	-
Airplane	RN	-	-	-	-	-	-	-	-	-	-	-	-	-	-	-	-	-	-	-	-	-	-	-	-	-	3937.433	-
Airplane	RO	-	-	-	-	-	-	-	-	-	-	-	-	-	-	-	-	-	-	-	-	-	-	-	-	-	4101.771	-
Airplane	RR	-	-	-	-	-	-	-	-	-	-	-	-	-	-	-	-	-	-	-	-	-	-	-	-	-	6354.405	-
Airplane	RS	-	-	-	-	-	-	-	-	-	-	-	-	-	-	-	-	-	-	-	-	-	-	-	-	-	1481.715	-
Airplane	SC	-	-	-	-	-	-	-	-	-	-	-	-	-	-	-	-	-	-	-	-	-	-	-	-	-	941.938	-
Airplane	SE	-	-	-	-	-	-	-	-	-	-	-	-	-	-	-	-	-	-	-	-	-	-	-	-	-	2922.011	-
Airplane	SP	4815.239	3277.409	5305.581	5305.581	2621.393	4177.928	1356.123	1178.424	1237.212	3968.163	782.944	1354.787	2156.436	3918.728	3700.947	3553.978	3730.341	545.121	573.179	3937.433	4101.771	6354.405	1481.715	941.938	2923.347	-	2372.881
Airplane	TO	-	-	-	-	-	-	-	-	-	-	-	-	-	-	-	-	-	-	-	-	-	-	-	-	-	2372.881	-

Appendix A: Routine Vaccines

Table 36 - Routine Vaccines

Routine Vaccines	AC	AL	AM	AP	BA	CE	DF	ES	GO	MA	MG	MS	MT	PA	PB
BCG	1.161	3.610	5.803	1.109	13.719	8.896	2.814	3.883	6.729	8.038	17.911	3.120	4.279	10.144	4.146
Polio	3.677	11.433	18.378	3.512	43.443	28.172	8.910	12.296	21.307	25.455	56.720	9.879	13.549	32.122	13.129
Polio1	1.305	3.921	6.314	1.238	15.926	10.223	3.301	4.505	7.995	9.168	20.723	3.421	4.445	11.230	4.457
Polio4	1.267	3.872	6.233	1.260	15.893	10.147	3.028	4.439	8.121	9.073	20.508	3.402	4.356	11.049	4.401
Hepatitis B	1.226	3.811	6.126	1.171	14.481	9.391	2.970	4.099	7.102	8.485	18.907	3.293	4.516	10.707	4.376
Rotavirus	2.323	7.221	11.607	2.218	27.438	17.793	5.627	7.766	13.457	16.077	35.823	6.239	8.557	20.288	8.292
Meningococcal C	2.452	7.622	12.252	2.341	28.962	18.781	5.940	8.198	14.205	16.970	37.813	6.586	9.033	21.415	8.753
Meningococcal C1	1.305	3.921	6.314	1.238	15.926	10.223	3.301	4.505	7.995	9.168	20.723	3.421	4.445	11.230	4.457
Dtp Penta	3.677	11.433	18.378	3.512	43.443	28.172	8.910	12.296	21.307	25.455	56.720	9.879	13.549	32.122	13.129
Pneumococcal	2.452	7.622	12.252	2.341	28.962	18.781	5.940	8.198	14.205	16.970	37.813	6.586	9.033	21.415	8.753
Pneumococcal 1	1.305	3.921	6.314	1.238	15.926	10.223	3.301	4.505	7.995	9.168	20.723	3.421	4.445	11.230	4.457
Yellow fever 9m	1.226	3.811	6.126	1.171	14.481	9.391	2.970	4.099	7.102	8.485	18.907	3.293	4.516	10.707	4.376
Yellow fever 4a	1.267	3.872	6.233	1.260	15.893	10.147	3.028	4.439	8.121	9.073	20.508	3.402	4.356	11.049	4.401
Dtp1	1.305	3.921	6.314	1.238	15.926	10.223	3.301	4.505	7.995	9.168	20.723	3.421	4.445	11.230	4.457
Dtp2	1.305	3.921	6.314	1.238	15.926	10.223	3.301	4.505	7.995	9.168	20.723	3.421	4.445	11.230	4.457
TetraViral	1.305	3.921	6.314	1.238	15.926	10.223	3.301	4.505	7.995	9.168	20.723	3.421	4.445	11.230	4.457
Hepatitis A	1.305	3.921	6.314	1.238	15.926	10.223	3.301	4.505	7.995	9.168	20.723	3.421	4.445	11.230	4.457
Varicella	1.267	3.872	6.233	1.260	15.893	10.147	3.028	4.439	8.121	9.073	20.508	3.402	4.356	11.049	4.401
Dtpa	1.305	3.921	6.314	1.238	15.926	10.223	3.301	4.505	7.995	9.168	20.723	3.421	4.445	11.230	4.457
Dtp	1.267	3.872	6.233	1.260	15.893	10.147	3.028	4.439	8.121	9.073	20.508	3.402	4.356	11.049	4.401
Hepatitis B PW	3.880	11.399	18.234	3.839	42.744	28.171	12.000	12.208	18.358	24.889	56.637	9.792	13.563	31.685	13.061
Dtpa PW	1.293	3.800	6.078	1.280	14.248	9.390	4.000	4.069	6.119	8.296	18.879	3.264	4.521	10.562	4.354
Dt PW	3.880	11.399	18.234	3.839	42.744	28.171	12.000	12.208	18.358	24.889	56.637	9.792	13.563	31.685	13.061
Papillomavirus	5.306	16.476	24.814	4.961	65.430	40.256	11.622	17.410	31.949	37.383	82.036	13.243	15.915	45.903	16.802
Dtabd	6.170	23.525	28.910	5.973	105.835	64.996	21.920	28.926	50.589	49.450	152.656	19.767	24.743	60.673	28.575

Routine Vaccines	PE	PI	PR	RJ	RN	RO	RR	RS	SC	SE	SP	TO
BCG	9.336	3.401	10.502	14.045	3.213	1.882	1.028	9.206	7.138	2.308	38.853	1.757
Polio	29.564	10.770	33.257	44.475	10.173	5.959	3.256	29.151	22.605	7.310	123.035	5.563
Polio1	10.678	3.698	12.293	17.498	3.705	2.193	968	10.936	7.601	2.658	47.035	1.990
Polio4	10.473	3.656	12.225	17.319	3.662	2.170	919	11.017	7.587	2.601	47.236	1.904
Hepatitis B	9.855	3.590	11.086	14.825	3.391	1.986	1.085	9.717	7.535	2.437	41.012	1.854
Rotavirus	18.672	6.802	21.005	28.090	6.425	3.764	2.057	18.411	14.277	4.617	77.707	3.513
Meningococcal C	19.710	7.180	22.172	29.650	6.782	3.973	2.171	19.434	15.070	4.873	82.024	3.708
Meningococcal C1	10.678	3.698	12.293	17.498	3.705	2.193	968	10.936	7.601	2.658	47.035	1.990
Dtp Penta	29.564	10.770	33.257	44.475	10.173	5.959	3.256	29.151	22.605	7.310	123.035	5.563
Pneumococcal	19.710	7.180	22.172	29.650	6.782	3.973	2.171	19.434	15.070	4.873	82.024	3.708
Pneumococcal 1	10.678	3.698	12.293	17.498	3.705	2.193	968	10.936	7.601	2.658	47.035	1.990
Yellow fever 9m	9.855	3.590	11.086	14.825	3.391	1.986	1.085	9.717	7.535	2.437	41.012	1.854
Yellow fever 4a	10.473	3.656	12.225	17.319	3.662	2.170	919	11.017	7.587	2.601	47.236	1.904
Dtp1	10.678	3.698	12.293	17.498	3.705	2.193	968	10.936	7.601	2.658	47.035	1.990
Dtp2	10.678	3.698	12.293	17.498	3.705	2.193	968	10.936	7.601	2.658	47.035	1.990
Tetra Viral	10.678	3.698	12.293	17.498	3.705	2.193	968	10.936	7.601	2.658	47.035	1.990
Hepatitis A	10.678	3.698	12.293	17.498	3.705	2.193	968	10.936	7.601	2.658	47.035	1.990
Varicella	10.473	3.656	12.225	17.319	3.662	2.170	919	11.017	7.587	2.601	47.236	1.904
Dtpa	10.678	3.698	12.293	17.498	3.705	2.193	968	10.936	7.601	2.658	47.035	1.990
Dtp	10.473	3.656	12.225	17.319	3.662	2.170	919	11.017	7.587	2.601	47.236	1.904
Hepatitis B PW	29.964	11.415	33.309	44.465	10.334	5.928	3.247	29.128	22.546	7.562	123.293	5.451
Dtpa PW	9.988	3.805	11.103	14.822	3.445	1.976	1.082	9.709	7.515	2.521	41.098	1.817
Dt PW	29.964	11.415	33.309	44.465	10.334	5.928	3.247	29.128	22.546	7.562	123.293	5.451
Papillomavirus	44.205	15.091	46.788	66.925	15.402	8.310	3.449	42.167	28.528	10.758	187.628	7.912
Dtabd	68.037	23.093	81.931	123.995	25.195	12.642	4.443	81.795	51.978	16.404	330.977	11.176